ARO 14090.1-EX

RESEARCH REPORT

LEVEL

A STUDY OF HIGH SPEED FRICTION

Ernest Rabinowicz, Nam P. Suh and
Forest J. Carignan

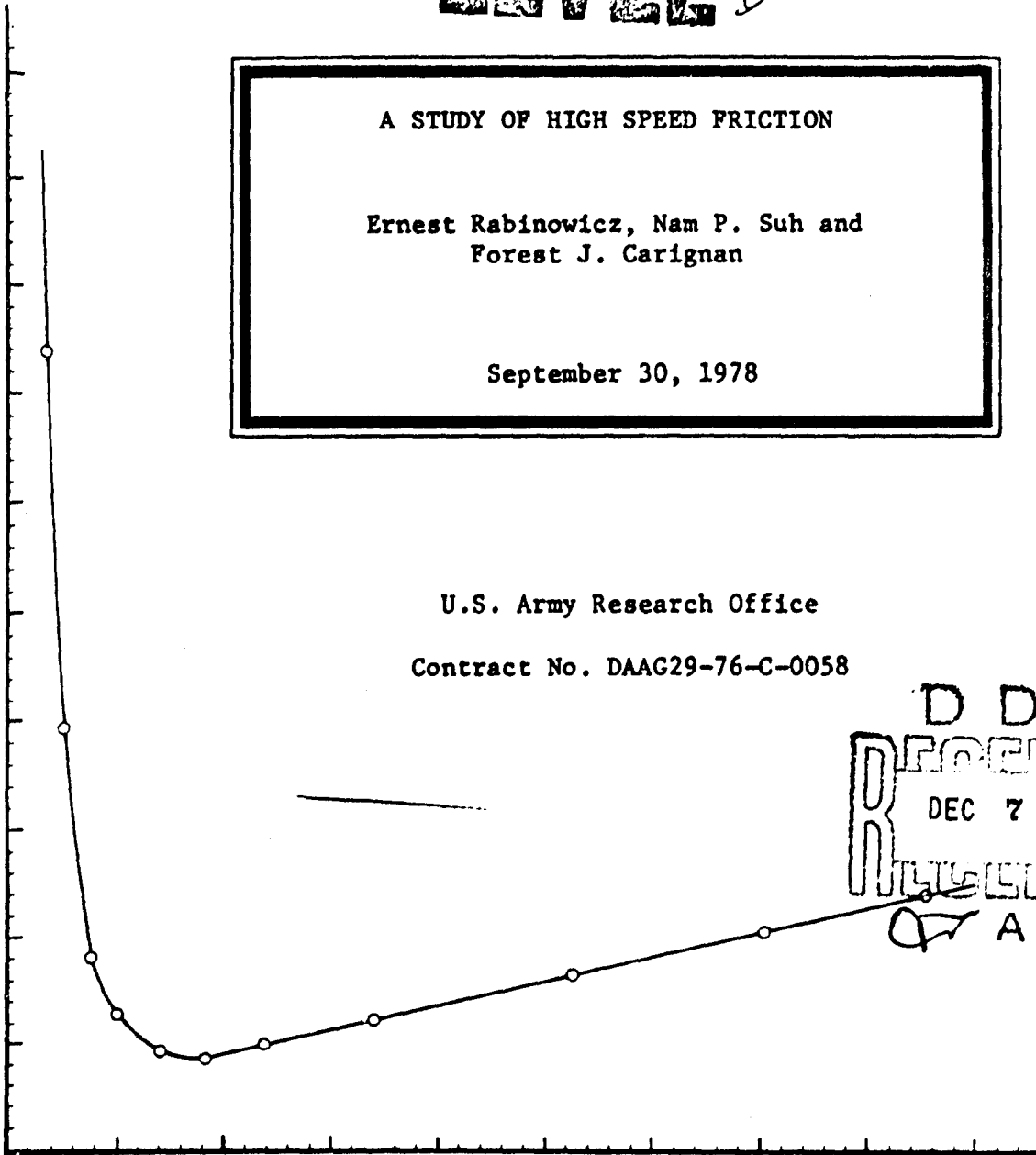September 30, 1978

D D C

RECEIVED

DEC 7 1978

A

SURFACE LABORATORY
DEPARTMENT OF MECHANICAL ENGINEERING
MASSACHUSETTS INSTITUTE OF TECHNOLOGY
CAMBRIDGE, MASSACHUSETTS

092

REPORT DOCUMENTATION PAGE		READ INSTRUCTIONS BEFORE COMPLETING FORM
1. REPORT NUMBER	2. GOVT ACCESSION NO.	3. RECIPIENT'S CATALOG NUMBER
4. TITLE (and Subtitle) A STUDY OF HIGH SPEED FRICTION.		5. TYPE OF REPORT & PERIOD COVERED Final report.
		6. PERFORMING ORG. REPORT NUMBER
7. AUTHOR(s) Ernest Rabinowicz, Nam P. Suh and Forest Carignan		8. CONTRACT OR GRANT NUMBER(s) DAAG29-76-C-0058
9. PERFORMING ORGANIZATION NAME AND ADDRESS Department of Mechanical Engineering Massachusetts Institute of Technology Cambridge, MA 02139		10. PROGRAM ELEMENT, PROJECT, TASK AREA & WORK UNIT NUMBERS
11. CONTROLLING OFFICE NAME AND ADDRESS U.S. Army Research Office Box 12211 Research Triangle Park, NC 27709		12. REPORT DATE 30 September 30, 1978 13. NUMBER OF PAGES
14. MONITORING AGENCY NAME & ADDRESS(If different from Controlling Office) 138p.		15. SECURITY CLASS. (of this report) Unclassified 15a. DECLASSIFICATION/DOWNGRADING SCHEDULE

16. DISTRIBUTION STATEMENT (of this Report)

Approved for public release; distribution unlimited.

ARO

14090.1-EX

17. DISTRIBUTION STATEMENT (of the abstract entered in Block 20, if different from Report)

NA

18. SUPPLEMENTARY NOTES

19. KEY WORDS (Continue on reverse side if necessary and identify by block number)

20. ABSTRACT (Continue on reverse side if necessary and identify by block number)

A high speed friction and wear machine has been developed for operation in the 100-500 feet per second regime. Normal loads up to ten pounds are used with the upper limit determined by the force transducer. Signals corresponding to the frictional and normal forces are electronically divided to indicate the friction coefficient. All data is recorded on a high speed oscillograph. Wear of test materials is determined by weight loss measurement. Interfacial temperature measurements via thermoelectric effects and optical pyrometry can be made. The

DD FORM 1473 EDITION OF 1 NOV 65 IS OBSOLETE
1 JAN 73

apparatus and associated instrumentation is described in detail.

Results indicate a decreasing friction coefficient with increasing sliding speed. This is due to thermal softening, leading to the presence of low shear films at the interface. However, full hydrodynamic lubrication is not reached in the range of loads and velocities tested so the friction coefficient does not get below 0.14.

The wear coefficient increases with sliding speed very rapidly. This is probably due to the change in hardness of the test materials at high temperatures.

The following materials were tested against 4140 steel: 70-30 brass, gliding metal, copper, copper-16% lead, nylon, DQ3, Rulon A, vulcanized fiber, constantan, zinc, bismuth, Delrin, solder, grafite, iron, polycarbonate, polyethylene and woods metal.

A study of high speed friction

Final report

Ernest Rabinowicz, Nam P. Suh and Forest J. Carignan

September 30, 1978

U.S. Army Research Office

Contract No. DAAG29-76-C-0058

Department of Mechanical Engineering
Massachusetts Institute of Technology
Cambridge, Massachusetts 02139

Friction and Wear
at High
Sliding Speeds

by

Ernest Rabinowicz, Nam P. Suh and Forest J. Carignan

Abstract

A high speed friction and wear machine has been developed for operation in the 100-500 feet per second regime. Normal loads up to ten pounds are used with the upper limit determined by the force transducer. Signals corresponding to the frictional and normal forces are electronically divided to indicate the friction coefficient. All data is recorded on a high speed oscillograph. Wear of test materials is determined by weight loss measurement. Interfacial temperature measurements via thermoelectric effects and optical pyrometry can be made. The apparatus and associated instrumentation is described in detail.

Results indicate a decreasing friction coefficient with increasing sliding speed. This is due to thermal softening, leading to the presence of low shear films at the interface. However, full hydrodynamic lubrication is not reached in the range of loads and velocities tested so the friction coefficient does not get below 0.14.

The wear coefficient increases with sliding speed very rapidly. This is probably due to the change in hardness of the test materials at high temperatures.

The following materials were tested against 4140 steel: 70-30 brass, gilding metal, copper, copper-16% lead, nylon, D03, Rulon A, vulcanized fiber, constantan, zinc, bismuth, Delrin, solder, grafite, iron, polycarbonate, polyethylene and woods metal.

TABLE OF CONTENTS

LIST OF FIGURES

LIST OF TABLES

Introduction

The aim of this project has been to undertake sliding experiments at relatively high speeds, in the range 50 feet/sec to 500 ft/sec (15 to 150 m/sec), and to measure friction, wear and surface temperature. A wide variety of materials would be tested, with special emphasis on those of value in ballistic applications. Hopefully, the results would be of interest to those interested in high speed friction as well as to those concerned with ballistics.

Perhaps some comments on past research in this field would be in order. As is well known, the prediction of friction forces to be encountered in high speed sliding is a complex one, since on top of all the considerations applicable to any sliding situation (the compatibility of the surfaces, the state of contamination or lubrication of the interface, the load, the speed, the geometry and the surface roughness, etc.) there are complications introduced by the high surface temperatures and the high thermal gradient at the surface, both present as result of frictional heating.

The consequence of the surface heating is to leave a soft surface layer on a harder substrate, leading to a sharply reduced friction coefficient. This phenomenon has been labelled 'melt lubrication' whether or not surface melting occurs. (In fact the question of whether melting does or does not occur in any situation is a complex one, and investigators have on occasion had to retract previously published views. For example Bowden for a number of years explained his high speed friction results in terms of a continuous molten surface layer, but had to revise this explanation when calculations showed that his sliding system had insufficient kinetic energy to induce a very considerable degree of surface melting).

-1-

When it becomes necessary to analyse the behavior of a ballistic projec-
tile in a gun, (itself an extremely complex problem), what is generally done
is to make a highly simplified assumption about the friction, to analyse the
consequence of the assumption on the projectile motion and the wear of the
system, and then to measure the motion and the wear rate. If the agreement
between analysis and experiment is reasonable, it is concluded that the assump-
tions were quite probably correct. Given the complexity of the analysis and
the fact that the friction forces are but a small proportion of all the
forces involved, while wear theories and measurements are not very precise,
this is not necessarily a correct procedure. Specifically, it would be dan-
gerous to rely on assumptions tested out in this way to design optimum bal-
listic systems.

The subject of high temperature friction has been reasonably well cov-
ered in the tribological literature. Perhaps the pioneering work was that of
Johnson, Swikert and Bisson, who in 1947 showed, using a pin on disk apparatus,
that the friction dropped as the sliding speed was increased to 100 ft/sec.
Sternlicht and Apkarian (1960) used a pin-on-disk machine built by W. W. Shugarts at
Franklin Institute to measure the friction and wear of various elemental
metal riders (Mo, W, Cr, Cu, Ag, Al) against a copper plated and chromium
plated disk. Bowden and Freitag (1958) and Bowden and Persson (1961) used a
suspended ball technique to study the friction and surface damage of a variety
of materials against a bearing steel ball. More recently, Allen and McKillop
(1968) have used a contacting annulus geometry to study friction at high
sliding speeds.

In general, these workers carried out one or a limited number of tests

with each combination tested, so that the temperature profile, and the influence of the temperature profile on the friction, was not well defined. Moreover, no attempt was made to devise material combinations giving optimum friction and wear resistance. No attempt was made to analyse the fluctuations encountered in the friction coefficient values.

From the ballistic side, there seem to have been few papers (at least readily available ones). Herzfeld and Kosson in 1953 analysed the motion of a projectile in a bore and showed fairly good agreement with experimental results on assuming that a molten surface layer formed immediately after movement began. They found evidence for drastic fluctuation in the frictional resistance. Krafft in 1955, measured the frictional interaction between a spinning projectile and a target, and deduced various friction coefficient values suggestive of melt lubrication.

Until recently, there seem to have been few attempts to link closely the experimental data obtained from high speed friction tests with those derived from ballistic tests. The work carried out by Montgomery (1976) has greatly helped to close this gap, while at the same time pointing out systematic discrepancies between the two sets of data. In a sense, our study might be regarded as an attempt to derive more data of the kind analysed by Montgomery.

Our research was carried out during the two-year period August 16, 1976 to August 15, 1978. Mr. Forest Carignan worked on the project throughout this period, for most of this period   as Research Assistant and then for the last few months as Research Engineer. His M.S. Thesis, "Friction and Wear at High Sliding Speeds" which contains an extensive account of the work carried out under the project, is appended to this report as Appendix A. The work carried out in the last few months is summarized as appendix B.

-3-

Apparatus

The high speed friction apparatus used in these tests was based on that designed by J. Potter as a B.S. degree project in 1973. Mr. Potter purchased or built many components of the driving system, but did not assemble the apparatus as a whole. Nevertheless, the availability of parts of the apparatus greatly shortened the time required to get the project to the stage where experimental results could be obtained. A detailed description of the apparatus is given in Appendix A.

Results

The results obtained during the project are fully described in appendices A and B.

Discussion

The experimental results obtained in this work form a further indication of what appears to be a serious disagreement with regard to friction values obtained during high speed sliding. In order to illustrate the problem, we have tabulated in table 1 the experimental values obtained using the various methods. Since sliding speed is such an important variable, we have only considered data at 100 m/sec and 200 m/sec (for our own experiments we considered the top sliding speed of 150 m/sec).

Bowden and his co-workers at Cambridge University have used a technique involving a ball spinning at very high speeds and then slowed down by contact against one or more stationary specimens. In some of their tests they got very high friction values with friction coefficients above 0.5, but they frequently obtained very low friction values. Of the data shown in Table 1, 16 out of 54 (or 30%) are below 0.10, while 8 out of 54 (or 15%) are below 0.05. Montgomery (1976a) cites friction results based on ballistic tests at Picatinny Arsenal. Only two values are tabulated, but in fact his paper gives many values obtained at many sliding speeds, and it seems that of the 24 friction coefficient values obtained above 80 m/sec, none is above .05, and in fact the highest is 0.027.

In contrast, the friction values obtained in the 1950's at the Franklin Institute using a pin on disk apparatus, and conveniently collected by Montgomery (1976b) are all quite high, in the range 0.50 to 0.25 as are the values obtained by Sternlicht and Apkarian (1960) with the Franklin Institute apparatus. Our own friction values, again

obtained with a pin on disk tester, are also generally high, although we have on one occasion got down to 0.14.

To some extent the discrepancy can be explained away (for example in the case of the ballistic tests an external source of heat was available) but we do not feel that the discrepancy has been resolved. Certainly it seems that the phenomenon of 'melt lubrication,' in which a complete liquid layer derived from one or both sliding metals is present at the interface and provides very low friction, is not as prevalent or as drastic as many have hypothesized. Also, to the extent that our samples showed a relatively modest drop in friction or the sliding speed was increased, we saw few indications of the kind of frictional oscillations that might have been excited by a steeper negative slope. A letter by Allan (1976) is of interest in discussing melting and vibrations observed in guns during World War II.

Our experimental results suggested that generally the wear rate per unit sliding distance increased significantly as the sliding speed increased. This effect was specially marked in the case of some of the polymers, in which case there was often an increase by several orders of magnitude. However, in a ballistic situation that would represent the wear of the driving band of the shell rather than the wear of the gun barrel and hence, a phenomenon of limited importance. We were not able to measure wear of the steel surface very reliably, and thus our tests don't throw much light on the wear of the gun barrel.

Perhaps our major disappointment was that our technique of sliding a pin against a disk with a sharp projecting edge did not seem to reproduce the imprinting phenomenon very well, and thus we did not seem to get results that would give the magnitudes of the additional forces

arising during the imprinting stage. Probably, the geometry of a pin sliding over a grooved disk would be preferrable.

As regards materials selections for use in driving bands, our tests pointed out the superiority of teflon-based materials. These did not give as low friction as teflon often does in low speed sliding tests, but the friction was relatively low, relatively constant, and with a small but regular negative slope. If compositions with sufficient mechanical strength can be found, they would appear to have considerable potential.

Acknowledgements

References

1. C. W. Allen and A. A. McKillop, Melt lubrication of an annular-thrust surface, ASME paper 68-LubS-1968.

2. J. F. Allen, 'Melting by friction,' Letter on p 480 of Physics Bulletin, November, 1976.

3. F. P. Bowden and E. H. Freitag, "The friction of solids at very high speeds," Proc. Roy. Soc., 248A, 350-367, 1958.

4. F. P. Bowden and P. A. Persson, "Deformation, heating and melting of solids in high-speed friction," Proc. Rov. Soc., 260A, 433-458, 1961.

5. C. M. Herzfeld and R. L. Kosson, "A Theory of Bore Friction," Report 851, Ballistics Research Laboratories, March 1953.

6. R. L. Johnson, M. A. Swikert and E. E. Bisson, NASA Technical Note 1442, 1947.

7. J. M. Krafft, "Surface Friction in Ballistic Penetration" J. Appl. Phys., 26, 1248-1253, 1955.

8. D. R. Miller, 'Friction and abrasion of hard solids at high sliding speeds,' Proc. Roy. Soc., 269A, 368-384, 1962.

9. R. W. Montgomery, 'Surface melting of rotating bands,' Wear, 38, 235-243, 1976a.

10. J. R. Potter, 'Design of a high speed/high temperature friction apparatus,' B.S. thesis in Mechanical Engineering, M.I.T., June 1973.

Table I. Friction coefficient values

I. Spinning ball apparatus

	Stationary material	Moving material	Load	f at 100 m/sec	f at 200 m/sec
Bowden and Freitag (1958)	Copper	Steel	30 g	Seized	0.5
	Alumium alloy	steel	25 g	0.7	0.4
	bismuth	steel	15 g	0.07	0.04
	antimony	steel	30 g	0.28	0.18
	tungsten	steel	40 g	0.38	0.25
	molybdenum	steel	40 g	–	0.36
	molybdenum	copper	40 g	–	0.53
	diamond	steel	50 g	.05	.02
	diamond	chromium	50g	.06	.12
	diamond	copper	50g	.03	.04
Bowden & Persson (1961)	bismuth	steel	5 kg	0.142	0.097
	woods alloy	steel	5 kg	0.04	0.2
	lead	steel	5 kg	0.28	0.18
	tin	steel	5 kg	0.11	0.06
	silver nitrate	steel	5 kg	0.04	0.02
	copper	steel	5 kg	0.21	0.17
	steel	steel	5 kg	0.09	0.07
	nylon	steel	5 kg	0.15	0.12
	teflon	steel	5 kg	0.21	0.17
	rubber	steel	5 kg	1.1	0.7
	glass	steel	5 kg	0.23	0.18
D.R. Miller (1962)	diamond	steel	50 g	0.012	0.08
	silicon carbide	steel	50 g	0.18	0.11
	silicon carbide	chromium	50 g	0.22	0.16
	titanium carbide	steel	50 g	0.16	0.10
	sapphire	steel	50 g	0.13	0.11
	sapphire	copper	50 g	0.18	0.13
	sapphire	chromium	50 g	0.22	0.19

II. Shell on gun apparatus

Montgomery (1976a)	Stationary	Moving	Load	f at 100 m/sec	f at 150 m/sec
	gilding metal	gun steel	High	0.02	.011

III. Pin on disk apparatus

	Stationary	Moving	Load	f at 100 m/sec	f at 150 m/sec
Montgomery (1976b)	gilding metal	gun steel	10 kg	0.39	0.32
	annealed iron	gun steel	10 kg	0.36	0.25
	copper	gun steel	10 kg	-	0.38
	projectile steel	gun steel	10 kg	0.50	0.28
	aluminum	chromium	8 kg	-	0.59
Sternlicht & Apkarian (1960)	copper	chromium	8 kg	0.53	0.47
	silver	chromium	8 kg	0.53	0.48
	tungsten	copper	8 kg	-	0.46
	molybdenum	copper	8 kg	-	0.41
	chromium	copper	8 kg	0.51	0.47
	aluminum	copper	8 kg	-	0.95

IV. Pin on disk apparatus

	Stationary	Moving	Load	f at 100 m/sec	f at 150 m/sec
This report Appendix A					
	gilding metal	4140 steel	2 kg	.60	.55
	Rulon A (teflon based)	4140 steel	2 kg	.28	.24
	DQ3 (teflon based)	4140	2 kg	.30	.20
	Nylon	4140	2 kg	.50	.30
	Cu84 Pb16	4140	2 kg	.52	.58
	Copper	4140	2 kg	.31	.52
	Zinc	4140	2 kg	.44	.38
	Constantan	4140	2 kg	.25	.21
	Vulcanized fiber (axial)	4140	2 kg	.35	.26
	Vulcanized fiber (radial)	4140	2 kg	.51	.43
This report Appendix B					
	Bismuth	4140	2 kg	.18	.14
	Sintered Iron	4140	2 kg	.85	.75
	Wood's metal	4140	2 kg	.50	.50
	Eutectic Solder	4140	2 kg	.83	.83
	Bismuth	Eutectic solder	2 kg	.30	.30
	Bearing steel	Eutectic solder	2 kg	--	.22

A.I. INTRODUCTION

Throughout the history of mankind friction and wear tests have been unwittingly conducted. However, advances in this field (called tribology) have until recently been almost non-existent. It 'as been and is still widely felt that control over friction and wear is governed by folklore. Statements like "use oil", "make it smoother", or "bronze isn't bad" are typical examples. Quantitative work in tribology has been advancing rapidly, and there are some areas in which qualitative information is still needed. Friction and wear at high speeds is one of these areas.

There are several areas where high speed sliding is a problem. Interest in this area stems from problems of wear in gun tubes. Guns have existed for many years and from a tribology standpoint very little has been done to improve their performance. Another situation is met in some high speed turbines which keep a close blade-housing clearance by wearing the two together. For another example, trains can encounter sliding situations of up to a few hundred feet per second. Machines in general are being run at higher speeds as efficiency becomes more important and as technology advances.

The purpose of this report is not to specifically decide what material would make the best gun tube, but rather to scientifically analyze the whole high speed sliding

situation. Insight into problems of high speed sliding in general will hopefully be the result.

In contrast to the millions of friction and wear experiments unconsciously run every day, high speed testing requires a special apparatus. In this report a device for conducting such tests is discussed in detail. Special attention has been placed on examining temperature rises which occur at a sliding interface. Increased temperatures are felt to be the most significant difference between low and high speed sliding situations. Appropriate instrumentation for high speed force measurements has also been developed.

Included are the results of 200 tests conducted with various materials on 4140 steel. Wear and friction coefficients have been plotted as a function of sliding speed. The normal loads were identical and some temperature rise results are also shown. Both qualitative and quantitative information has been obtained, but more work is still needed. Part of the problem lies in deciding where future efforts should be concentrated.

A.II. EXPERIMENTAL APPARATUS
A. ROTARY SYSTEM

In order to obtain surface speeds of 500 feet per second (fps) a large diameter (14 inch) steel disc was chosen to be spun at 10,000 rpm. As is well known, the basic factor limiting the surface speed of a rotating disc is not the disc diameter but mainly the strength and density of the disc (Appendix A). There is a square law proportionality between rotational induced stress and surface speed. There were three basic reasons for using a 14 inch diameter disc instead of a smaller disc spun faster. The larger disc has more surface area available for testing. If the outer periphery is used for tests, it presents a nearly flat surface to the test specimen. Lastly, there is some practical difficulty encountered in going above 10,000 rpm. At the other extreme, a larger disc intended to be spun more slowly would have been harder to fabricate.

A 4140 steel hot rolled plate was turned and ground to a finished diameter of 14 inches and a thickness of .74 inches. The outer edge was chosen to be the test surface, since a pin can traverse it axially while maintaining a constant surface speed. This edge is also preferable to the sides of the disc in regard to the likelihood of dynamic unbalance from test loads. This factor is secondary, because due to the disc's large moment of inertia a single side load

might also be stable. Were this not so, it would be necessary to load the disc equally from both sides. Smooth running at 10,000 rpm was obtained without any dynamic balancing, but the radial disc runout was approximately .002 inches. The force transducer picked this up and produced oscillations in the normal force. The oscillations had amplitudes of one-half the full signal and severely limited the usable range of test loads. The transducer arm is capable of providing a fairly constant normal force at low frequency but it will not respond to gross variations as rapid as the wheel rotational frequency. The mass and springiness of the transducer arm transform a .002 inch oscillation (a gross variation) of the specimen into some normal load. Typically, a 5 pound normal load would be applied and it would vary from 2.5 to 7.5 pounds sinusoidally. Eliminating this load variation was desirable, so a means for machining the outer edge of the disc while on the apparatus was devised. A manually driven platform on which was mounted a special ceramic tool (10% TiO, 90% Al_2O_3) was used to turn the edge. The device was essentially a lathe, although the minimum surface speed attainable was 3000 feet per minute.

A second disc was fabricated with a projection on the outer surface for engraving tests. A sectional view is shown in Figure 1. The projection makes it possible to run tests at higher contact pressures than a flat surface will permit. It

```
                              ┌──────────────────────┐
                              │                      │
                              │        DISC          │
  Normal                      │                      │
  Force                       │                      │
         ──────▶ │ pin │   ┌──┤ projection  1/32 inch high by
                              │             1/32 inch wide
                              │                      │
                              └──────────────────────┘
```
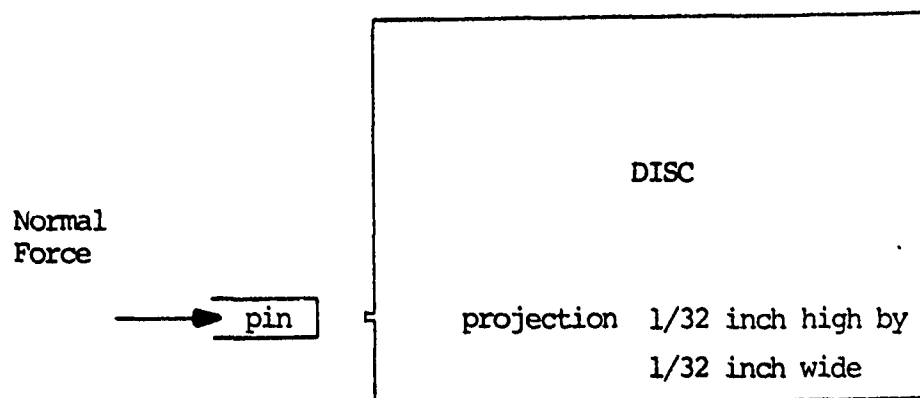
Figure A1. Sectional view of disc projection

is meant to simulate the engraving which occurs as a
projectile conforms to the rifling in a gun tube. It was
unnecessary to true the outer edge of this disc, and it would
have been difficult to do so without removing the projection.

An attempt to produce a copper surface which could
move at 500 fps was made by electroplating copper onto the
edge of the first disc. Stress considerations (Appendix A)
prevent the use of a solid copper disc, and the results of the
plating process were partially unsatisfactory. The disc was
mounted on a lathe, the outer edge was turned to produce a
clean surface, and the edge was thinly alkaline brush plated
(11). The plating was then built up using a copper sulfate
plating bath to a calculated .02 inch thickness. The entire
process was conducted while the disc was turning at 20 rpm
with a portion of it in the plating bath (Figure 2). In

4140 steel
disc with
lacquer
coating on
both sides

20 rpm

Lathe
Headstock

3 Jaw
Chuck

copper
sulfate
solution

Copper brush to
electrically
contact the disc

−   +

DC
Supply

Copper anode

Pyrex dish

Figure A2. Disc edge plating process

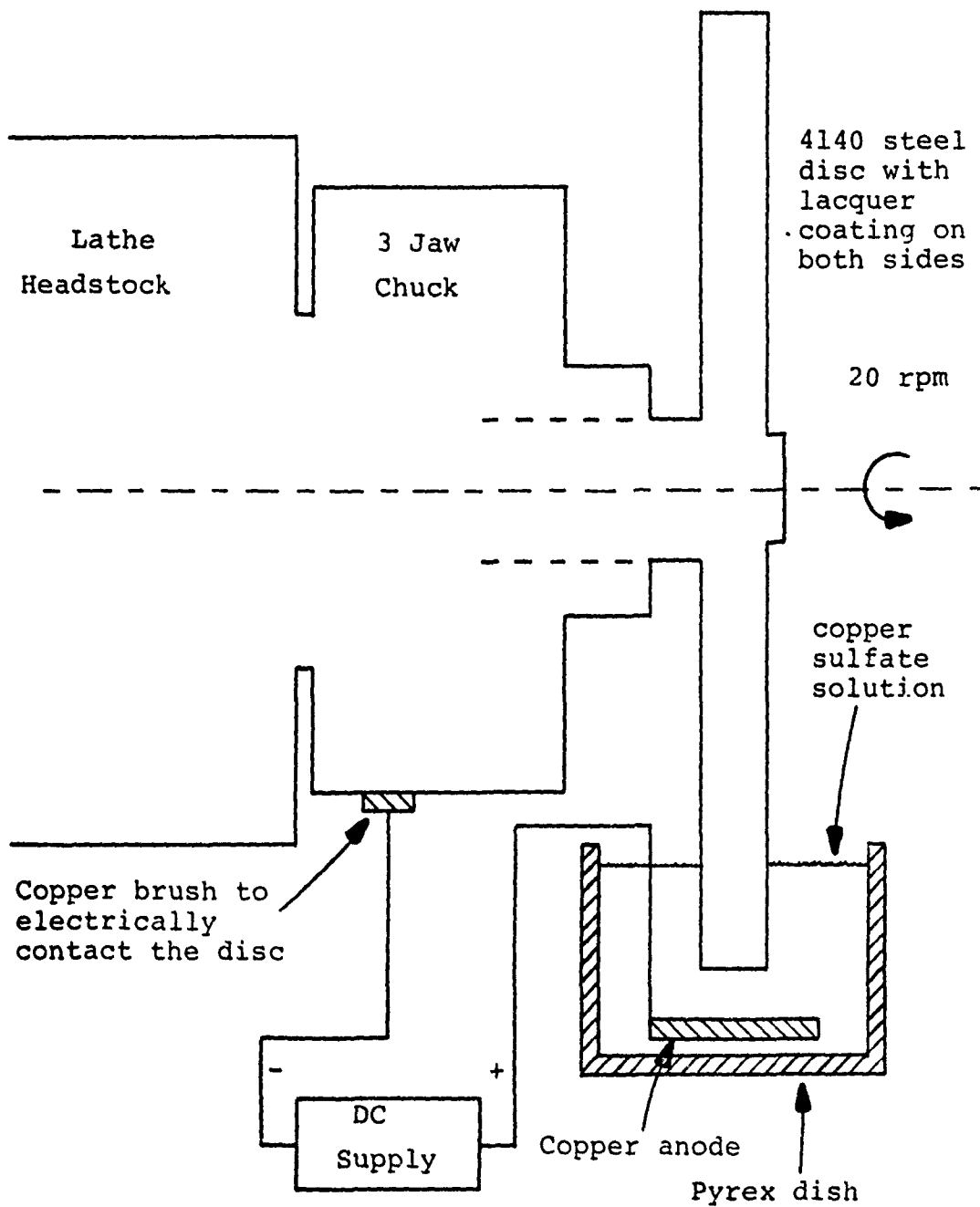practice the electroplating resist on the sides of the disc did not hold up for the forty hour plating process and the edge coating was only a few mils thick. It was also somewhat porous and hence it was not used. Future attempts could be more successful and might be pursued.

The disc is driven by a five horsepower induction motor through a variable speed drive and a step-up gearbelt arrangement. Disc speed control from 1100 to 10,000 rpm (50 to 600 fps) is obtained through a 60 cycle stepper motor which actuates the variable speed drive. Originally a handwheel controlled the speed setting, but remote operation was preferable. A stepper motor was chosen because it is reversible and can be stalled without damage. The original handwheel should have been operated only when the induction motor was running to prevent damage to the variable speed drive. This became a necessary condition for the stepper motor to receive power. An electromagnetic clutch is installed between the gearbox and the gearbelt pulley to allow increased versatility and safety.

The disc shaft bearings are mounted in a portion of an automobile engine block for rigidity and alignment. The bearings are from an ultra-light series and are unshielded and unsealed. They can be lubricated continuously or intermittently by dropping oil into their side. In practice only intermittent lubrication has been used. The bearings are

lightly loaded and no heating is evident in the course of a test. Figure 3 is a diagram of the drive system.

Approximately 75 fifty pound sandbags and a three inch layer of plywood were placed around the disc to absorb stored kinetic energy in the slight chance of a catastrophic disc or bearing failure. The system displays no tendency to be unstable, but since 60,000 foot pounds of energy is stored at 10,000 rpm safety is a major concern. Disc stress is kept below one-half of the yield stress. Motor controls are essentially failsafe; the speed cannot be increased without continuously holding a switch and a power shutdown resets the system to off.

Disc speed is measured by an optical tachometer which senses an unpainted strip of the disc or shaft as it rotates. The change in reflectivity of the paint is picked up by a photodetector. A standard tachometer is mounted on the output of the variable speed drive before the clutch. All motor controls are shown in Appendix B. The optical tachometer circuitry is also included. Figures 4 and 5 are general views of the apparatus.

14 inch disc

Specimen position

Bearings housed in engine block

Gearbelt

Clutch

Stepper Motor

Variable Speed Drive

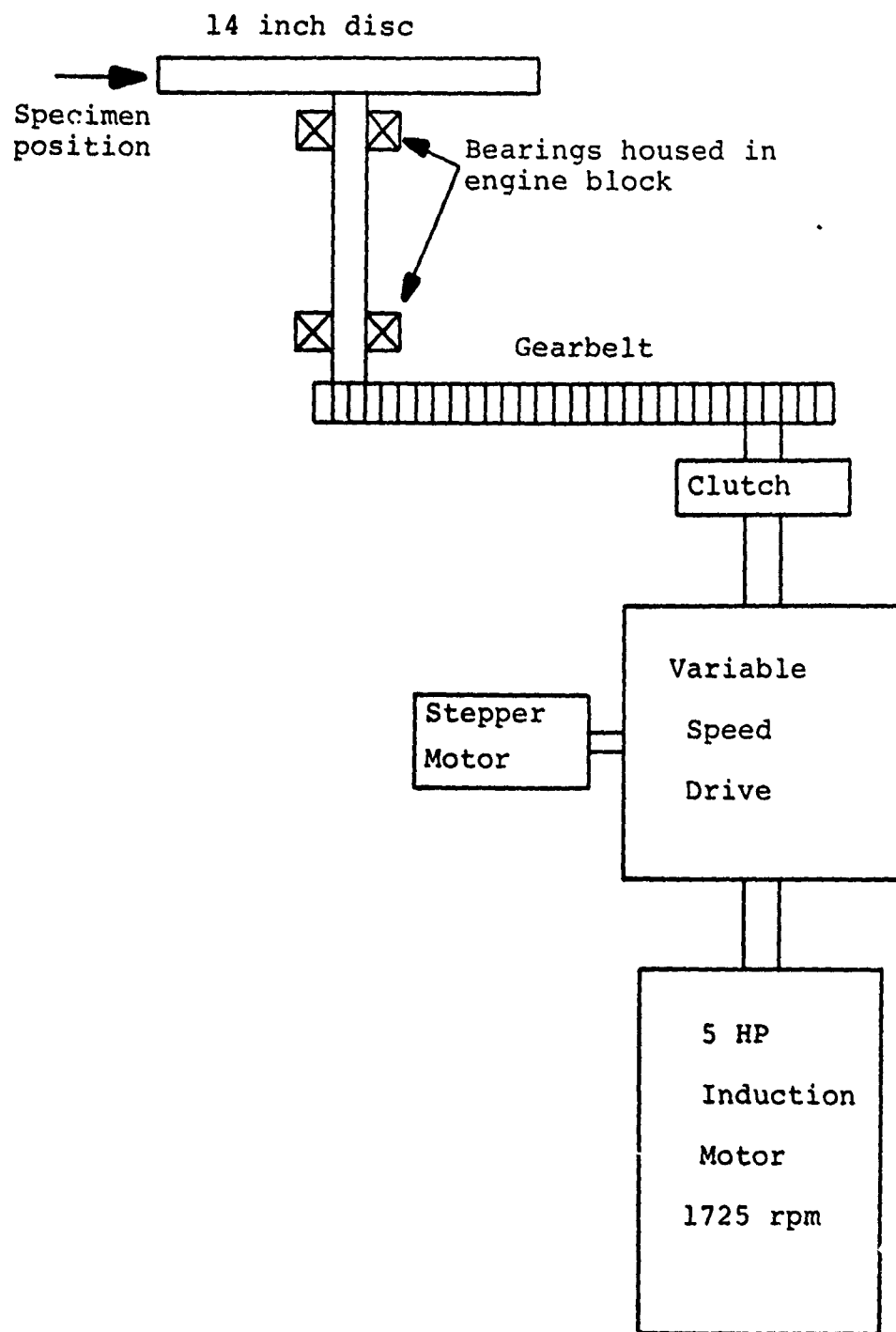5 HP Induction Motor 1725 rpm

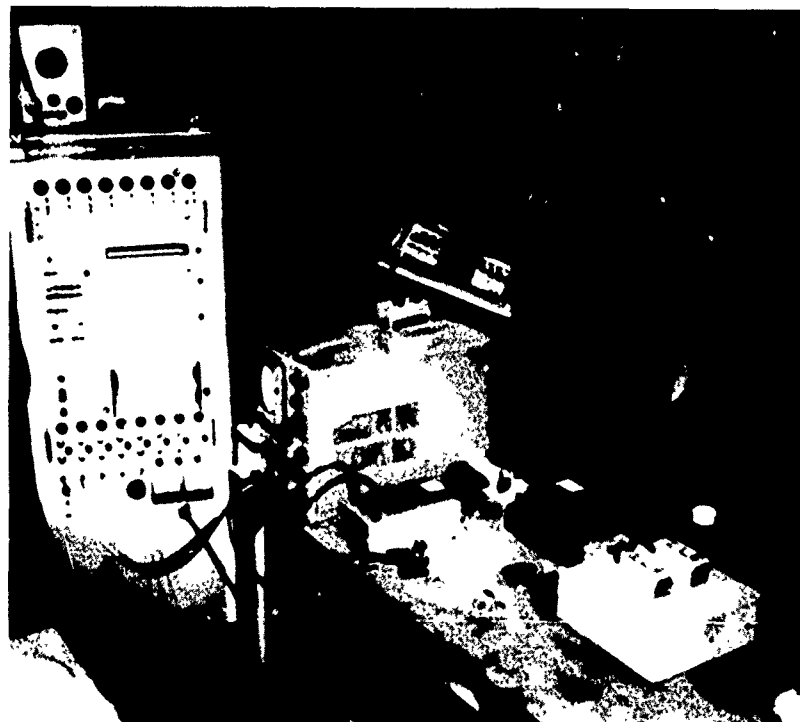Figure A3. Disc drive system

Figure A4. #1 general view of the apparatus

Figure A5. #2 general view of the apparatus
-A10-

A.2. TRANSDUCER SYSTEM

Firmly attached to the side of the engine block base is a platform which holds the transducer, to which is attached the pin wear specimen. By means of a motor driven screw shaft and linear bearings the transducer can be traversed axially along the edge of the disc. This can be done during a test or before it. In the latter case it can allow manual placement of the pin-disc contact region. If the traversing is done during a test the specimen follows a spiral trajectory on the disc edge. The adjustable traversing speed is independent of the disc speed and has a maximum value of 1.75 inches/second. This is just sufficient to allow a one-sixteenth inch specimen to not retrace its wear track during 100 fps tests. Specimens are generally larger than one-sixteenth inch, so tests usually retrace their wear track. Since in most practical situations a sliding surface does not always encounter a fresh surface this was not considered a detrimental feature.

In order to press the specimen against the disc the transducer is mounted on an arm attached to a pneumatic actuator. The air pressure determines the normal force and is controlled by a four-way solenoid valve. Manual or complete automatic control of the arm is possible by toggle switches or microswitches activated as the transducer traverses the disc. The electric solenoid has a response time of 10 milliseconds.

The normal force in pounds is roughly one-quarter of the air pressure in psi. The transducer platform is shown in Figure 6.

High speed friction measurements require a force measuring system with a fast response time. In addition, the system must be capable of sensing both the normal and frictional components, because under rapidly varying conditions a "constant" normal force as produced by a mass is not constant. For instrumentation reasons to be presented soon, it was also desirable to have electrical signals corresponding to both components.

A symmetrical strain gage beam transducer (6) was chosen which would give independent normal and frictional signals with identical frequency response on both axes. The first beam-transducer arm assembly constructed was found to have a combined natural frequency of 120 hertz. This was determined by letting the beam and arm vibrate without contacting the disc and looking at the resulting electrical signal. Damping was very low and 120 hertz is insufficient to even sense oscillations as the disc rotated. For example, at 7200 rpm disc runout produces 120 hertz oscillations. There is nothing to make the transducer follow the disc at speeds higher than this. The specimen gets pushed out by the rotating eccentric disc and it does not follow the disc back in. Phenomenon similar to valve float in internal combustion

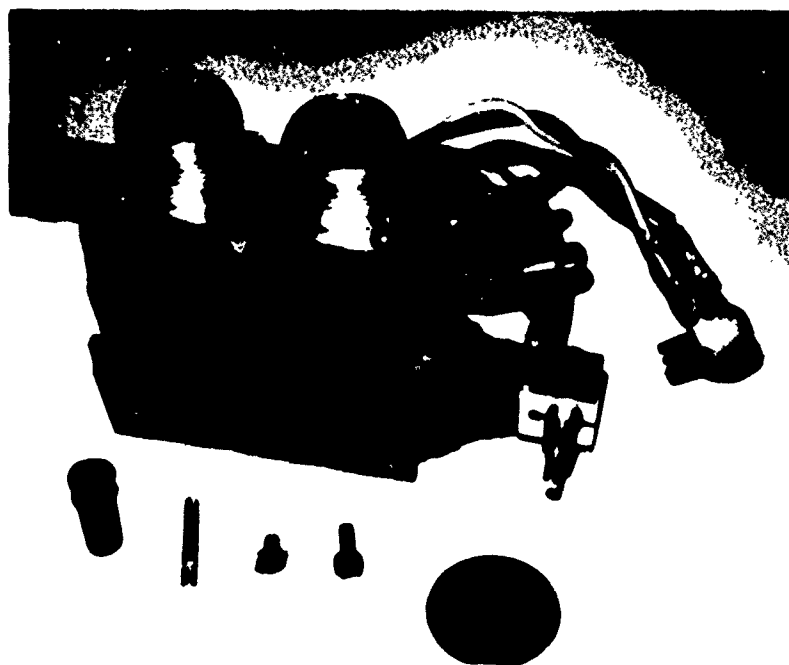Figure **A6.** View of transducer platform

Figure **A7.** Transducer with some typical specimens

engines is the result. In engines, the natural frequency of the valve-spring combination is too low to allow the valve to close at high engine speeds. In the transducer, the specimen contacts the disc for only a fraction of each revolution, and very smooth but erroneous signals are the result.

The second beam-transducer arm assembly had a natural frequency of approximately 3 kilohertz for both the normal and frictional components. This was sufficient, but it was necessary to make a slightly different third transducer because the second one failed by fatigue at the start of a test. All tests are now run on this third transducer (Appendix C) which holds specimens up to 3/4 inch long and .267 inch diameter. Its frequency response is greater than 2 kilohertz and one eighth inch pins are used for most tests. The transducer is shown in Figure 7.

A means for heating specimens up to several hundred degrees Centigrade has been incorporated into the transducer. A resistance heating coil surrounds the one-eighth inch pin and power is supplied by a highly filtered direct current source (Appendix D). Alternating current could be used to heat the specimen but 60 cycle noise becomes a problem. A chromel-alumel thermocouple of .004 inch diameter is inserted in a hole in the specimen to monitor its temperature. Because it is undesirable to overheat the strain gages, water cooling was provided in the head of the transducer which eliminates

this problem. It is important to keep the mass of the transducer head to a minimum for high frequency response, and silicon rubber is used to protect the strain gages and increase damping. The water cooling tubing increases damping without adding significantly to the mass of the head.

It is necessary to divide the instantaneous friction force by the normal force in order to get the value of its coefficient of friction f. For all tests run with the first transducer the friction and normal force signals were recorded on a strip-chart recorder. Then the friction trace was divided by the normal trace to give a value of f. Due to the rapidly changing forces this was difficult to do accurately. An electronic analog divider was therefore constructed which would do this automatically during each test. The friction force and the normal force are each transformed into a signal corresponding to .8 pounds per volt (or 8 pounds per volt) up to ten volts. The frequency response of this part of the electronic network has been limited to 10 kilohertz to minimize noise, but the divider has a frequency response of 750 kilohertz. It was convenient to put a lower limit on the voltage going into the divider in order to eliminate the instability occurring when dividing by zero. A block diagram of the instrumentation is shown in Figure 8. A detailed schematic is in Appendix E.
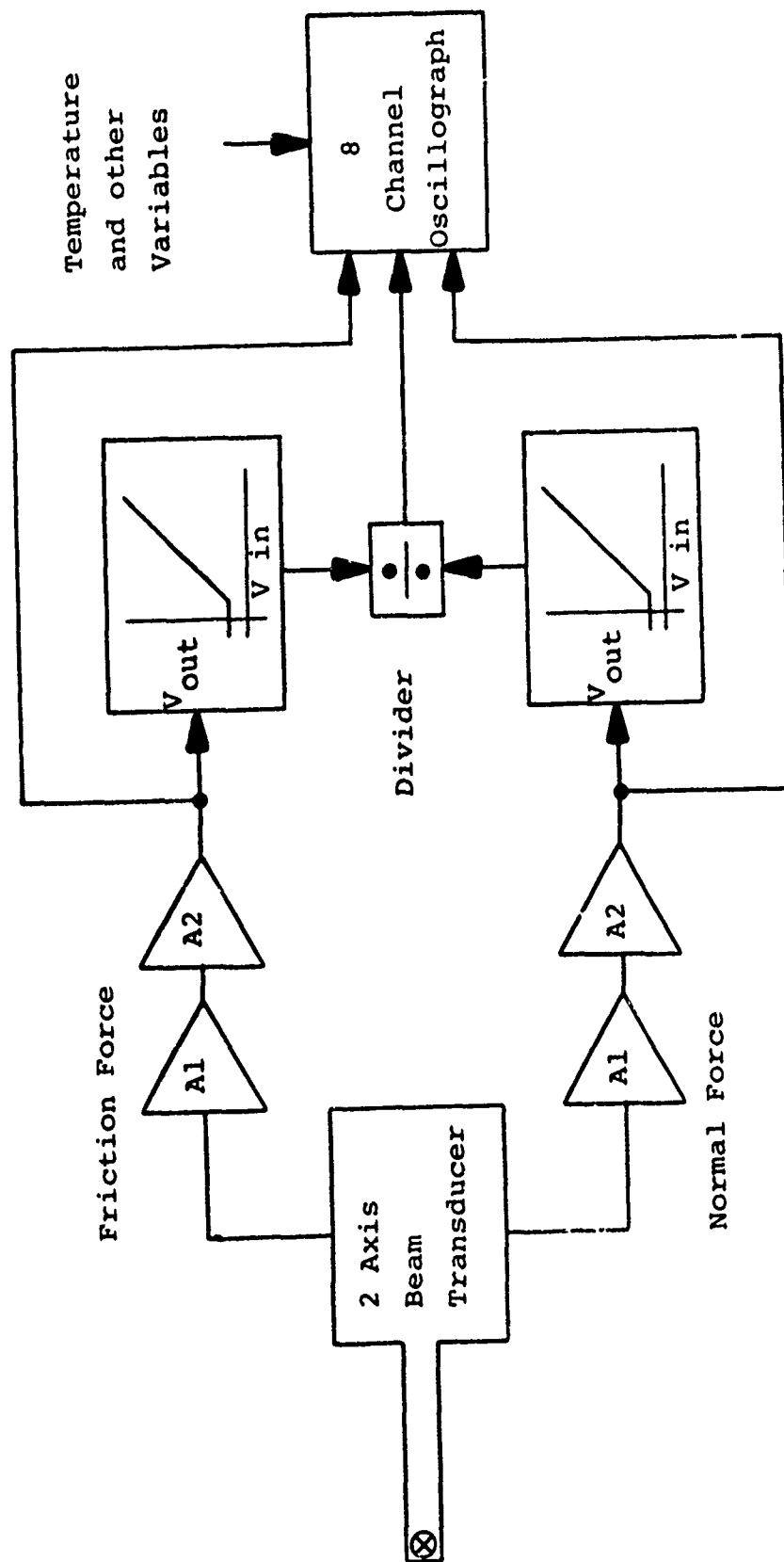
Figure A8. Block diagram of the amplifier and divider circuit

A3. TEMPERATURE MEASUREMENT

The importance of accurately determining the interfacial sliding temperature during a test lies in the fact that a molten fluid layer is expected to affect· friction and wear characteristics. Hence it is of interest to see if the melting temperature of one of the sliding surfaces is in fact reached. The melting range of materials in question is quite small, and a purely theoretical approach (Appendix F) is not likely to yield a credible quantitative result. A satisfactory method of measuring temperatures around 1000°C would be acceptable as gilding metal melts in this range. Temperature information about other materials would be useful but efforts have been concentrated on gilding metal.

A) THERMOELECTRIC METHODS

A method which has been tried involves using the pin specimen and the disc as two elements of a thermocouple. This is a very simple method to implement and one which would seem to give accurate results. To electrically contact the disc it was necessary to fit a slip ring to the rotating shaft. There is a high electrical resistance through the ball bearings and electrical contact cannot be made through the engine block. The transducer platform had to be electrically isolated from the rest of the apparatus. In practice, two things present

difficulties. The first is the electrical noise experienced during sliding and the second are the problems associated with thermocouple calibration. The full scale thermocouple output is on the order of a few millivolts, and during sliding whenever interfacial junctions are broken and formed the EMF output jumps abruptly. If the pin is not contacting the disc there is a large induced voltage of tens of volts appearing on the thermocouple leads. This can be reduced significantly by a shunting resistor across the thermocouple leads at the measuring instrument, but even with a 50 ohm resistor the noise is a few millivolts. This output can be filtered, and this problem can be reduced to manageable proportions. A suitable thermocouple circuit is shown in Figure 9. 60 cycle pickup can be subtracted out from the DC signal component. The second difficulty is more of a problem.

In order to obtain a temperature from the thermal induced EMF it is necessary to refer to calibration tables for the materials used. Unfortunately, 4140 steel and any other metal is not a standard thermocouple pair, so calibrations had to be performed. 4140 steel wire of .05 inch diameter was machined and swaged from 5/16 inch rod. Pin materials which could easily be swaged from larger stock were similarly reduced. Low melting point materials were melted and drawn up fine pyrex tubing with a vacuum to make wire. Zinc, which is brittle, was formed into wire the same way. Calibration
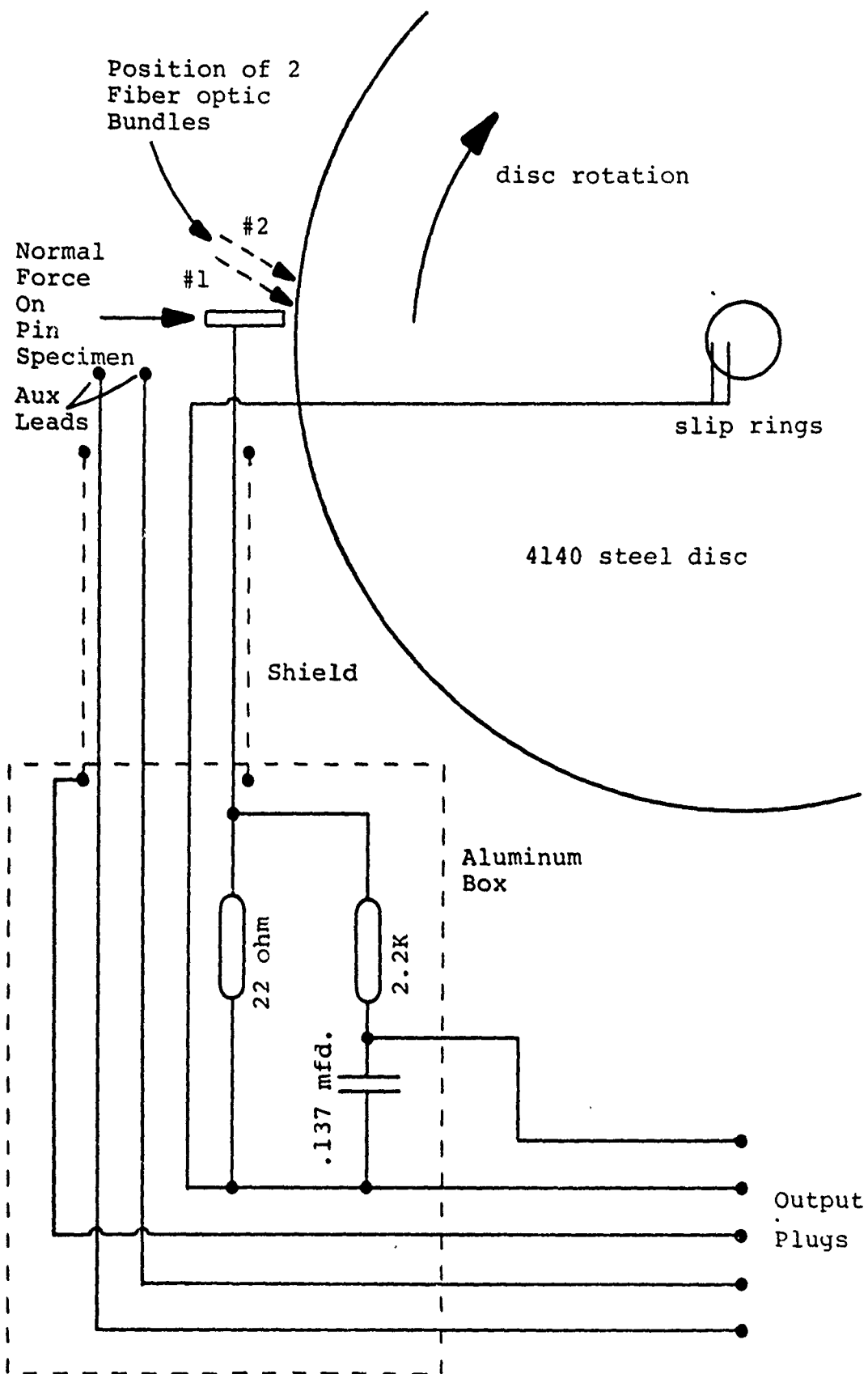
Figure A9. Thermocouple circuit with fiber optic placement

thermocouples were then made. A standard chromel-alumel thermocouple was placed in thermal contact with the pair being tested to indicate the actual junction temperature. The two thermocouples were then heated in an electric furnace. Cold junctions were used for both thermocouples, and their outputs were put into an X-Y recorder to give an EMF versus temperature (chromel-alumel millivolts) plot. Usually the calibration did not melt the test materials so the plot was produced upon cooling to minimize electrical noise from the furnace.

Plots of 4140 steel versus gilding metal, copper, 70-30 brass, constantan, and zinc are shown in Figures 10 through 14. A gilding metal-4140 thermocouple has a parabolic EMF output which peaks considerably before the gilding metal melts. With the exception of constantan, the same is true of the other materials tested.

It is generally true that all thermocouple materials exhibit parabolic temperature-EMF relationships (7). The governing equation is of the form

$$E = C_1(T_1 - T_2) + C_2(T_1^2 - T_2^2)$$

where E = millivolts

T_1 = measuring junction temperature, $^\circ F$

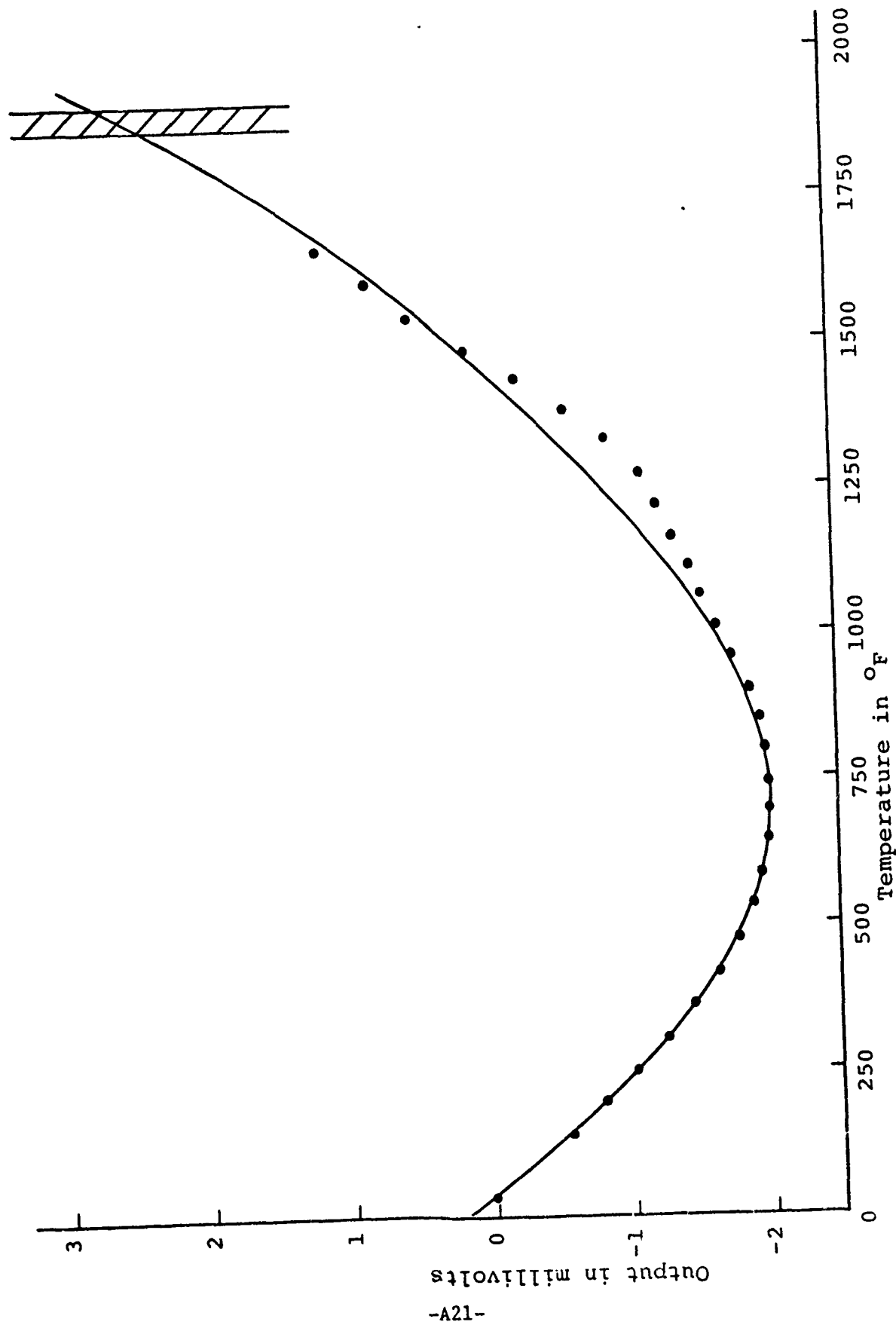T_2 = cold junction temperature, $^\circ F$

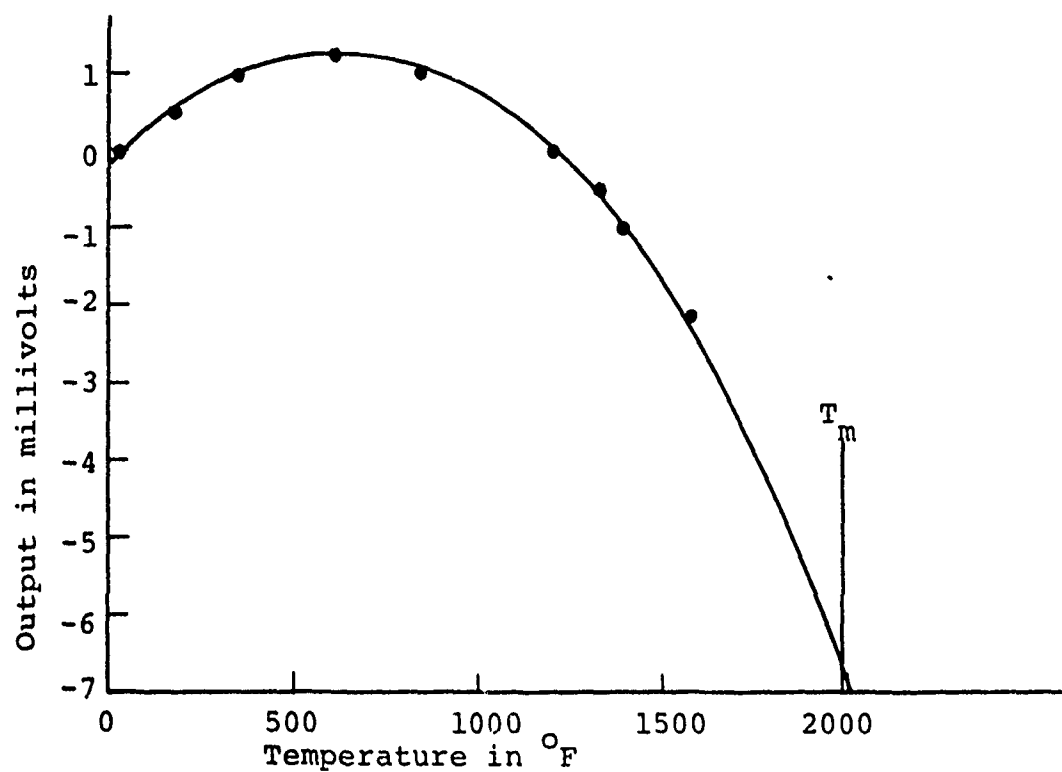Figure A10. Gilding metal-4140 thermocouple calibration

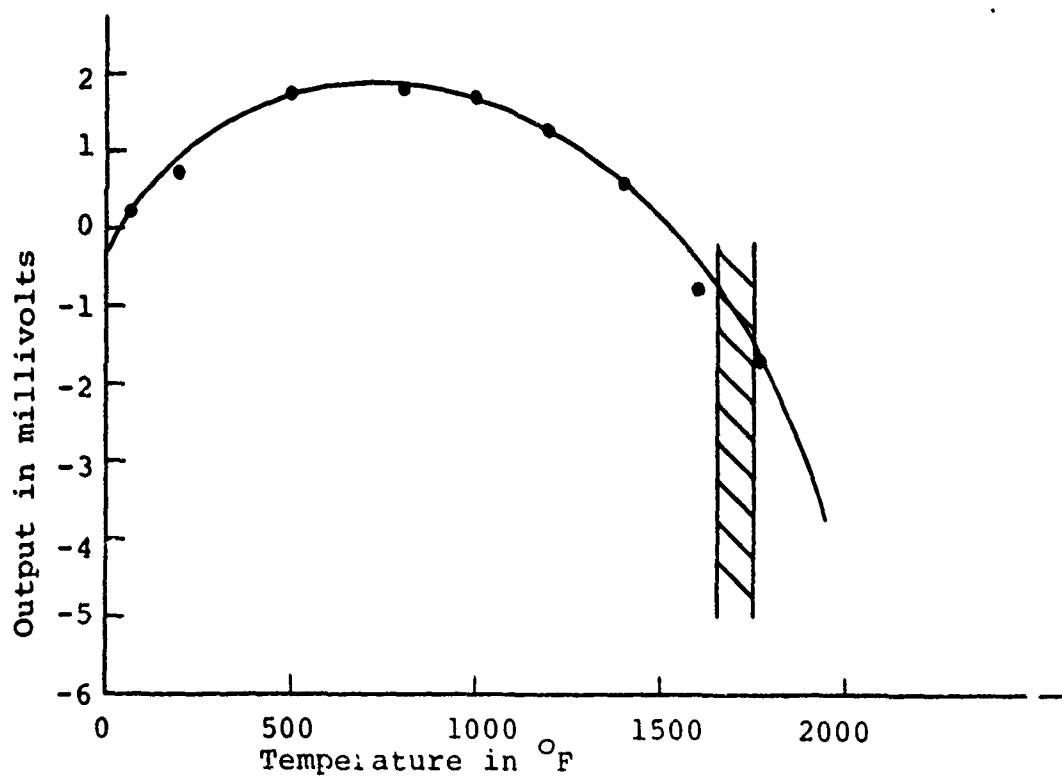Figure A11. Copper-4140 thermocouple calibration
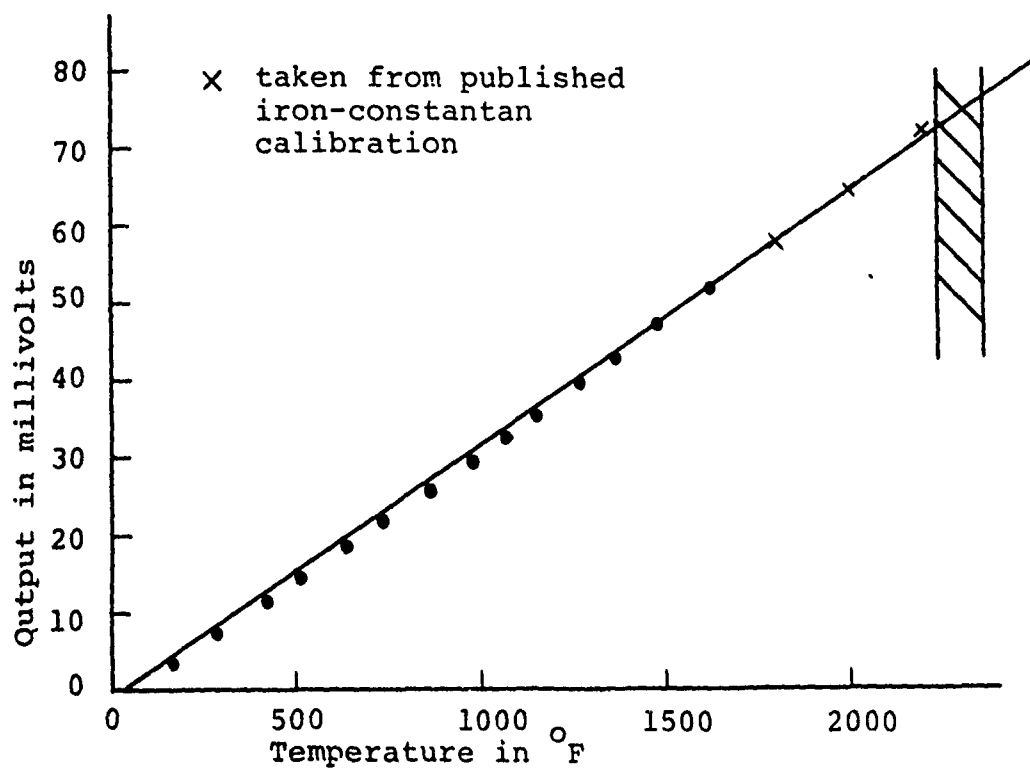

Figure A12. 70-30 Brass-4140 thermocouple

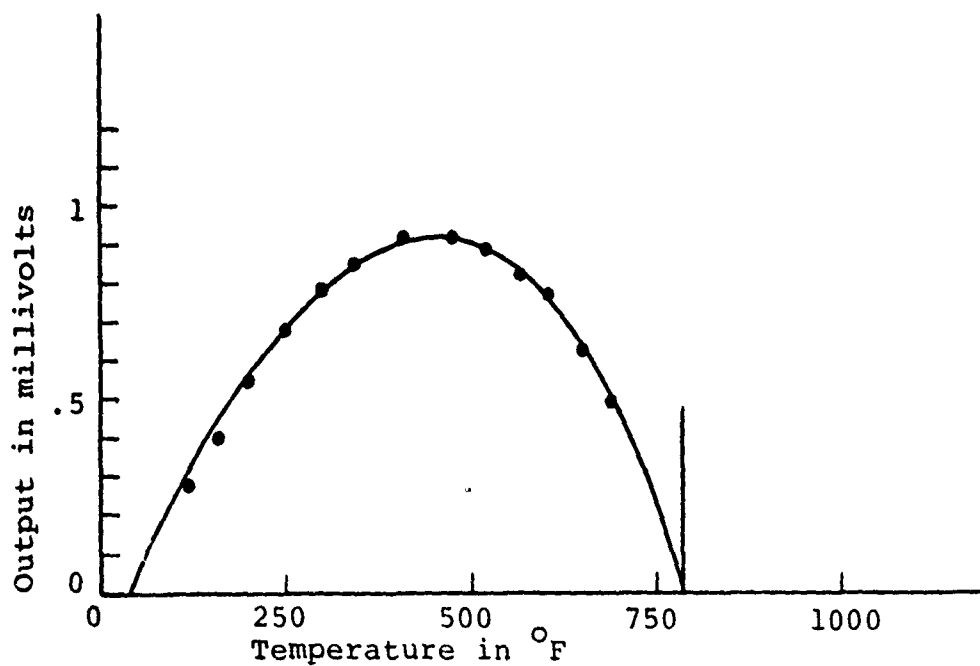Figure A13. Constantan-4140 thermocouple calibration

Figure A14. Zinc-4140 thermocouple calibration

The values of C_1 and C_2 are characteristic of a specific pair of thermocouple materials. C_1 is the result of the Peltier EMF and C_2 results from the Thomson EMF. A gilding metal-4140 thermocouple gives (from the calibration curve)

$$E = -.0058(T_1 - T_2) + .000004(T_1^2 - T_2^2) .$$

In general, thermocouple materials are not used in the range where they have zero slope. In this region they have a very low voltage-temperature output and an indicated EMF corresponds to 2 different temperatures. The material combinations of interest here cannot be optimized in regard to their operating region.

The result is a temperature-voltage relationship which is well defined for a single thermocouple junction at a roughly known temperature but which is unknown for a sliding interface. In sliding there are junctions at many different temperatures and they all get averaged together in the output. Even if the EMF output were not parabolic with temperature it would not be straightforward to say what the interfacial temperature was. If it is assumed that all the junctions are at one temperature, interpretation of the EMF output is straightforward. Otherwise, the junction is a problem in applied statistics and probability. If some other means of measuring temperature were available, a calibration of a sliding thermocouple could possibly be made as long as test conditions were not varied. This would ensure identical

junction characteristics. Without a calibration or some statistical supporting evidence a disc-pin thermocouple is not likely to yield very accurate results.

A.3.B) RADIATION THERMOMETRY

A more promising method of temperature measurement towards which considerable effort has been made uses optical pyrometry techniques. For any given temperature objects emit radiation of a well defined spectrum and intensity. The total radiant energy emitted by an object is given by the Stefan-Boltzmann law to be (24):

$$W = \varepsilon \sigma T^4$$

where W = radiant power emitted per unit area (watts/cm^2)

ε = emissivity

σ = Stefan-Boltzmann constant (5.673 X 10^{-12} watts/cm^2°K^4)

T = absolute temperature (°K)

In words, the Stefan-Boltzmann law states that the power radiated by a physical body is directly proportional to the fourth power of its absolute temperature. The chart of Figure 15 plots temperature versus radiance which is defined as intensity radiated per unit projected area of source per unit solid angle.
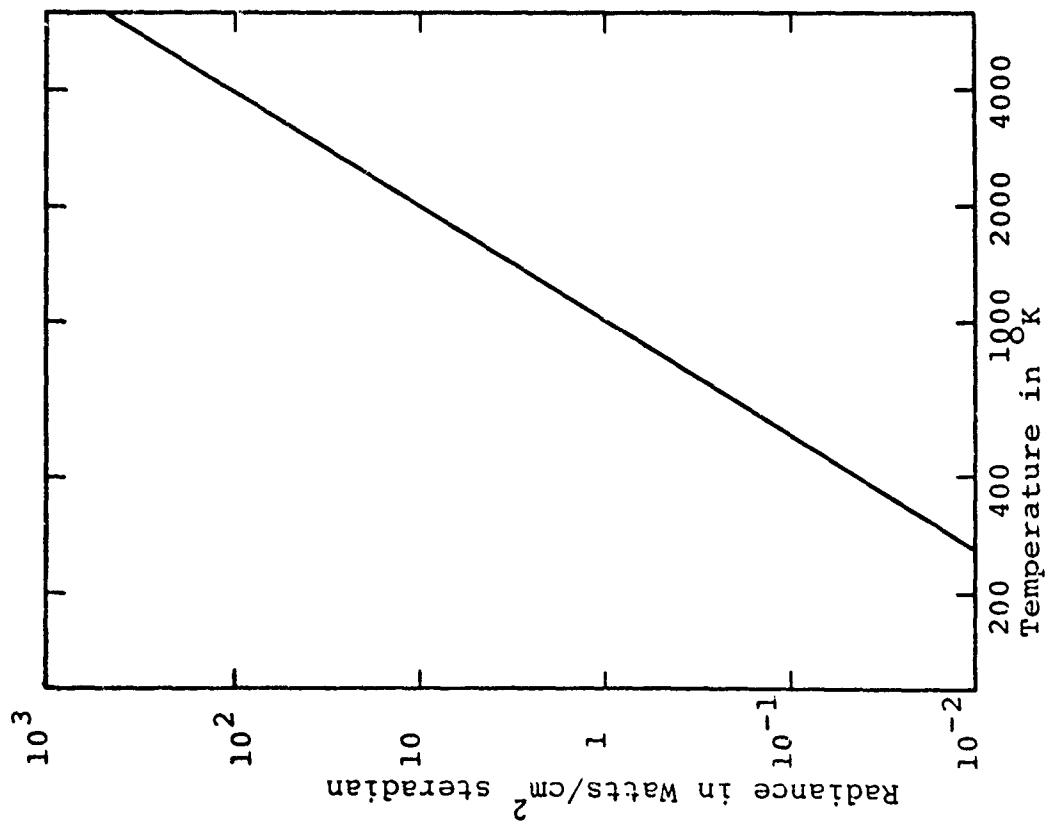
Figure A16. Spectral energy distribution for 4 different temperatures

Figure A15. Total radiant energy output versus temperature for a black body

The spectral radiant energy distribution for a black body is given by Planck's radiation equation (7)

$$W = C1/\lambda^5(e^{C2/\lambda T} - 1)$$

where W = hemispherical spectral radiant intensity, watts/$(cm^2$-micron)

C1 = 37,413, (watts-micron^4)/cm^2

C2 = 14,388, microns-$^\circ$K

λ = wavelength of radiation, microns

T = absolute temperature of blackbody, $^\circ$K

The distribution takes the form shown in Figure 16, with the peak for each curve determined by Wein's displacement formula (10),

$$\lambda_m T = 2893 \text{ micron degrees.}$$

As temperature increases, the peak of the radiation shifts steadily towards shorter wavelengths.

The total radiant power emitted by an object depends markedly on the emissivity of the object. The uncertainty with which the emissivity is known is one problem in radiation pyrometry. If the total radiated power from an object is measured, and if its emissivity is known, it is possible to accurately determine its temperature.

In the temperature range we are working in (greater than 25°C) a lead selenide detector (9) closely covers a large

part of the spectral energy emitted (Figure 17). It essentially measures total radiant power. The detector output is non-linear (varies as T^4) but this is not a problem. The difficulty is that the emissivity of the system in question could vary from .1 to .8. With a lead selenide detector the indicated temperature would vary several hundred degrees. This is unacceptable, but there are solutions.

Two-color pyrometers (24) can be used which are based on the principle that the ratio of radiation emitted in two narrow frequency bands is independent of emissivity but dependent on temperature. For example, if the emissivity is 1 an object could emit 10 units of energy at wavelength A and 5 units of energy at wavelength B. If the emissivity goes down to .1, there is 1 unit of energy at A and .5 units at B, but the ratio is the same. This pyrometry technique is essentially emissivity independent. However, it is expensive and it would have been difficult to make a satisfactory unit. Instead, a pyrometer which is emissivity insensitive was designed and built. It is relatively simple and is described in detail.

The brightness of a hot object increases with temperature much more rapidly than does the total radiation which it emits. Between 1000°C and 1500°C the brightness increases about a hundred times while the total radiation increases by a factor of less than four. The brightness
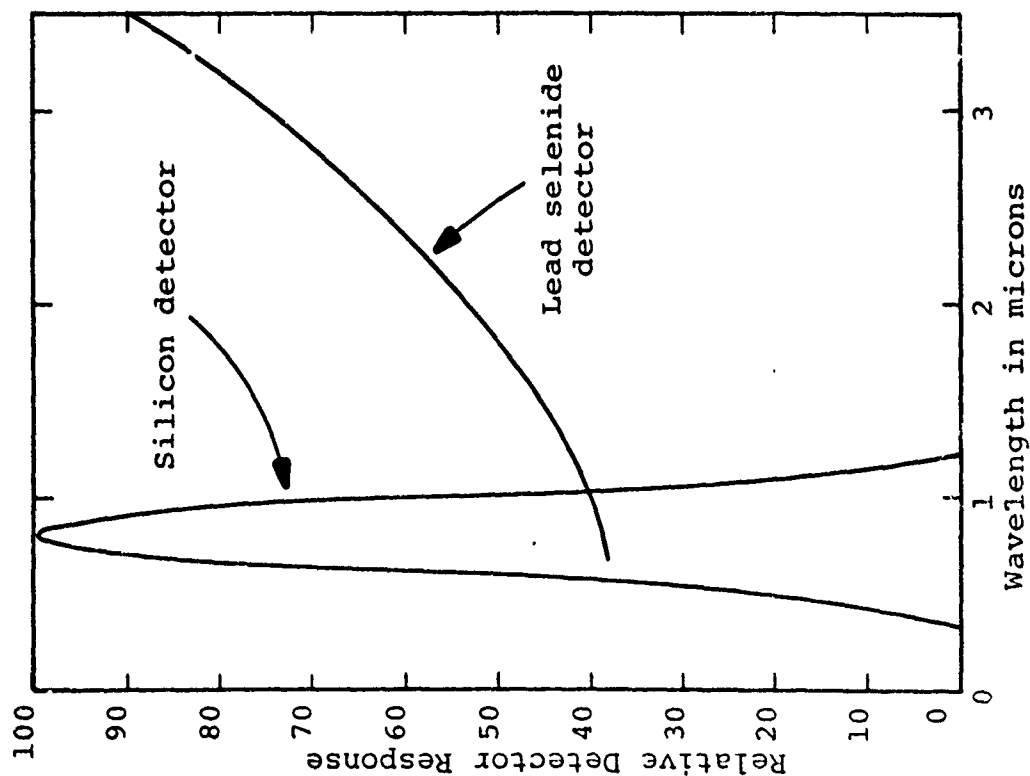
-A28-

Figure A18. Variation in intensity of total and short wavelength energy

Figure A17. Spectral sensitivity of silicon and lead selenide detectors

corresponds to short wavelength radiation, which is a much more sensitive measure of temperature than the total radiation.

This feature is illustrated in Figure 18 in which the changes in intensity of total radiation and of short wavelength radiation over a small range of temperatures are compared. If the radiation R is reduced to ER, as by a change in emissivity, the temperature indicated by a total radiation pyrometer will drop to T1. But if the pyrometer only measures short wavelength radiation, the indicated temperature will drop much less, to T2.

In words, the total radiation from a body varies in proportion to the 4th power of temperature and the short wavelength radiation varies in proportion to a higher power of temperature (2). If use is made of a silicon phototransistor, one of the cheapest and most common photodetectors available, its output around 1000°C varies in proportion to the 13th power of the absolute temperature. In consequence, a 13% change in output due to some cause, say a change in emissivity, results in only a 1% change in indicated temperature. It is therefore emissivity insensitive.

The spectral sensitivity of a silicon photodetector (21) is shown in Figure 17. It responds only up to 1.2 microns and in general an object below 600°C does not have

sufficient short wavelength radiation to be measurable. For this reason, a silicon detector has a 600°C lower limit on temperatures it can measure. There is no upper limit, but output changes so rapidly with temperature that only a few hundred degrees Centigrade can be accommodate on any scale. The pyrometer built using a silicon phototransistor has a calibrated output-temperature curve shown in Figure 19. Two distinct values of emissivity were plotted along with an "average" value of .4. The lower value of the scale can be easily increased.

Radiation was transmitted to the sensor via a two foot length of glass fiber optics .062 inch in diameter. The fiber ends have an acceptance angle of 60 degrees and can be positioned very close to the object whose temperature is to be measured. As long as all the area within the 60 degree cone of vision of the fiber bundle is at the same temperature the distance away from the fiber end is irrelevant. In calibration, the ends of the bundle, which are encased in a metal tip, were placed in a water-cooled holder so they would not overheat. The target temperature reached 950 degrees Centigrade and it was .5 inch away from the fiber end.

Plastic fiber optic bundles cannot be used because they transmit radiation in the wavelengths of interest very poorly and also because they might melt upon calibration. The glass fibers used respond up to 2 microns, and it is difficult
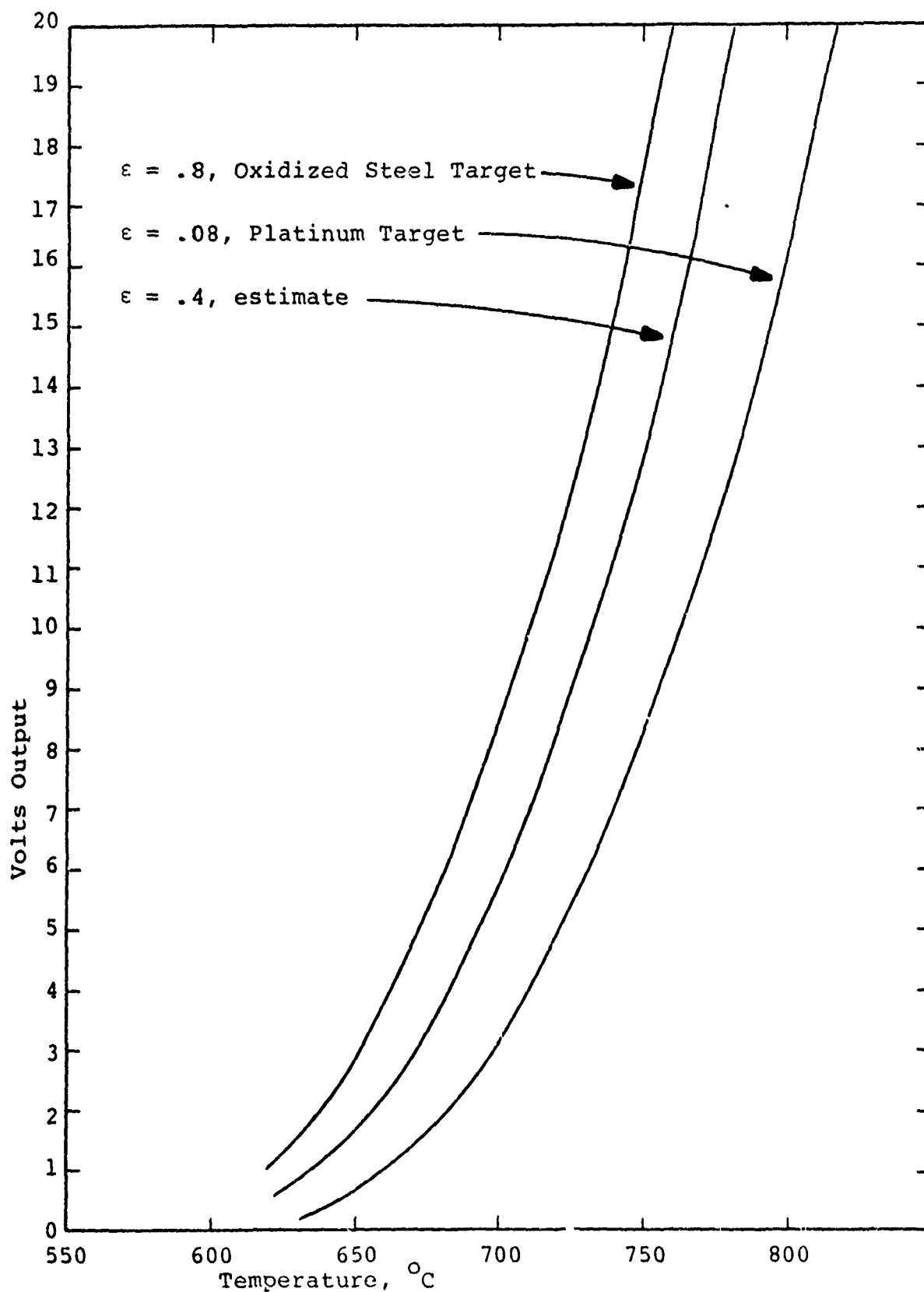
Figure A19. Optical pyrometer calibration

-A32

to obtain fibers that will transmit longer wavelengths than that.

A typical response time of the silicon pyrometer is 10 microseconds, fast enough for any tests conducted. The output is noise free and very stable. A schematic is shown in Appendix G.

A.4 WEAR MEASUREMENT

Measuring the wear of a test pin is a very simple procedure requiring the weighing of the pin before and after a test. A Mettler H15 balance is used for this purpose. It has a .1 milligram accuracy. The pin is easily removed from the transducer unmarred by loosening one screw. If it is desirable to measure the weight loss of the disc after a test, it is necessary to weigh a 30 pound disc to an accuracy of milligrams. This can be done, but it is not a simple procedure.

An extremely precise high capacity balance is located in the Gage Laboratory at MIT. It can be used for weights up to 100 pounds, although its sensitivity decreases with increasing weight. With a disc and holder combined weight of approximately 30 pounds it is possible to discern a 5 milligram weight change, or one part in a few million.

The necessity of cleaning the disc before each weighing is important and for reproducibility any paint that was on the side of the disc has to be removed (paint was needed for the optical tachometer). There are also some threaded holes on the sides of the disc which should not contain small amounts of moisture or degreaser. One-tenth of a drop of water weighs 5 milligrams.

After a test with gilding metal (brass), there is a substantial amount of brass smeared onto the disc. This would represent a large weight gain, and it is necessary to remove the brass completely to determine how much of the steel has worn away. This can be done with a solution of 5 parts ammonium hydroxide and 3 parts hydrogen peroxide (100) which dissolves the brass and does no harm to the steel. Reverse electroplating in an alkaline solution might also work but is more dangerous, difficult, and likely to disturb the steel disc. The necessity of having to remove brass indicates that there was a significant amount of brass to brass contact during a test, but initially the steel would have been worn.

After the disc is cleaned and the test material removed, it can be weighed. Problems arising from the moisture absorption of the PMMA disc holder were not realized until many tests were conducted, after which an aluminum holder was made. It seems that after the handling, metal removal, rinsing, and degreasing the accuracy to which the weight loss can be determined is only plus or minus 15 milligrams. Rust and residual moisture seem to present the most difficulty, as a two and one-half square foot area of clean steel with internal threads and mounting holes is susceptible to contamination. Since a typical weight loss is on the order of the weighing accuracy or less, it is difficult to draw conclusions on disc weight loss. If sizable amounts

of disc wear could be produced, the weighing errors would be minimized. The balance is shown in Figure 20.

There is another method of measuring disc wear which has not yet been tried but which seems promising. If an accurate profile of the disc edge can be taken before and after a test, the wear volume can be easily calculated knowing the circumference of the disc. It is assumed that the worn profile is the same all around the disc, and this is probably not an inaccurate assumption. The profile can be taken on a "Talysurf 4" surface measuring instrument which is in the Gage Laboratory at MIT. It produces a graphical presentation of the surface in question, magnified up to 100,000 times vertically and 100 times horizontally. This would mean that a .2 inch section of the disc edge could be examined and a 20 inch long chart would be produced with all the hills and valleys of the disc edge. If a wear track 5 microinches deep by .02 inch wide were produced, the vertical deflection on the graph would be .5 inch and the wear could be computed to be .5 milligram. The accuracy of this method would be much higher than that obtained through direct weight loss measurement, although the brass would still have to be removed. A picture of the Talysurf 4 with the disc is shown in Figure 21..

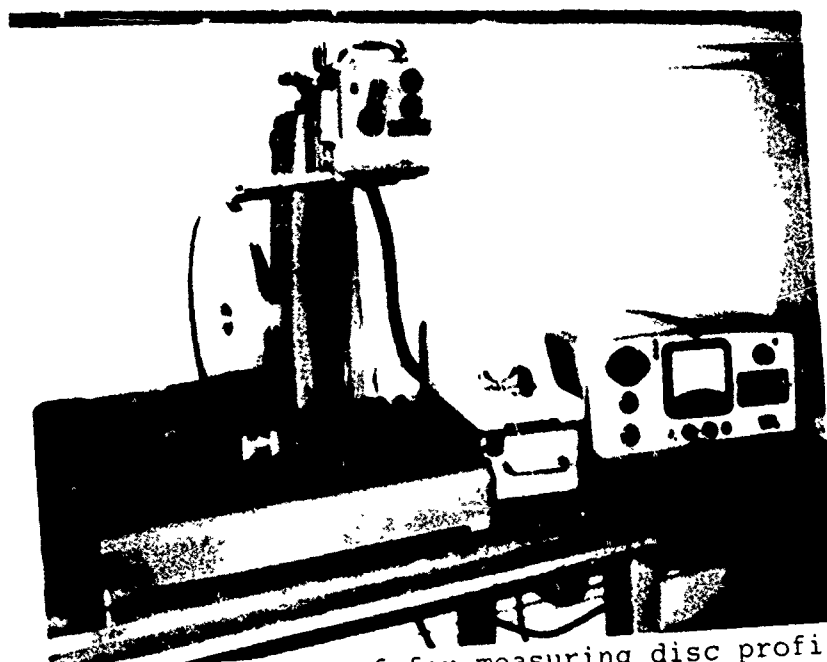Figure **A20.** View of balance used to weigh disc

Figure **A21.** Talysurf for measuring disc profile

A.5 DATA ACQUISITION

A high speed recording instrument was necessary to provide a record of test results. The number of independent recording channels deemed necessary was four, but more channels would have been desirable. After some investigation, a used Sanborn model 4500 oscillograph was purchased. It was equiped with 8 recording channels although provisions for a total of 24 channels were included. A corresponding set of 8 medium gain and 8 low gain amplifiers were also obtained. All the recording instrumentation was mounted on a movable 19 inch panel rack.

Light beam oscillographs produce a permanent copy of data on light sensitive paper. They utilize the movement of a very small glass-enclosed mirror which reflects ultraviolet light onto the paper. The mirror is actually a band of metal through which an electric current is passed. It is in a magnetic field and the torque resulting from the current (V X B) moves the band and therefore the reflected light spot. There has to be one mirror, called a galvanometer, for each channel.

Due to the naure of the device, there are no large masses to move and the oscillograph has a frequency response at 3 kilohertz that is down 3 db (.707 of the input signal). The 8 inch wide paper can move at speeds of .25 to 100 inches

per second (ips). After the data is recorded, it takes a
minute for the result to appear on the paper. The recording
darkens with light and when not in use it should be stored in
a light-proof box.

AIII. TEST PROCEDURES

Specimens for testing are usually made .125 inches in diameter and from .15 to .8 inches long. They are solvent degreased before use and are weighed to the nearest tenth of a milligram.

The disc preparation starts by abrasion with 120 grit emery cloth at the lowest rotational speed. 240 grit emery is then used, followed by wiping with a paper towel wet with trichloroethylene. The paper towel should remove any abrasive particles and leave the disc clean on a macroscopic level. If the disc is weighed before testing it should be cleaned first. The basic function of the emery cloth is in the removal of specimen material from the disc. There is often a large buildup of adhered material, and if there isn't only 240 grit emery is necessary.

The pin specimen contacts the disc slightly above its horizontal centerline. This reduces the likelihood of stick-slip frictional vibrations. These vibrations are more likely to occur if the pin makes contact below the centerline.

The amplifiers and instrumentation should be on for a few hours for them to reach thermal equilibrium. They can be used immediately after being turned on but they drift considerably. In any case each amplifier used in the

oscillograph is calibrated and zeroed, and the strain gage amplifiers are zeroed. The divider has no adjustments to be made. Calibration of the force transducer is done with a mass and pulley system but is not necessary for each test. Calibration depends on resistor ratios in the amplifier circuitry and they are not usually changed. Zeroing all amplifiers takes only a few minutes.

The air pressure should be set to the desired value; 24 psi is used for most tests. The disc motor is activated, and then the clutch is engaged. The speed is increased to the desired value as indicated on the optical tachometer. If the specimen is to traverse the disc edge the platform motor is turned on to initiate a test, otherwise the solenoid is switched manually on and off. Solenoid switching is done by microswitches during a traversing test. Usually a chart speed of 5 or 10 ips is used, and a test lasts a fraction of a second. Friction force, normal force, coefficient of friction, and pyrometer outputs gradually appear on the recording, which is then stored until it can be analyzed.

FRICTION RESULTS

The classical friction law states that friction force is proportional to normal load L

$$F = fL$$

where f (friction coefficient) is the proportionality constant (15). The value of f is said to be independent of the apparent area of contact and of the sliding speed. Were this the case, friction data taken at low speeds would be applicable to high speed situations.

In actuality f is not independent of sliding speed, and it depends somewhat on the apparent area of contact. Both of these statements are based on changes in material properties which occur at high sliding speeds. The principal change is in hardness which comes about through large temperature rises. Taken to the limit, hardness goes to zero at melting and friction may be governed by hydrodynamic fluid lubrication. Some work has been done on hydrodynamic lubrication at high sliding speeds (26). The results indicate that fully hydrodynamic lubrication does not occur until a non-dimensional bearing pressure, W^*, is greater than about .2:

$$W^* = \frac{W}{L \; x}$$

where   w = load per unit width

        L = volumetric latent heat

        x = length of slider

Values of W^* below .2 indicate that the leading edge
of the slider is not lubricated by liquid metal. In all tests
run W^* was usually less than .002. This does not indicate
that melting did not occur, but it explains friction values
which are not as low as those obtained in, say, journal
bearings.

Figures 22 through 32 show friction coefficient as a
function of sliding speed for the materials tested. The
normal load was approximately constant at 5 lbs and the pin
diameter was either .25 inches or .125 inches. The pin size
was changed to accomodate smaller available samples and is not
expected to have changed friction results appreciably.

Work on the problem of projectile friction in gun
tubes has been conducted (8, 12, 13, 14, 18, 19, 20). The
results indicate unstable and high f values occurring at the
PV values used in this paper. An explanation to this scatter
has been said to lie in the fact that heat flux (PVf) is not
the sole independent variable in high speed sliding. It
therefore will not give a unique value of friction coefficient
(14). This is certainly true, and the apparent area of the
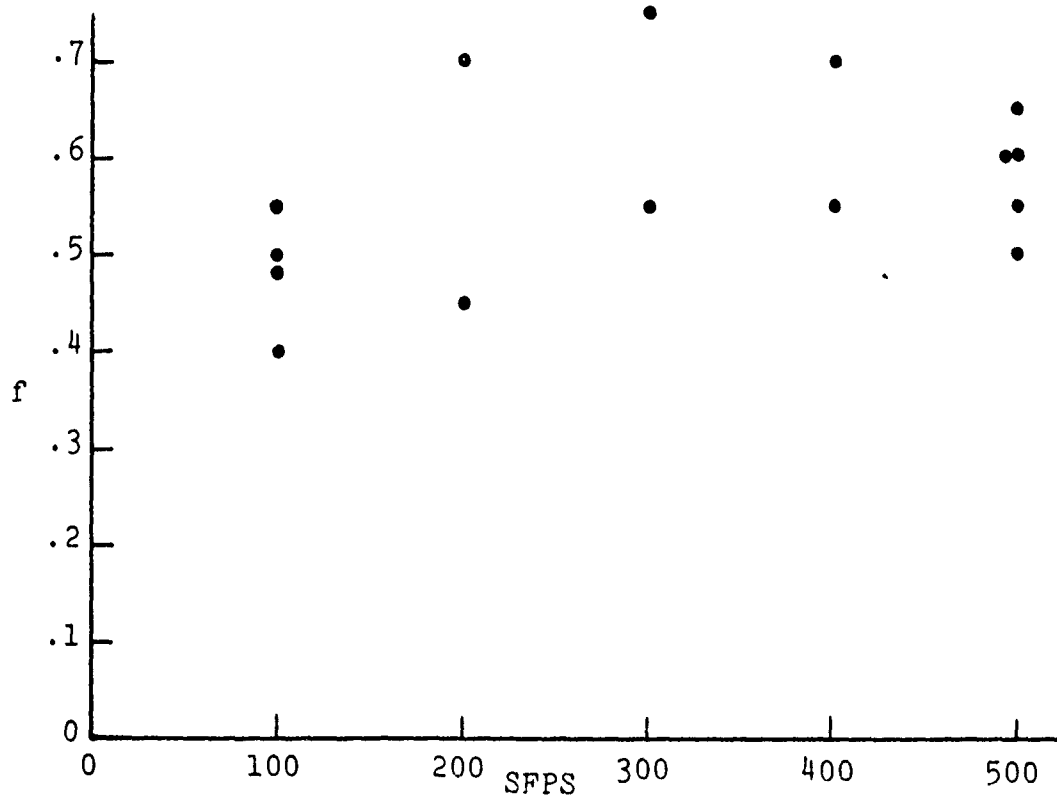sliding contact is probably the most important second
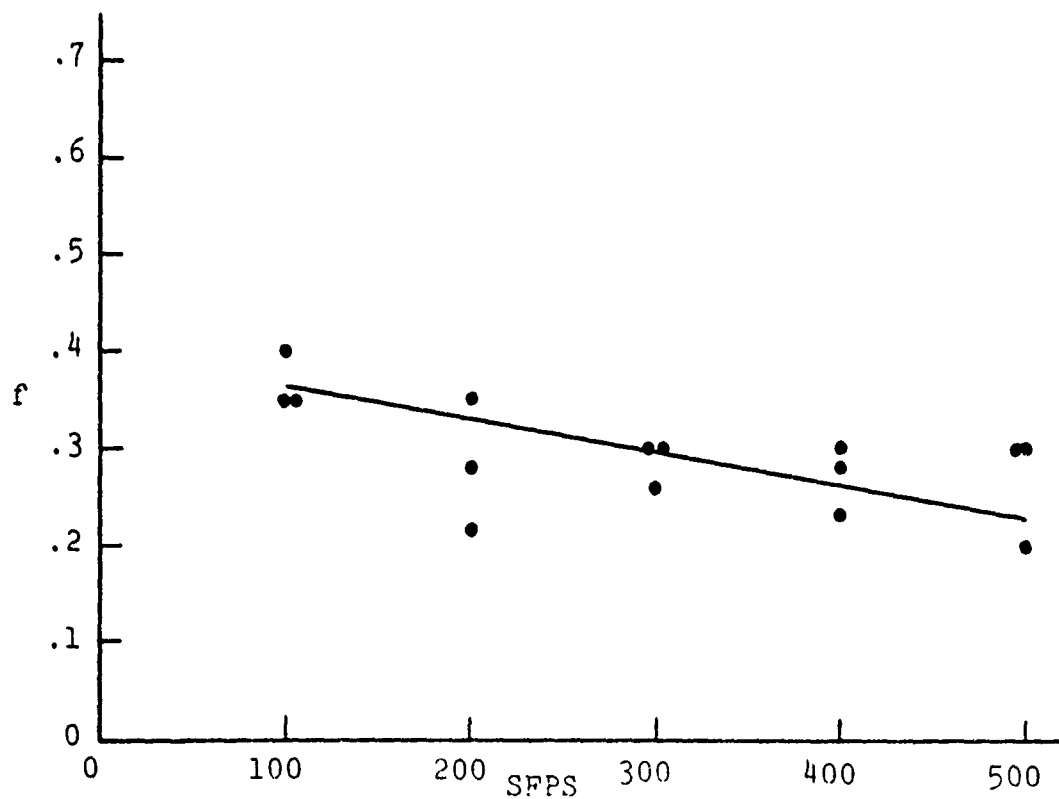variable.

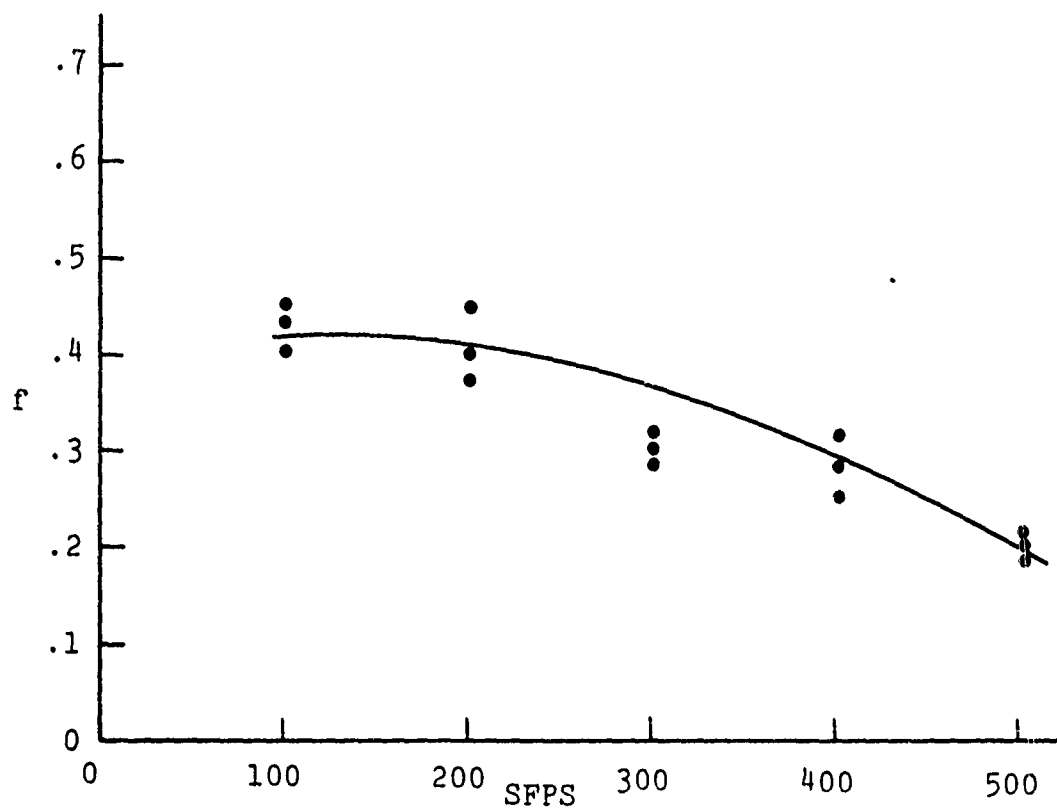Figure A22. Gilding Metal on 4140

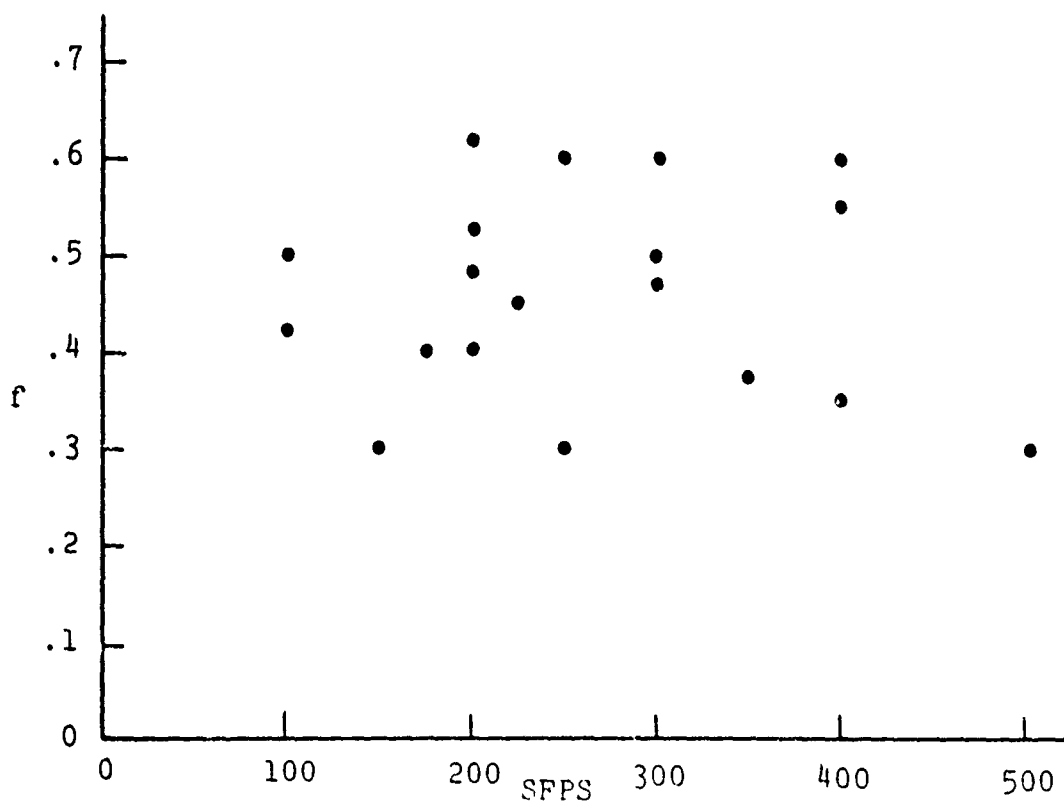Figure A.23. Rulon A on 4140

Figure A24. DQ3 on 4140
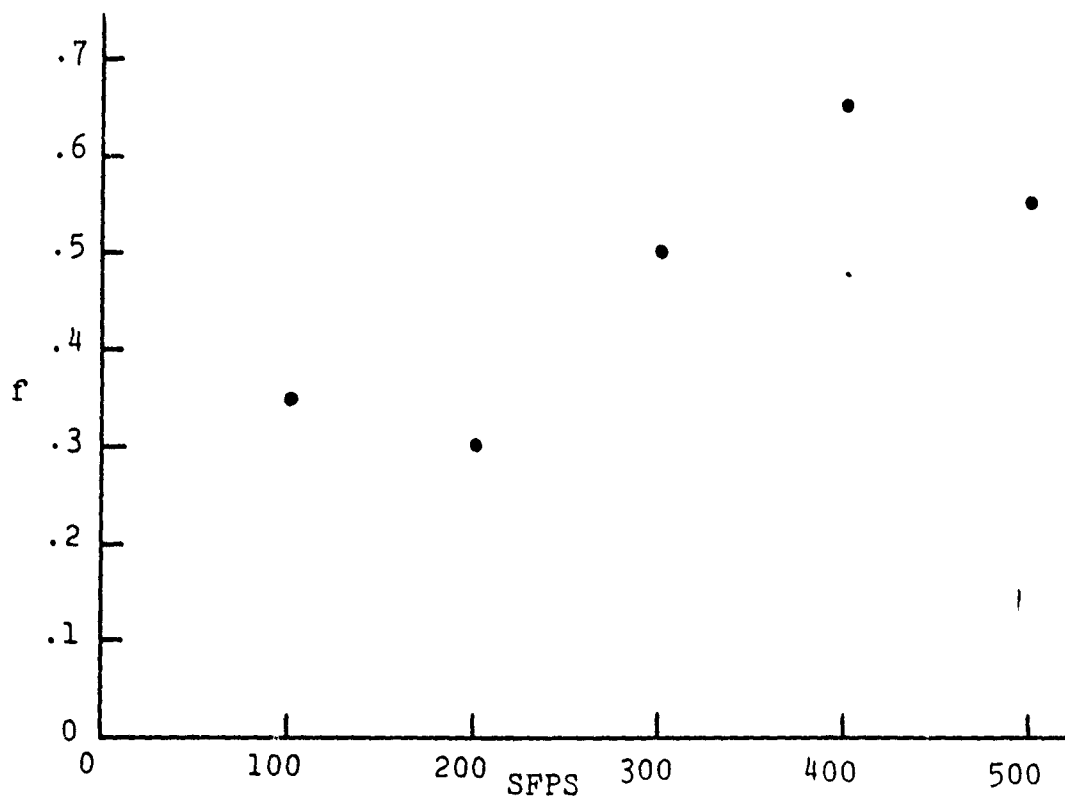

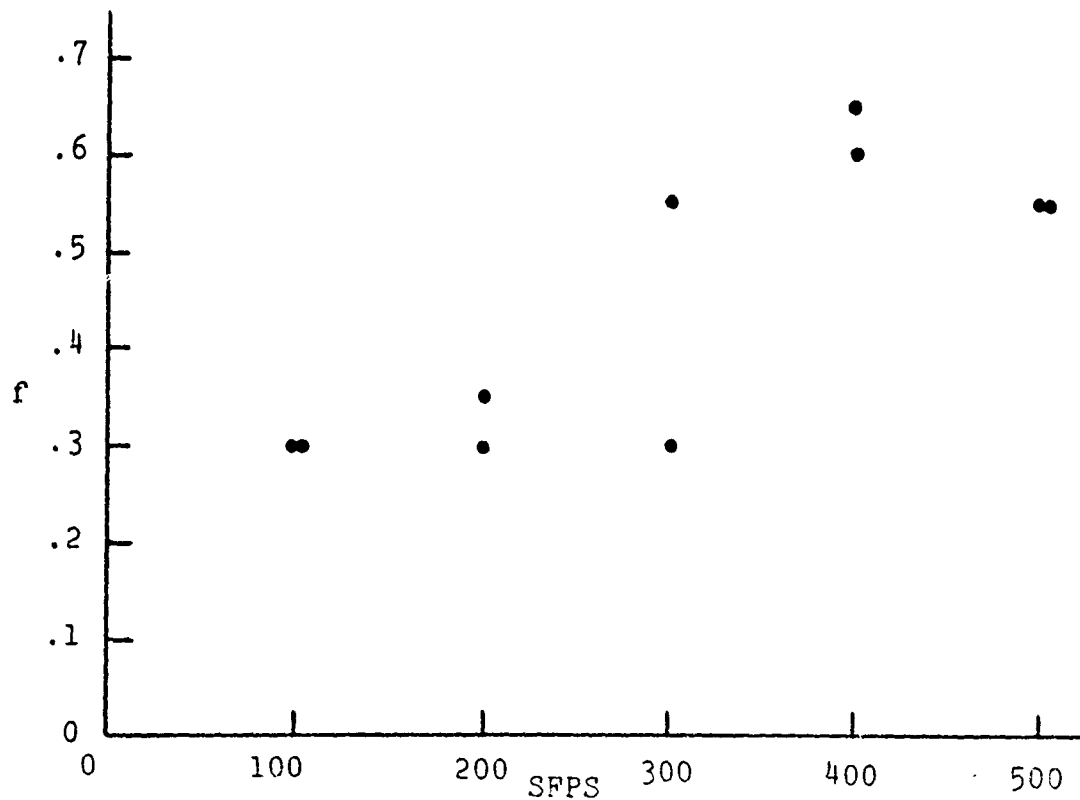Figure A25. Nylon on 4140

A45-

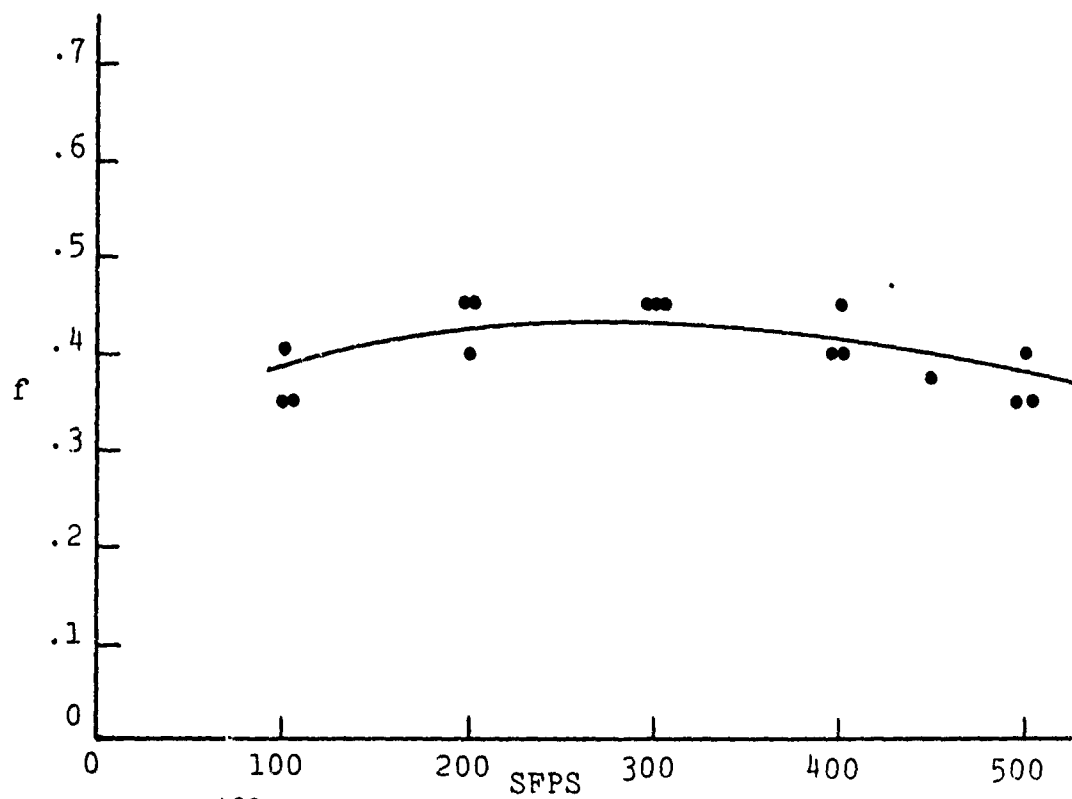Figure A26. Copper-16% Lead on 4140

Figure A27. Copper on 4140

Figure A28. Zinc on 4140
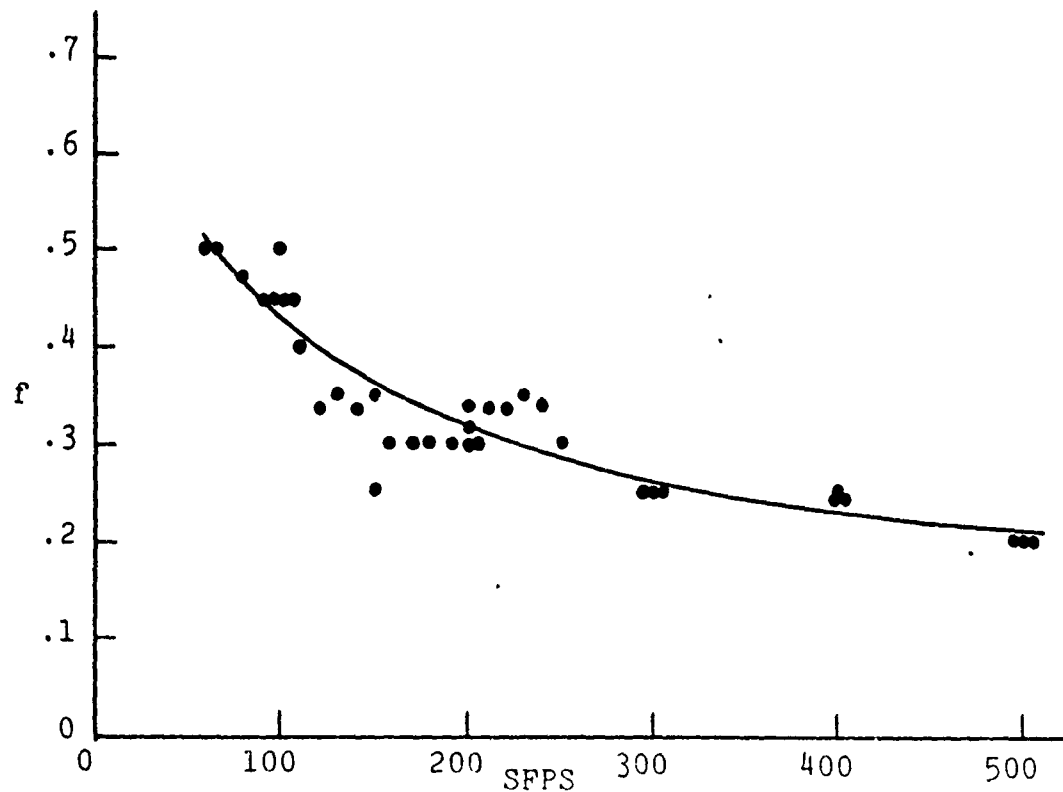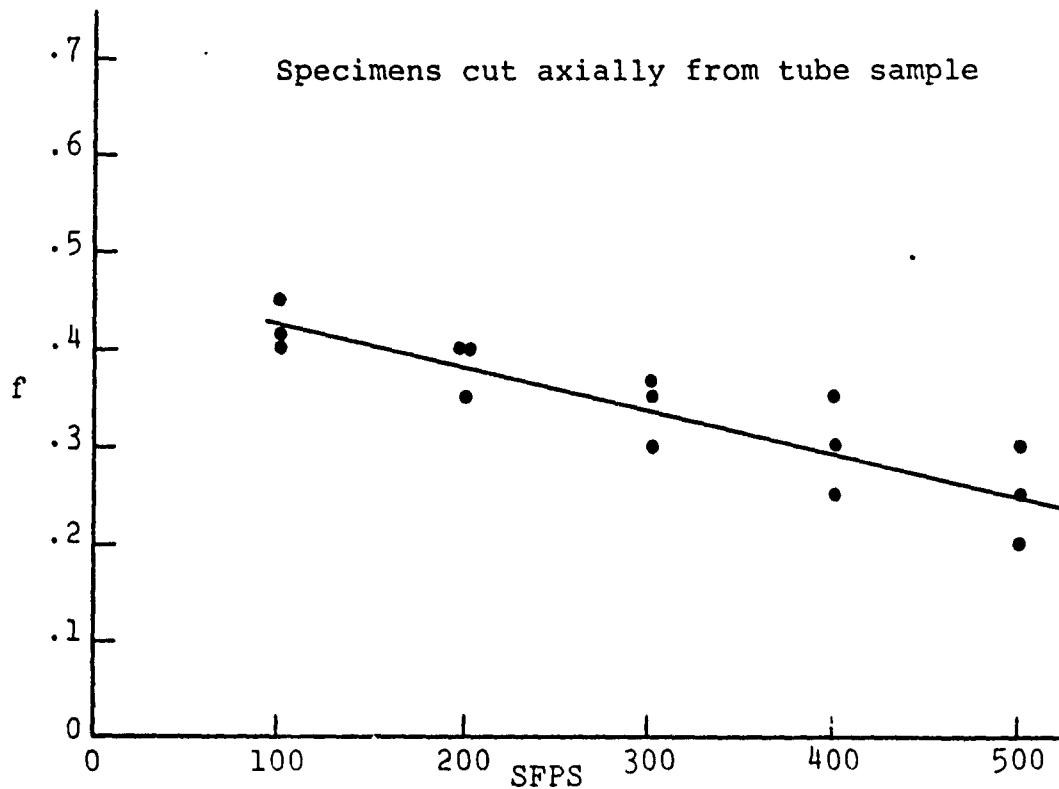

Figure A29. Constantan on 4140

Specimens cut axially from tube sample

Figure A30, National Vulcanized Fiber on 4140
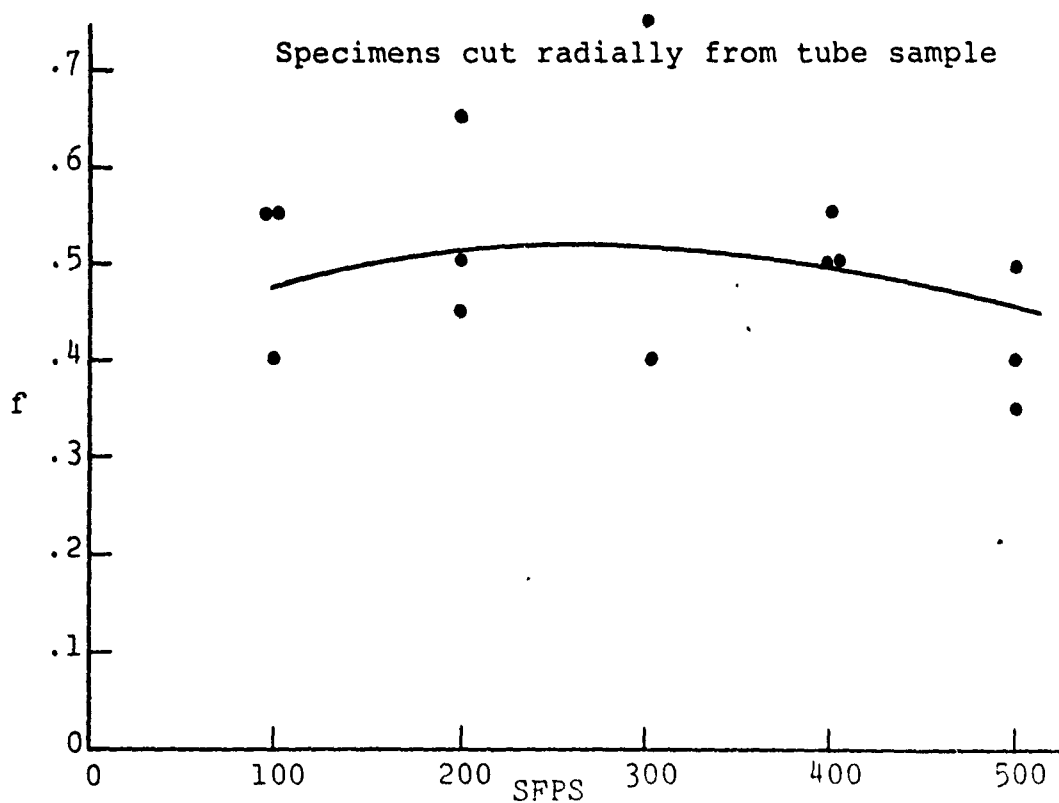

Specimens cut radially from tube sample

Figure A31. National Vulcanized Fiber on 4140

Although there was some scatter in the data presented in this report, most test results were consistent. A reasonably constant apparent area of contact certainly helped. The analog divider was extremely useful in processing test signals and was certainly more accurate than hand-calculations would have been. The accuracy of f calculations can conservatively be estimated as + or - 10 of that indicated in a specific test. Any friction values between .1 and 1 cannot be realistically taken to more than 2 decimal places (example, .35, not .353), and the 2nd place is not usually exact.

Surface layers of oxides and contaminants usually reduce f and can make it difficult to obtain reproducible results. Disc preparation as described in the procedure produced a consistent surface. Some variation in test results occurred when the disc was not abraded following disc weight loss measurements. Even if no visible material were left on the disc, surface conditions are not the same as they are on a freshly abraded surface.

From an applications viewpoint, more situations will arise in practice where repeated sliding occurs. Clean surface test conditions only simulate a device when it is first used. Deciding exactly what to do about this problem is not easy. It would be unfortunate to have accumulated large quantities of data only to discover that much of it had no practical value.

A.IV.2 WEAR RESULTS

There are two possible wear mechanisms that predominate in a high speed sliding system. They are adhesive and abrasive wear. Adhesive wear is characterised by the transfer of material from one surface to another during contact. It occurs because of strong adhesive forces that exist between atoms in intimate contact. There is a fundamental law governing adhesive wear (15):

$$V = \frac{K \cdot L \cdot X}{3 P}$$

where   V = volume worn away

       K = wear coefficient

       X = distance slid

       L = normal load

       P = indentation hardness

K is the probability of forming a wear particle, and it is usually much smaller than one. The value of K depends not only on the parameters in the adhesive wear equation but also upon the material being slid against. For instance, sliding brass against nylon will not give the same K as sliding brass against steel.

The experimental determination of K is not difficult because it is the only unknown in the wear equation. There are some theoretical methods of determining K which depend on

material compatibility and surface energy of adhesion. Of interest here is the change in K with sliding velocity and temperature, for which theoretical methods are not established. The most important variable is probably the change in P with temperature. P goes down as temperature increases, but sliding temperature rises are not well formulated.

Wear coefficients were calculated for almost all of the tests conducted. K is a good characterization of wear rate. Figures 32 through 41 show K versus surface speed on linear or semi-log charts.

K values which differ by a factor of 3 under identical test conditions are common. The very large (10^2) variations in K which occurred for similar tests with gilding metal (brass) have an explanation. During the initial stages of a test gilding metal is smeared onto the steel disc by a process of adhesive wear. The buildup is often as thick as a few mils and it increases with the duration of a test. The sliding of brass on brass versus brass on steel could be responsible for some change in K. However, this does not appear to be the major reason K changes so dramatically. What happens is a change in the wear mechanism occurs: 2 body abrasive wear predominates. The brass is deposited on the disc very irregularly, and the disc is transformed into a metal-cutting "file". There is a large difference in hardness between the

Figure A32. Constantan on 4140
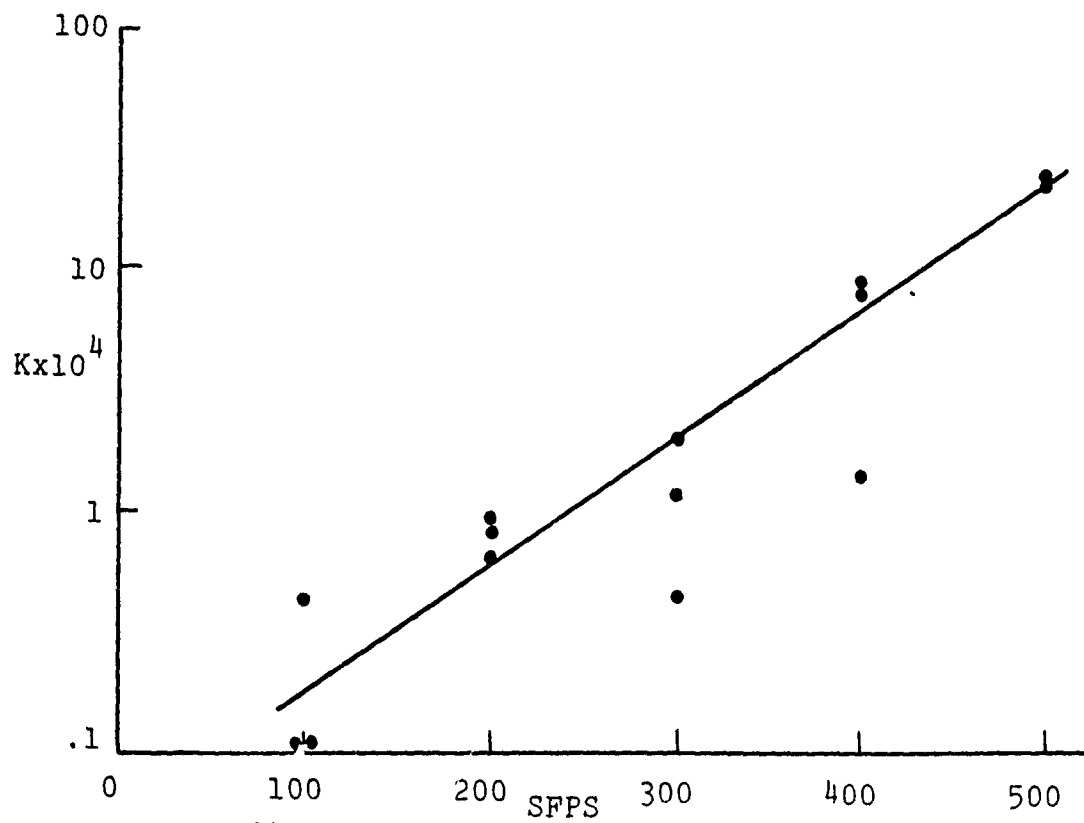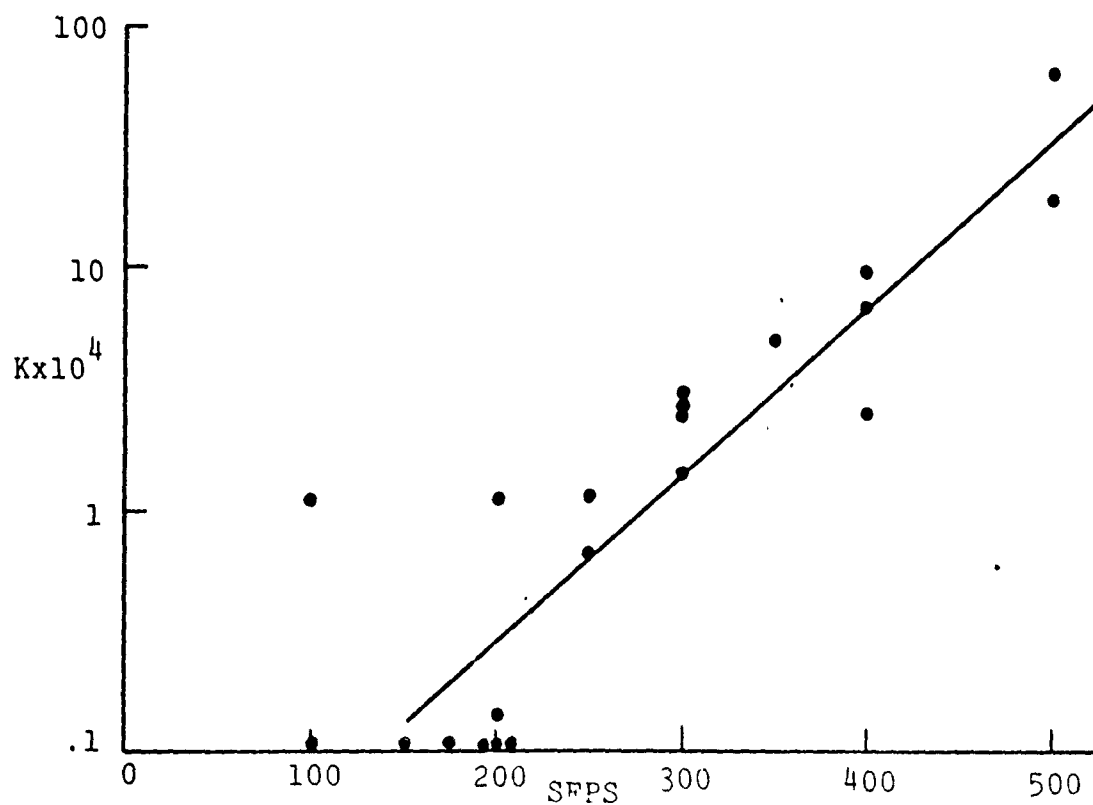

Figure A33. DQ3 on 4140
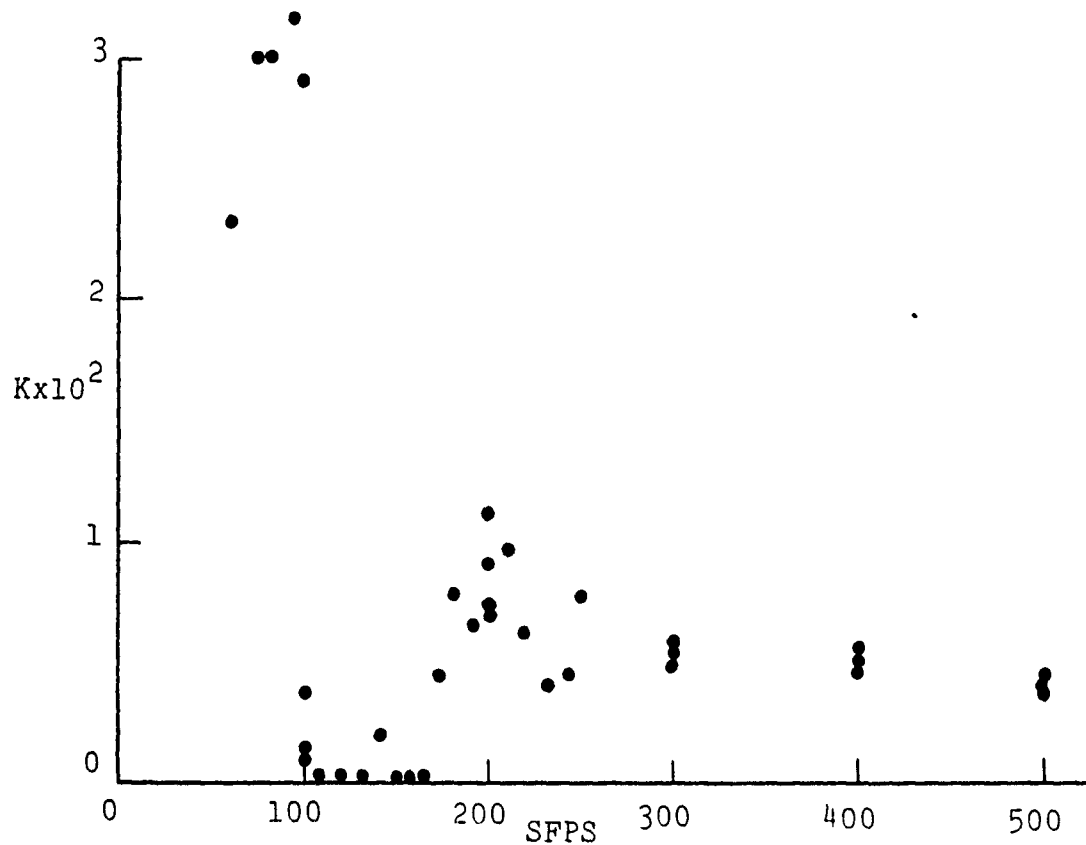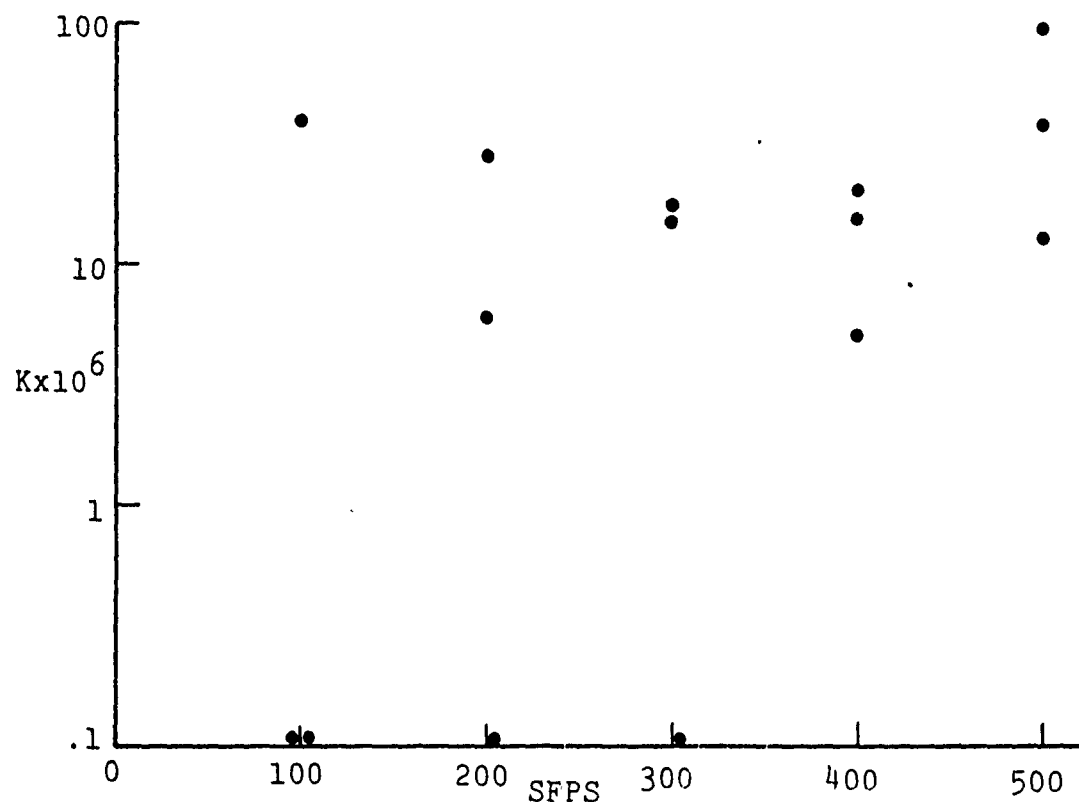
Figure A34. Zinc on 4140

Figure A35. Nylon on 4140
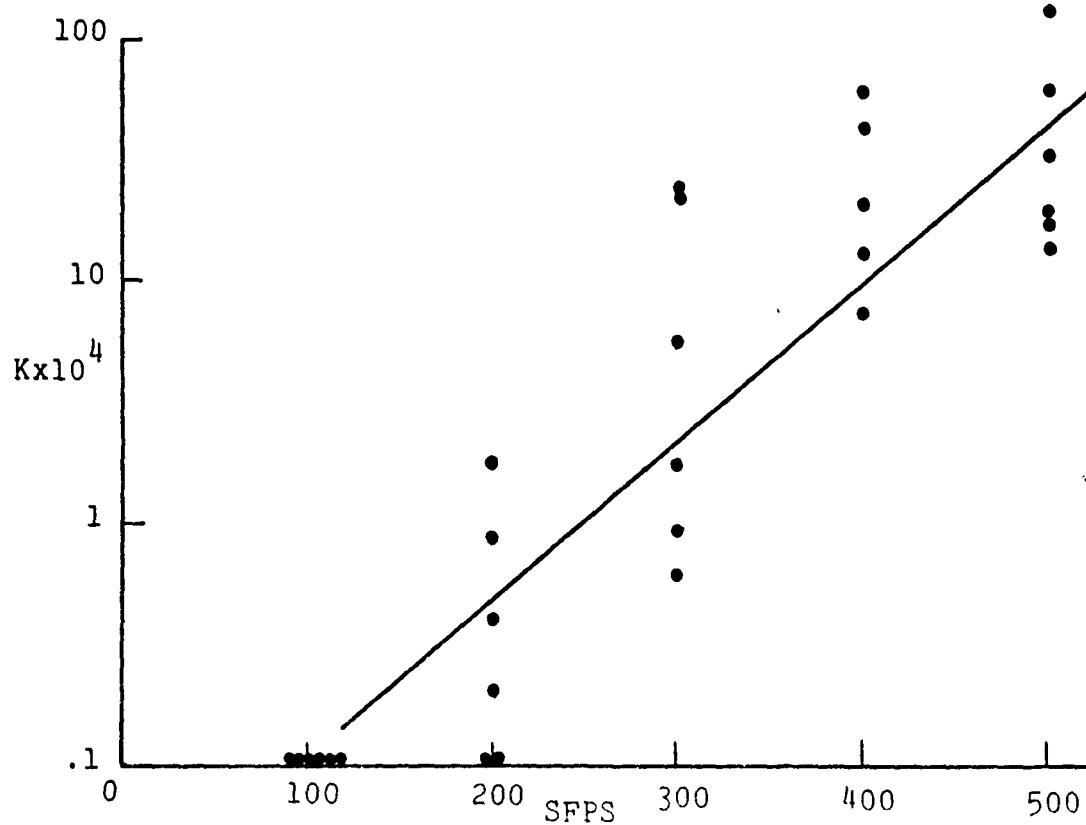
Figure A36. Rulon A on 4140

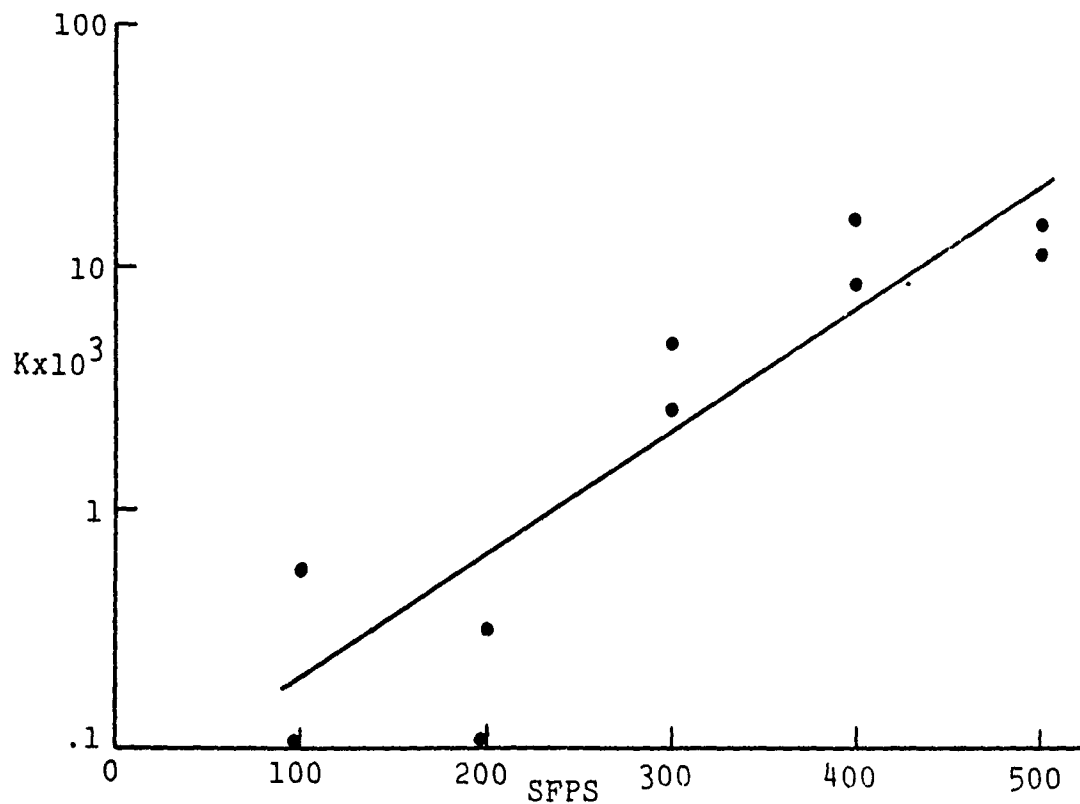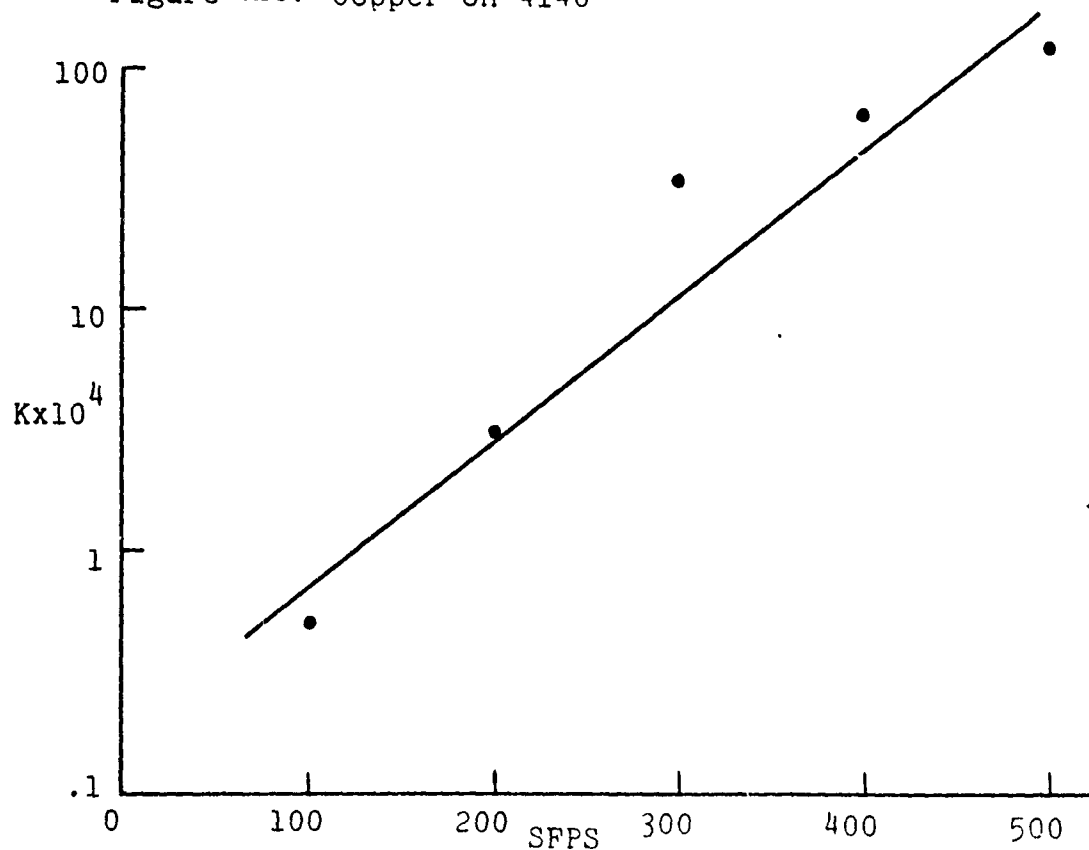Figure A37. National Vulcanized Fiber on 4140

Figure A38. Copper on 4140

Figure A39. Copper-16% lead on 4140

-A55-

brass "teeth" of the file (disc) and the brass pin. The bulk temperature of the pin is high and its hardness is therefore low. The teeth are cool when they contact the pin and scrape pieces of it away. The high values of K for some tests were the result of long (>.5 seconds) testing periods which resulted in abrasive wear.

There is an abrasive wear constant which quantifies this type of wear. It depends largely upon the geometric nature of the scraping surfaces: a file cuts well in one direction but poorly in the other. The majority of tests do not enter the abrasive wear regime, but those that do have high wear rates. The magnitude of K may decide which wear mechanism predominates. The transition from adhesive to abrasive wear does not occur at a well-defined point. It is not feasible to calculate an abrasive wear constant for the tests conducted, but low wear would dictate that abrasive action is to be avoided.

If K is known for some combinations of materials, it might actually be constant at high speeds if changes in P are accounted for. Hardness values at room temperature are used for all calculations, so K changes are reported. More information is needed on hardness as a function of temperature for test materials.

Most of the wear data thus far obtained has been on the specimen and not on the disc. Many tests in which the disc was weighed produced seemingly good results, but other tests indicate that the good data might be coincidental. Figure 42 shows the data points obtained. There is a general trend towards a decreasing weight loss and wear coefficient with increasing speed. This is the expected result, because the gilding metal gets soft at high temperatures. However, the experimental support for this is weak. The K values cannot be considered conservative, because brass on brass sliding accounts for much of the total sliding distance in the wear equation. It is certain that abrasive wear does not account for any significant part of the disc wear. The pin is at least three times softer than the steel, and abrasive wear of the harder material is minimal (15).
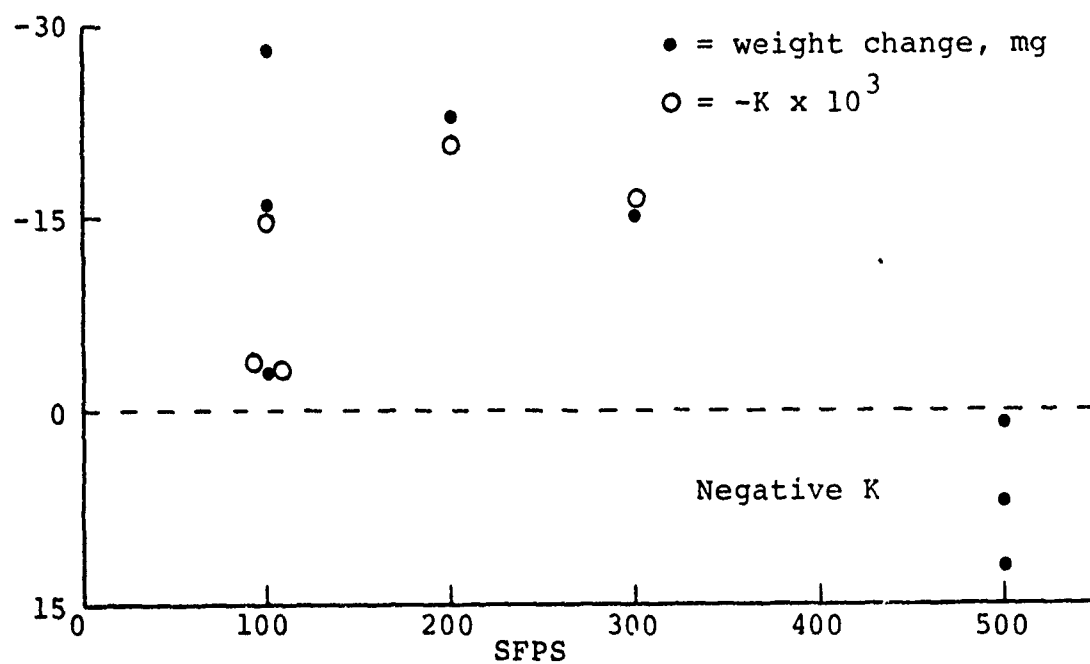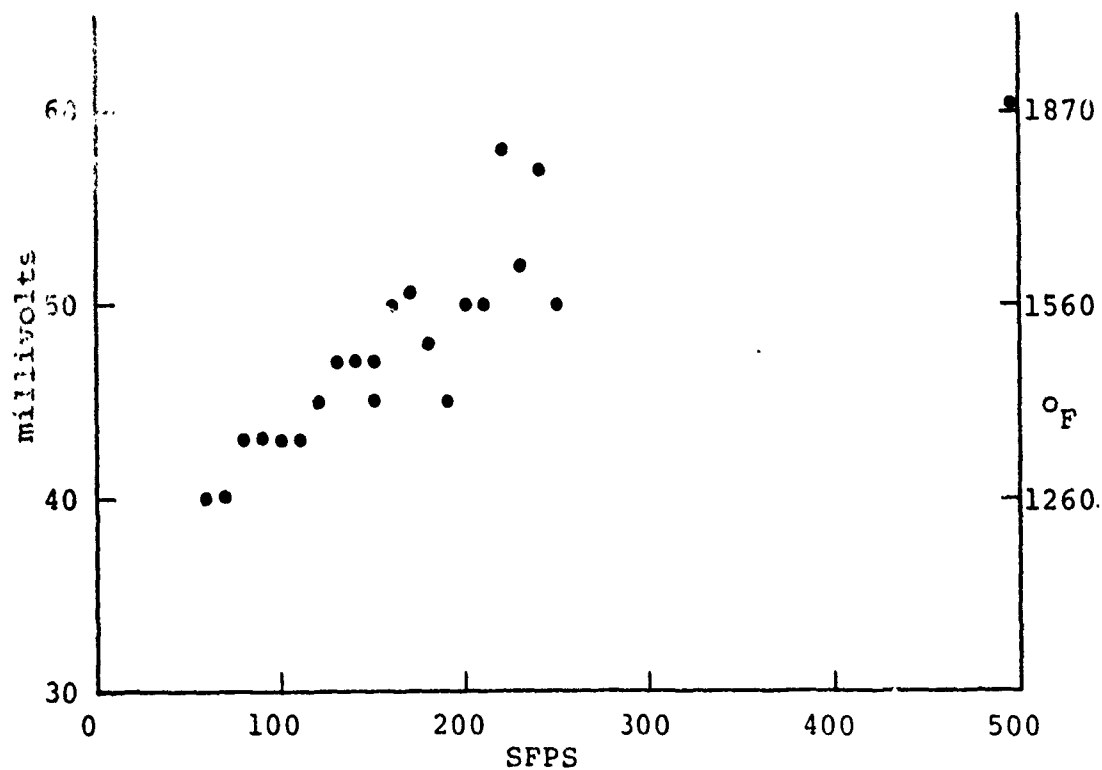
Figure A42. Disc weight loss measurement data

Figure A43. Constantan-4140 thermocouple
voltage-velocity data

AIV.3 TEMPERATURE MEASUREMENT RESULTS

A number of tests were conducted in the early stages of the project using constantan as the test specimen. It was the only material used with 4140 which produced a linearly increasing thermoelectric EMF. The data points taken are shown in Figure 43. It was decided that constantan was not a preferred material with which to run tests; its thermoelectric property was the only reason it was used. The constantan tests were not exhaustive because they were unlikely to produce a sound basis for general thermoelectric temperature measurement.

Some tests were run with 70-30 brass which produced inconclusive results. The EMF was approximately zero at the highest load X velocity X friction coefficient (PVf) values, but it had been higher at lower PVf values. This follows from the calibration curves but the accuracy to which the data can be interpreted is questionable.

During most tests, a layer of the specimen material is deposited on the disc. If brass is the specimen, there is a substantial amount of brass or brass sliding which occurs. This sliding produces no thermoelectric EMF. Instead, it shorts out nearby junctions of brass on steel which are producing an EMF. One solution is not to retrace an old wear track, but this is presently impractical and would not tipify common surfaces.

The dependence of thermoelectric methods on test material, metal transfer, and unknown junction characteristics led to other methods of temperature measurement. The optical method seemed the most promising, as it was independent of the above three parameters. Its limited temperature range is one drawback, but the method works well around the melting range of brass.

It is possible to place the fiber optic bundle inside a hole in the test specimen. This allows it to look directly at the pin-disc interface. However, the end of the bundle should be only about .025 inches away from the region to be measured. This is because only a small area should be in the fiber optic's 60° cone of vision. A test would therefore have only .025 inches of pin to wear away before reaching the fiber optic, which would probably be damaged in any test. Because of this, and the difficulty involved in setting up the specimen, another position for the fiber optics was found.

The interfacial temperature rise which is produced during a test is the same on the surface of the pin and on the surface of the disc. If the disc surface temperature can be measured, the pin temperature is also known. It is difficult, if not impossible, to optically measure the temperature of the disc when the specimen is covering it. It is possible to measure it immediately after the pin slides over it, and this is what has been done. Figure 9 shows the fiber optic

placement. The interface temperature can then be found, although it is obtained indirectly.

One dimensional heat flow in the radial direction is assumed (Appendix F). At the interface, there is zero thermal resistance ($H=\infty$). This means that if the interface was at $500^{\circ}C$ the disc was in intimate contact with a $500^{\circ}C$ temperature source. The duration of the contact is the time taken to slide a distance equal to the pin diameter. At 500 fps with a one-eighth inch pin this is 21 microseconds. A temperature profile in the disc can then be calculated for a $500^{\circ}C$ source in contact with a steel surface for 21 microseconds. The profile takes the form of a complimentary error function (16),

$$\frac{T - T_i}{T_f - T_i} = \text{erfc}\frac{x}{2\sqrt{\alpha\ t}}$$

where

    T = disc temperature

    T_i = initial disc temperature ($25^{\circ}C$)

    T_f = interface temperature

    α = thermal diffusivity of the disc steel (.018 inch^2/sec)

    t = time in seconds

    x = distance radially into disc from the interface (inches)

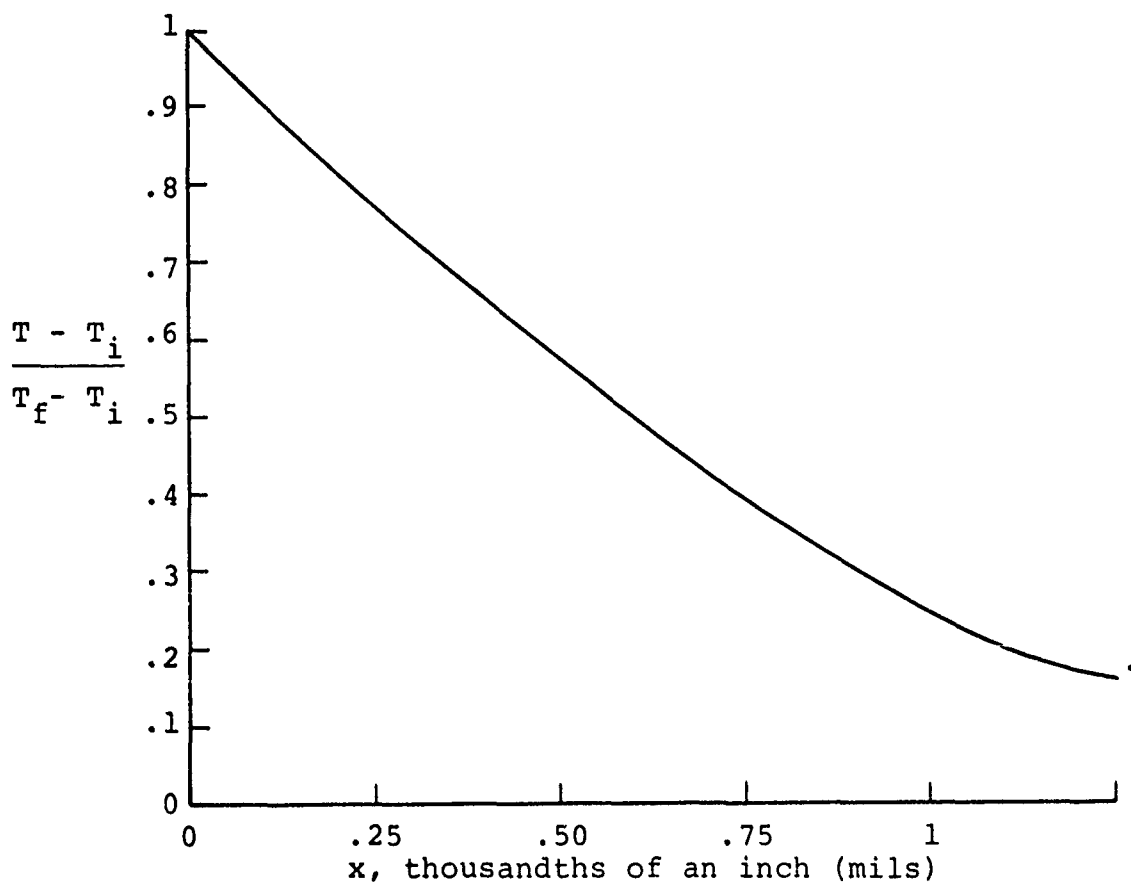The profile is shown in Figure 44 for a 21 microsecond contact time.

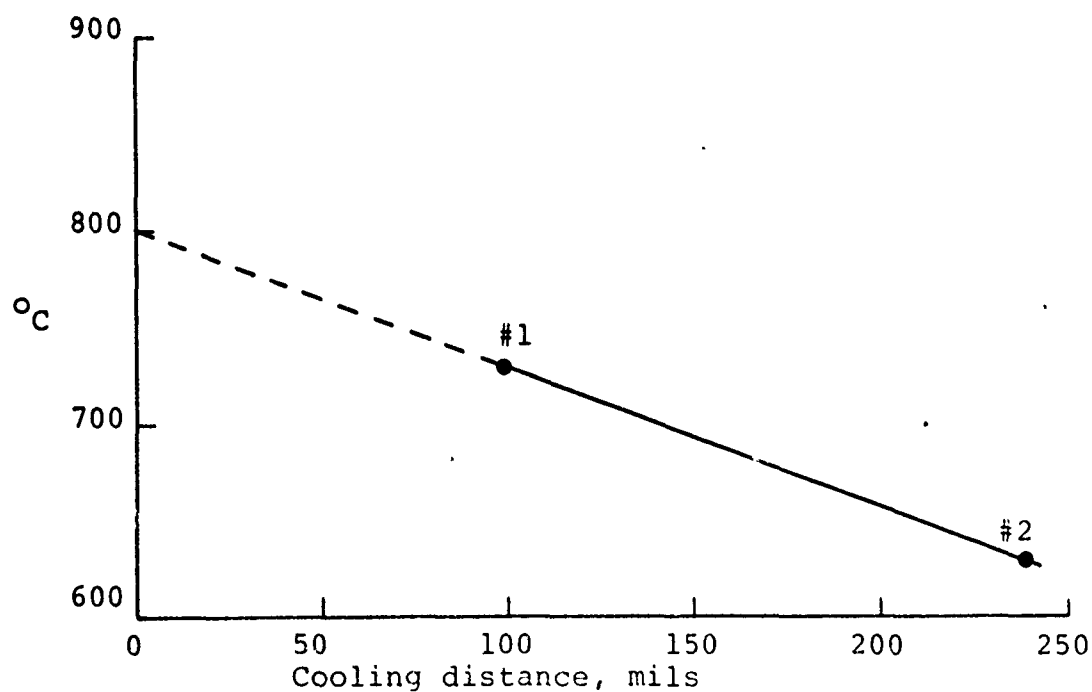Figure A44. Erfc temperature profile in disc for 500 fps tests with a 1/8 inch specimen

Figure A45. Surface temperature extrapolation from pyrometers #1 and #2

The surfa? temperature drop which occurs before the disc area in quest. n is under the fiber optic bundle has to be determined. ? the fiber bundle looks at the disc .125 inches above the , -disc contact area, the disc has 21 microseconds to c .. at 500 fps. There are three mechanisms of cooling. One is cooling by thermal conduction into the disc. The second is by forced convection, and the third is by radiation. An exact closed form solution to disc cooling with a complimentary error function initial condition has not been obtained. A numerical approach on a computer would be a good solution method. However, an analytical solution has been found which uses an exponential initial condition to approximate the error function. The solution and procedure is given in Appendix I. It can be seen from the results that in all test cases, thermal conduction into the disc accounts for all (>99%) of the surface cooling.

With two closely spaced fiber bundles (two distinct pyrometers) looking at the disc, two points are determined on a cooling curve. If the nature of the curve is known, extrapolation of the two points gives the interface temperature. If the curve is unknown, a low estimate would be to assume a constant dT/dt slope given by the two points and thus extend the curve.

For example, on one test, pyrometer 1 indicated $730^{\circ}C$ while pyrometer 2 indicated $630^{\circ}C$. #1 was .1 inch from the

interface, and #2 was .240 inch from the interface. As shown in Figure 45, the interface would have been 800°C. This is definitely a low estimate of the temperature obtained. Cooling occurs faster at higher temperature gradients, or immediately after the disc is no longer contacting the pin. Using the analytical approach with pyrometer #1's output, the interface temperature is 1280°C (Appendix I). This seems high, but not by much. The change in thermal conductivity with temperature would change the answer, as would a different cooling time (now taken to be the time to reach the middle of the fiber optic's viewing area).

The number of temperature points used to determine the experimental curve should be greater than 2. The curve is most likely well-behaved with no discontinuities. If three or four points were obtained sufficiently close to the contact region a good extrapolation could be made. An attempt at producing a four-element fiber optic array was unsuccessful. The fiber ends polished poorly and transmission losses were very high. The two fiber optic bundles in use are commercially polished. Greater than 60% of the radiation entering one end is transmitted out the other end. It is estimated that only 5% of the radiation was transmitted through the four-element array. Had it been successful, temperature points .1, .2, .3 and .4 inches from the contact region could have been obtained. Any future arrays should obtain points .05 inches apart instead of .1 inch apart.

The optical temperature measurement method is quite reliable. The main difficulty lies in physically positioning the fiber optics at desired points on the disc. The distance from the disc presents no problem; in the tests run it was .025 inch. The bundles look at a spot on the disc less than .1 inch in diameter.

The first time the optical pyrometer was tested the fibers were located .5 inches from the contact region. At 500 fps the disc had 84 microseconds to cool. The lower temperature limit on the pyrometer was 750°C and the pyrometer never responded with gilding metal test specimens. An assumption was made that the interface temperature would never get much higher than the lower melting point of the two test materials (brass in a brass-steel sliding situation) (15). Because of this, pure iron was used for two tests. It melts 500°C higher than gilding metal and it could reach a higher sliding temperature than the brass. The test results show that the iron definitely reached 830°C, which was the limit of the pyrometer. The test results are redrawn from the oscillograph recording in Figure 46. The rate of heat generation (PVf) is approximately the same for gilding metal and iron tests. The iron apparently rose to a much higher temperature than the brass, probably because the brass temperature rise was limited to its melting range (1000°C). At that temperature, the disc would have cooled sufficiently
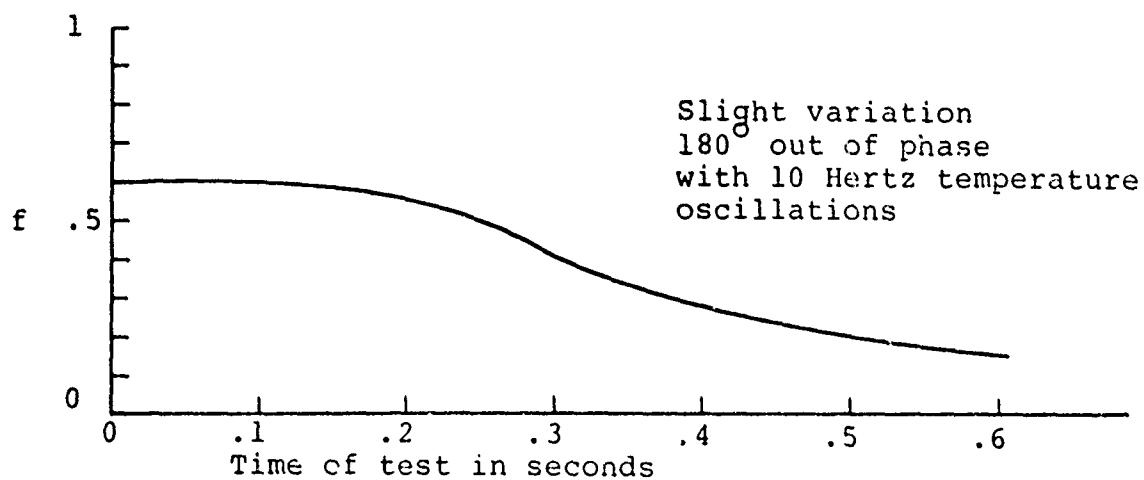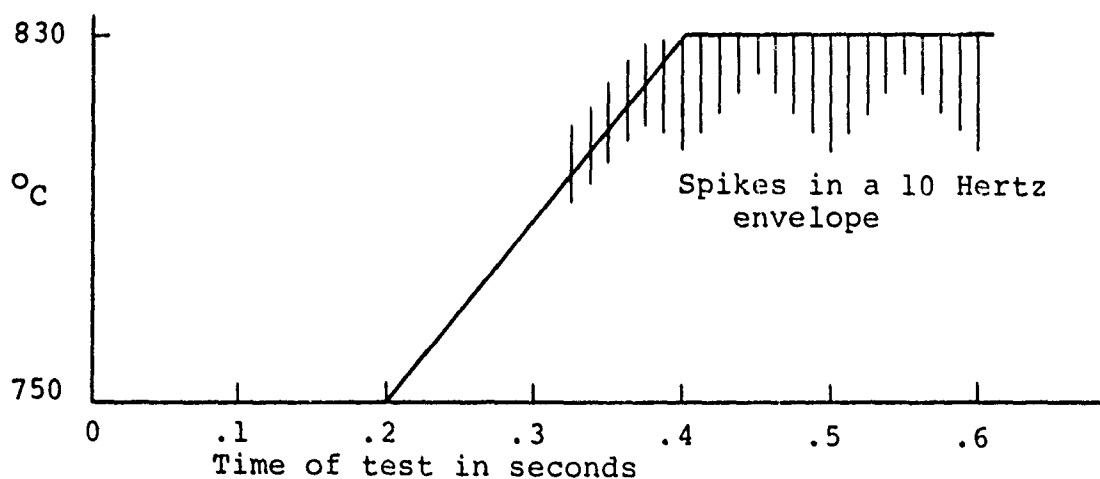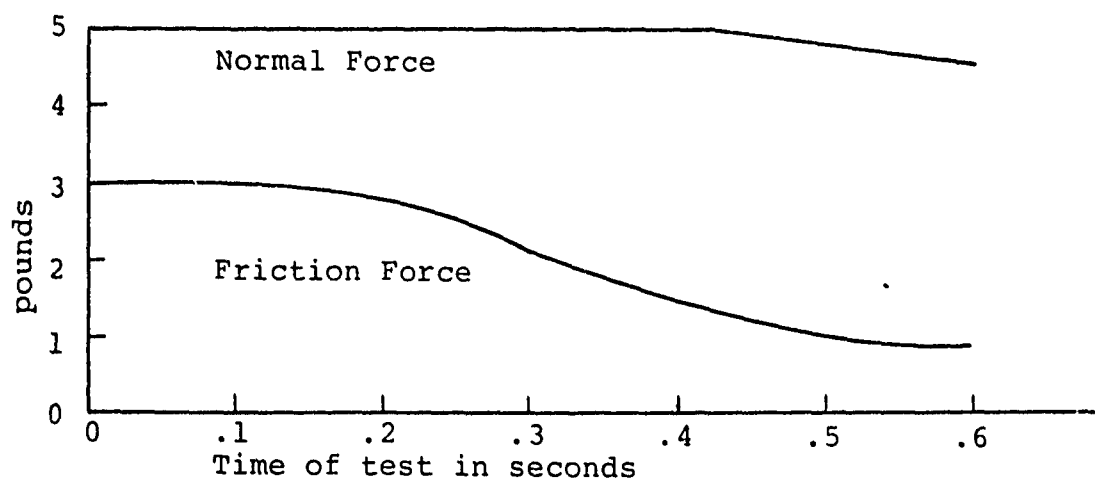
Figure A46. Test results from an iron on 4140 test

by the time it reached the fiber bundles that no reading would result. The interface temperature with iron was higher so the disc had not cooled enough to go below the pyrometer scale.

There is an interesting result that is clearly seen on the temperature trace with the iron specimen. A 10 hertz envelope surrounds the temperature profile after the pyrometer is saturated. There are no filters in the pyrometer, and the oscillations are definitely not electrical in origin. If the coefficient of friction trace is carefully examined, the same 10 hertz oscillations are visible. When the temperature oscillation is high, the f is low, and vice versa. The percent change is f is small, and its average value changes very little. It nevertheless supports one theory: as the temperature rises due to the PVf work put into the system, it will fall as f falls due to melting. Then f increases again, the temperature rises, and the oscillations continue. An analytical solution to this phenomenon was attempted but it was unmanageable.

Only three tests with gilding metal were conducted in which the pyrometers indicated something. They were tests at 300, 400, and 500 fps. The values shown in Figure 45 were taken from the 500 fps test. No oscillations were apparent, and the wide melting range for gilding metal may be the reason. Iron melts at a very specific temperature, and the friction probably changes dramatically at that temperature.

Gilding metal exhibits a gradual increase in "mushiness" until it reaches its liquidus temperature. The change in friction with temperature would probably be much lower for brass than for iron. Oscillations would therefore be more unlikely.

CONCLUSIONS

A large portion of the work described herein has been in the development of an apparatus to study high speed friction and wear phenomenon. The emphasis·has been on producing a limited amount of reliable data from which sound conclusions can be drawn. The measurement of interfacial sliding temperatures has received much attention because it is the least well known and perhaps the most important aspect of high speed friction and wear. Work in temperature determination still needs to be done but it is a matter of refining the existing setup. The optical pyrometer is considered a reliable method of temperature measurement and only in the last 8 of 199 recorded tests was it used.

All tests have been conducted at essentially the same normal load; the interface pressures could vary with the apparent area of contact. The disc projection has not yet been used and it will permit higher contact pressures to be used. Specimen preheating is an available means of simulating higher pressures and/or speeds.

Research is needed on the wear of the harder material, in this case the disc. Alternately, a plated disc might be utilized so that conventional wear measurements could be conducted on a hard pin.

For materials that melt f gradually decreases in value
with increasing speed. It does not get very low (<.1) in the
PV region investigated. Surface melting is responsible for
the decreasing f but the lack of a fully hydrodynamically
lubricated surface keeps it above .1. The real interest lies
in that region where only partial fluid lubrication occurs.
Materials that do not melt, like phenolics, are more difficult
to analyze.

The wear coefficient goes down with increasing surface
speed. An exception to this seemed to occur with constantan,
but constantan tests were conducted with a large pin and
interface temperatures could have been below the melting
point.

BIBLIOGRAPHY

1. J.F. Archard, The Temperature of Rubbing Surfaces, WEAR, Volume 2, 1958/59, pp. 438-455.

2. R. Barber and T. Land, The Place of Photovoltaic Detectors In Industrial Pyrometry, Temperature, Its Measurement and Control in Science and Industry, Volume 3, 1962, Reinhold Publishing Corp., N.Y.

3. F.P. Bowden and J.H. Brunton, The Behavior of Materials In a High Speed Environment, High Temperature Structures and Materials Proceedings of the Third Symposium on Naval Structural Mechanics, January 1963,N.Y., pp. 214-244.

4. F.P. Bowden and P.A. Persson, Deformation, Heating, and Melting of Solids in High-Speed Friction, Proceedings of the Royal Society, A, Volume 260, 1961, pp. 433-458.

5. H.S. Carslaw and J.C. Jaeger, Conduction of Heat In Solids, Oxford University Press, London, 1947.

6. Nathan H. Cook and Ernest Rabinowicz, Physical Measurement and Analysis, Addison-Wesley Publishing Company Inc., Reading Ma.

7. E.O. Doebelin, Measurement Systems: Application and Design, McGraw-Hill Book Company, N.Y. 1966.

8. C.M. Herzfeld and R.L. Kosson, A Theory of Bore Friction, BRL Report No. 851, Aberdeen Proving Ground, Maryland. March 1953.

9. Infrared Industries, Inc., Sensors Group, 5000 Series Detectors, Data Sheet No. 1008, Waltham, Ma. 1975.

10. P.W. Kruse, L.D. McGlauchlin, and R.B. McQuistan, Elements of Infrared Technology: Generation, Transmission, and Detection, John Wiley and Sons, 1962.

11. Metal Finishing Guidebook Directory, Brush Plating Techniques, 38th edition, 1970, pp. 45 -468.

12. R.S. Montgomery, Friction and Wear At High Sliding Speeds, WEAR 36, pp. 275-298, 1976 WVT-TR-75028 June 1975

13. R.S. Montgomery, Surface Melting of Rotating Bands, Report #WVT-TR-75060, Watervliet Arsenal, N.Y. Nov. 1965.

14. J.O. Pilcher and Emma M. Wineholt, Analysis of the Friction Behavior At High Sliding Velocities and Pressures For Gilding Metal, Annealed Iron, Copper and Projectile Steel, BRL Report No. 1955, January 1977.

15. Ernest Rabinowicz, Friction and Wear of Materials, John Wiley and Sons, Inc., N.Y. 1966.

16. W.M. Rohsenow and H.Y. Choi, Heat, Mass and Momentum Transfer, Prentice-Hall Inc., Englewood Cliffs, New Jersey. 1961.

17. Shock and Vibration Handbook, C.M. Harris and C.E. Crede, Volume 1, 1961. McGraw-Hill.

18. W.W. Shugarts Jr. and H.C. Rippel, Frictional Resistance, Heating and Wear At High Sliding Speeds, BRL Report No. F-2448, The Franklin Institute, Philadelphia Pa. August 31, 1956.

19. W.W. Shugarts Jr. and H.G. Clarke Jr., A High-Speed Friction and Wear Machine, The Franklin Institute.

20. W.W. Shugarts Jr. and H.G. Clarke Jr., Sliding Friction At High Speeds, The Franklin Institute, Interim Report No. I-2358-8, April 30, 1954.

21. Solid State Optoelectronics, Monsanto Commercial Products Co., Palo Alto, Ca., 1977 Catalog of Optoelectronic Products.

22. Standard Handbook for Mechanical Engineers, T. Baumeister and L.S. Marks, Seventh Edition, 1967, . McGraw-Hill.

23. R.W. Strachan, A Technique For Levitation Melting, Undercooling and Splat Cooling of Metals and Alloys, Department of Metallurgy, MIT, Phd. Thesis June 1967.

24. Riccardo Vanzetti, Practical Applications of Infrared Techniques, John Wiley and Sons, N.Y. 1972.

25. J.D. Welch, Automatic Feedrate Regulation in Numerically Controlled Contour Milling, MIT Electronic Systems Laboratory, Report 8436-R-1, 1960.

26. W.R.P. Wilson, Lubrication By a Melting Solid, ASME Paper No. 15-Lub-26, 1975

For a steel disc $\sigma_r|_{max} = 10{,}650$ psi at 10,000 rpm

and $\sigma_\theta|_{max} = 28{,}160$ psi

For a copper disc $\sigma_r|_{max} = 13{,}500$ psi

and $\sigma_\theta|_{max} = 35{,}780$ psi

If a 20 mil layer of copper were plated onto the steel disc,

$\sigma_r = 103$ psi and

$\sigma_\theta = 7{,}500$ psi

These stresses are sufficiently low that an electroplated coating would not fail due to rotational induced stress.

APPENDIX A

σ = stress, psi

ρ = mass density, lb-sec^2/in^4

R = outer disc radius, 6.8 inches

r = radius to point in question, inches

r_h = radius of center hole, .875 inches

μ = Poisson's ratio, .29 for 4140 steel and .355 for copper

ω = radians/second, 1047 at 10,000 rpm

With a center hole, the radial stress is

$$\sigma_r = \frac{3+\mu}{8} \rho\omega^2 \left[R^2 + r_h^2 - \frac{R^2 r_h^2}{r^2} - r^2 \right]$$

and the tangential stress is

$$\sigma_\theta = \frac{3+\mu}{8} \rho\omega^2 \left[R^2 + r_h^2 + \frac{R^2 r_h^2}{r^2} - \frac{1+3}{3+} r^2 \right]$$

The maximum radial stress occurs at $r = (Rr_h)^{1/2}$

$$\sigma_r|_{max} = \frac{3+\mu}{8} \rho\omega^2 \left[R - r_h \right]^2$$

and the maximum tangential stress occurs at the inner boundary (r_h)

$$\sigma_\theta|_{max} = \frac{3+\mu}{4} \rho\omega^2 \left[R^2 + \frac{1-\mu}{3+\mu} r_h^2 \right]$$

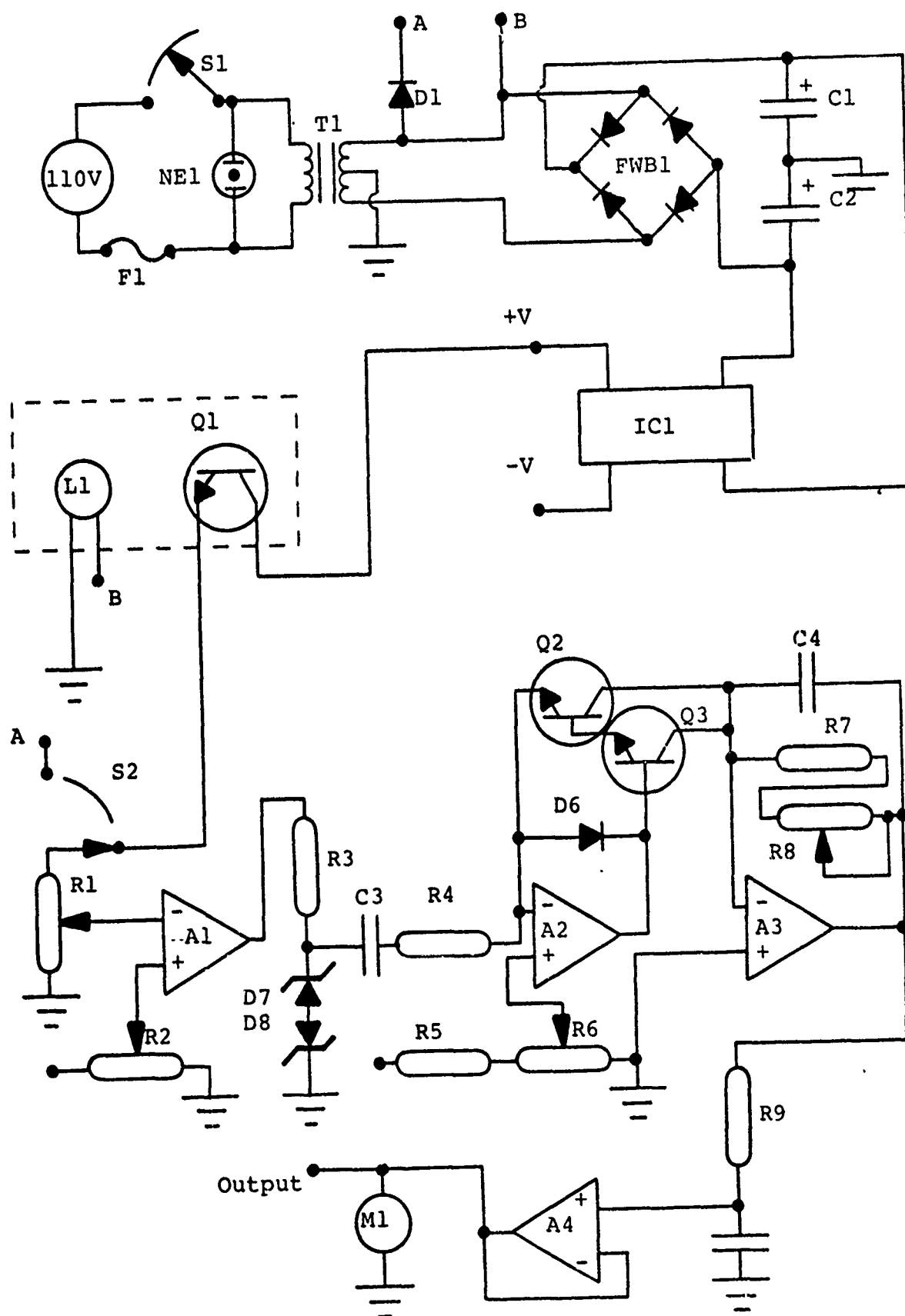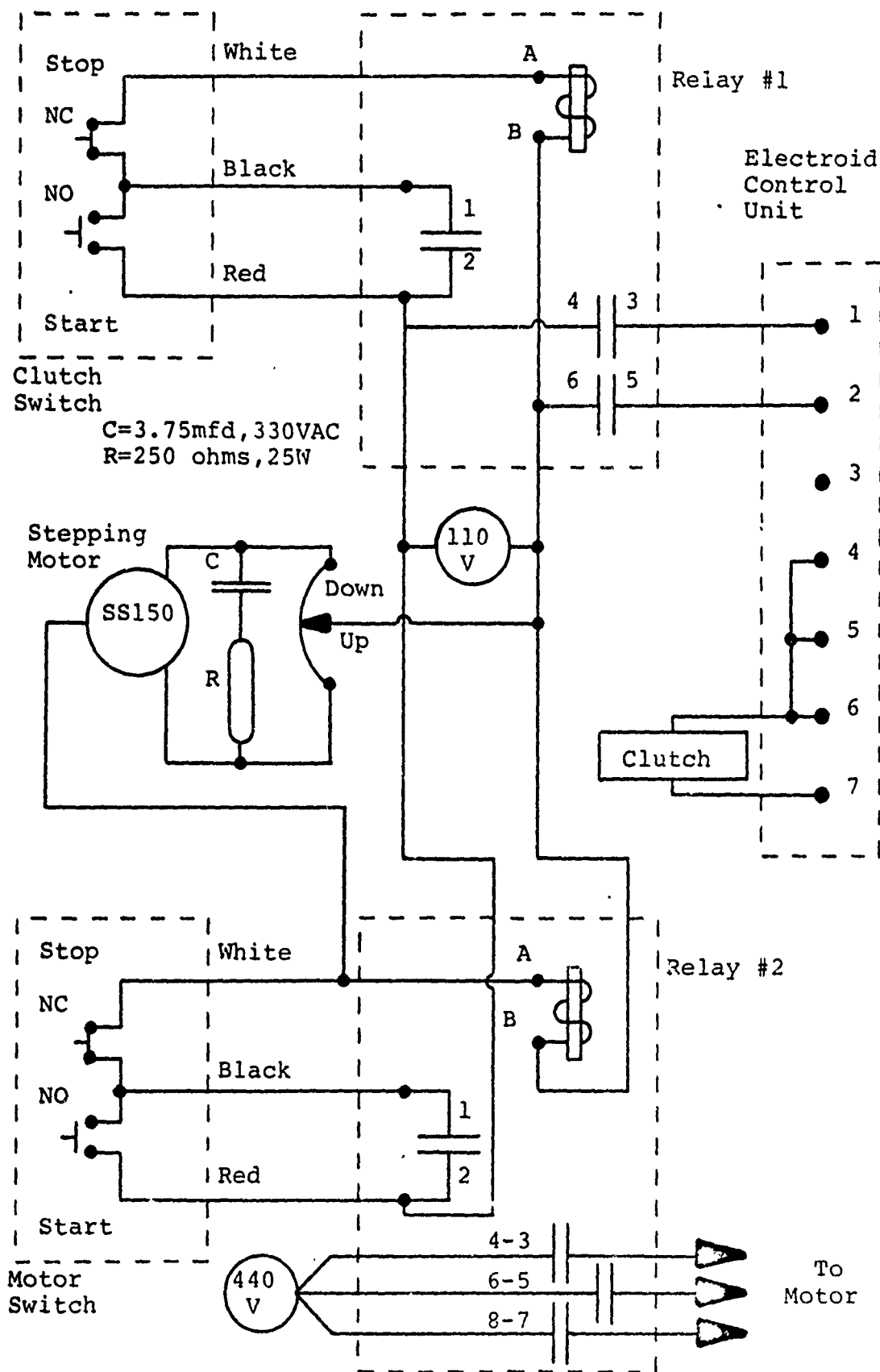Figure B2.   Optical Tachometer Schematic

Stop

White

A   Relay #1

NC

B

NO

Black

Electroid
Control
Unit

1
2

Red

Start

Clutch
Switch

C=3.75mfd,330VAC
R=250 ohms,25W

4 | 3   1

6 | 5   2

3

Stepping
Motor

C

4

SS150

Down

110
V

5

Up

R

6

Clutch

7

Stop

White

A   Relay #2

NC

B

NO

Black

1
2

Red

Start

Motor
Switch

440
V

4-3

6-5   To
Motor

8-7

Figure B1. Motor Controls.

A1-A2, A3-A4--747 dual op amp
IC1--#4501 dual 15 volt regulator
C1,C2--150 mfd, 20 volts
C3--.15 mfd
C4--.1 mfd
C5--50 mfd, 15 volt
D2-D5--Full wave bridge rectifier
D1,D6--1N4007
D7,D8--10 volt zener
L1-28 volt miniature incandescent lamp
M1--10 volt DC meter
R1--100K pot
R2--20K trimpot
R3--620 ohm
R4--1k
R5--12K
R6--5K trimpot
R7--22K
R8--5K pot
R9--10K
Q1--L14G2 phototransistor, GE
S1,S2--SPST
T1--24 VCT, 150 ma

S1--Power switch
S2--Calibrate switch, sends 60 cycle pulses to counting circuit
    and should give 3.6 volts output (3600 rpm)
R1--Sensitivity adjustment
R2--Calibration pot

Output 0 - 10 volts, 0 - 10,000 rpm

APPENDIX C

Transducer Specifications

The transducer can be modeled as the beam in this figure for frequency calculations (17):
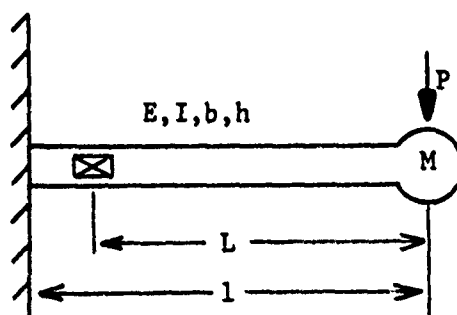

Figure C1. Beam vibration model

The lateral stiffness of a beam is

$$k = \frac{3EI}{l^3}$$

where

$$I = \frac{bh^3}{12}$$

and the natural frequency is

$$2\pi f = \sqrt{\frac{kg}{M+.23m}} = \sqrt{\frac{3EIg}{l^3 W}}$$

The following values are for the aluminum transducer in
Figure C2:

E = Young's modulus, 10×10^6 psi

I = moment of inertia, 3.26×10^{-4} inch^4

b = beam width, .25 inches

h = beam height, .25 inches

l = beam length, 1.075 inches

m = beam weight, .005 pounds

M = lumped weight at the end of the beam with
a typical specimen, .015 pounds

k = stiffness, pounds/inch

g = 386 in/sec^2

$W = M + .23m$

P = force in pounds

for the tranducer in use f = 2200 Hertz

The strain at the gages is

$$\varepsilon = \frac{6PL}{Ebh^2}$$

Transducer drawn 2X

Top View

Diagonal lines
represent strain gages

Front View

Primed numbers
indicate normal
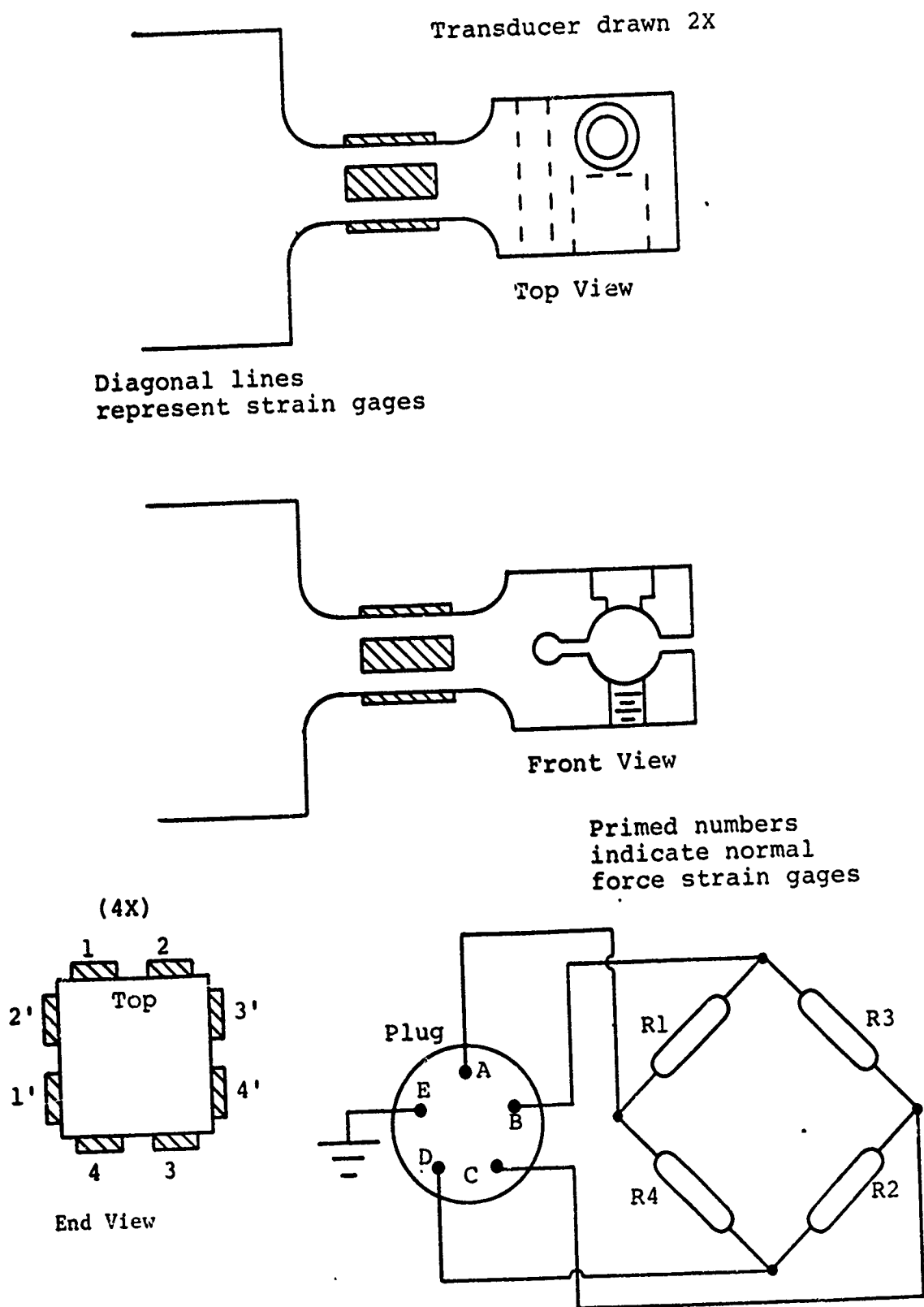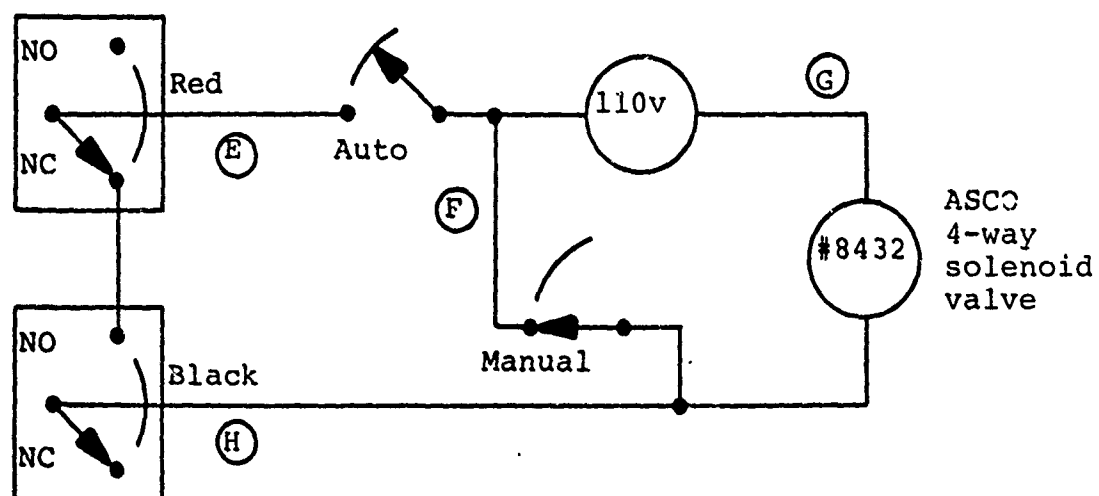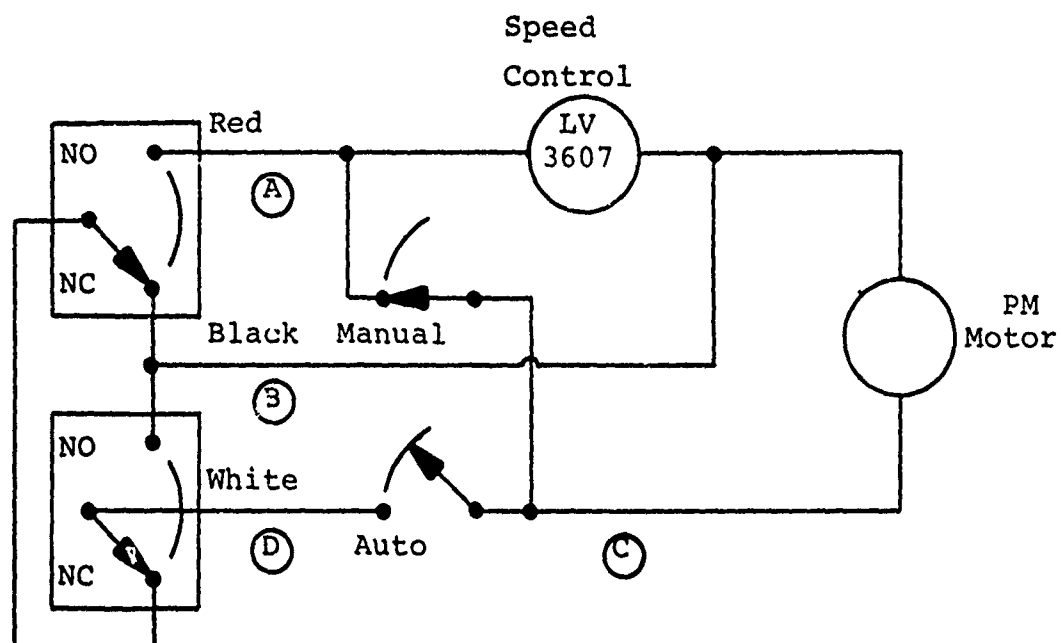force strain gages

(4X)

End View

Plug

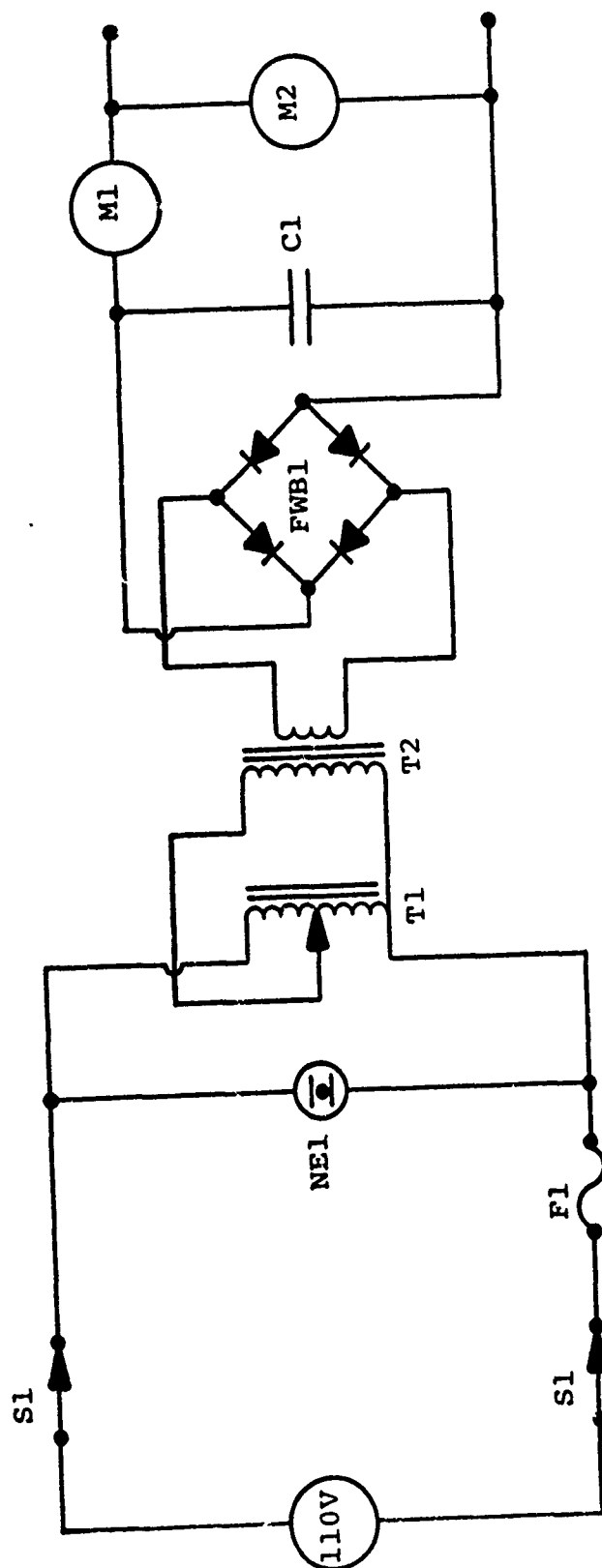Figure C2. Transducer configuration and plug connections

-A82-

Colors indicate leads from the limit switches
Circled letters indicate Amphenol plug contacts

Figure C3. Transducer platform controls

APPENDIX D

Specimen Heater

Power Supply

S1—DPST
F1—3 amp.
T1—2.5 amp autotransformer
T2—6.3 volt 20 amp sec., 110 volt primary
FWB1—25 amp full wave bridge rectifier
C1—220,000 mfd., 12 volts
M1—0-10 amps DC
M2—0-10 volts DC

Figure D1. Heater power supply schematic

APPENDIX E

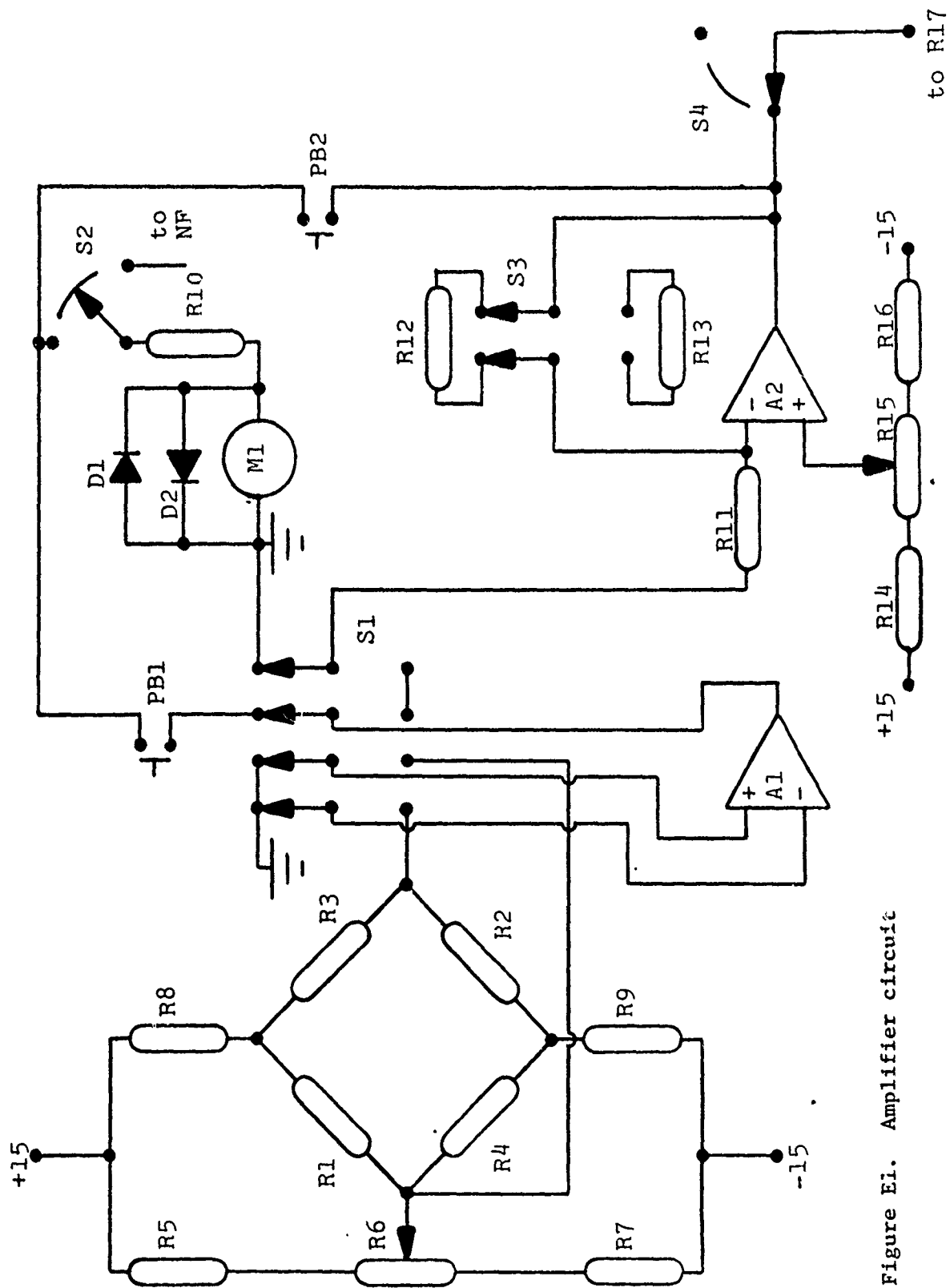## Amplifier and Divider
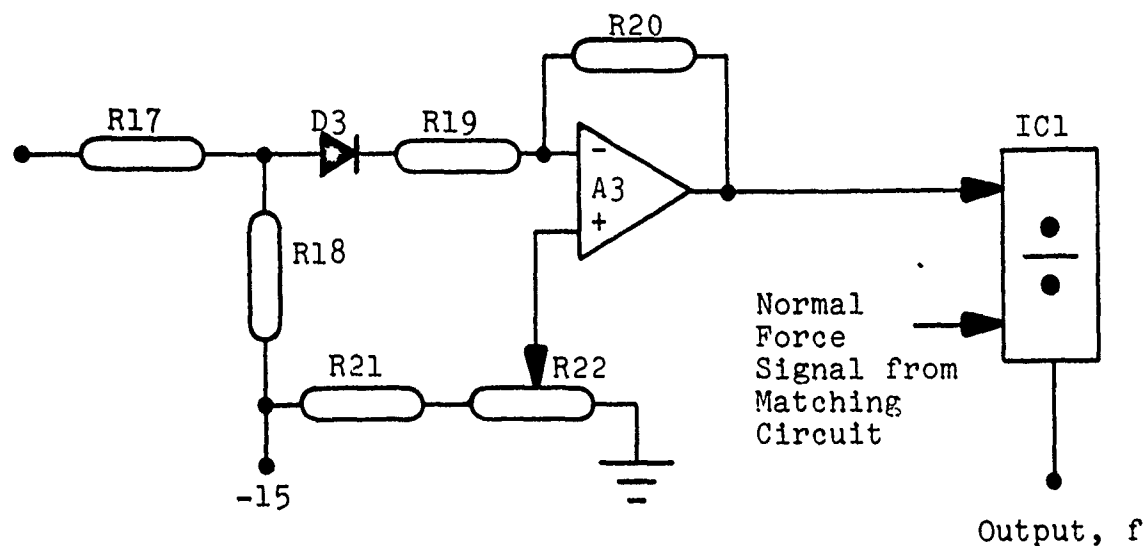## Circuitry

Figure Ei. Amplifier circuit

-87-

Figure E2. Divider circuit

S1—Test or run. Permits grounding of A1's inputs for zeroing with A1's trimpot if S3 is on. Also grounds A2's input for zeroing with pot 2 and S4

S3—Varies feedback resistor for A2 giving gain multiplies of 1X and 10X

PB1—Connects A1 to meter

PB2—Connects A2 to meter

R6—Zeroes strain gage bridge after A1 and A2 are zeroed

R15—(pot 2)—zeroes A2

S4—Disconnects divider from amplifiers

S2—Connects meter to normal force or friction force circuitry

```
A1--AD520 instrumentation amplifier
A2--AD509 op amp
A3--LM301AN op amp
IC1--AD532 divider
M1--50 microampere meter
D1,D2,D3--germanium signal diodes
R1-R4--strain gages
R5,R7--5K
R6--50 ohm pot
R8,R9,R19,R20,R21,R10--20K
R11--3K
R12--100K
R13,R14,R16,R18--10K
R15--100 ohm pot
R17--47K
R22--1K pot
PB1,PB2--momentary contact, spst
S1--4pdt
S2,S3--DPDT also S4
```

APPENDIX F

Theoretical Temperature Rise Calculations

High speed sliding exists as defined by Archard (1) if the dimensionless quantity

$$L = \frac{Va}{2K} \qquad \text{is greater than 5.}$$

where   V = velocity

a = radius of area of contact

K = thermal diffusivity

Even at the lowest operating speeds encountered in the apparatus described in this report this criterion is satisfied. The assumed junction model used when calculating the temperature of sliding surfaces is shown in Figure F1.
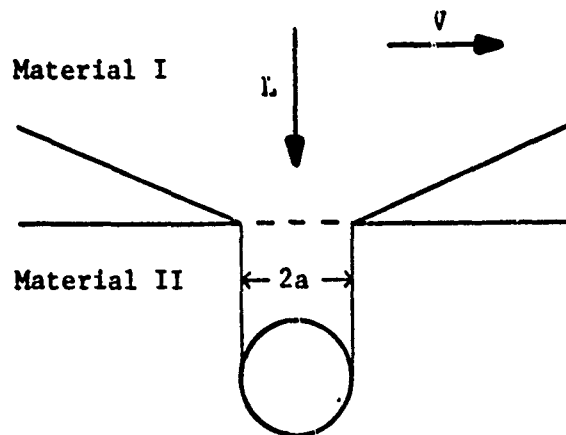

Figure F1.   Assumed junction model

Material I would be the specimen and material II would
be the disc. At sufficiently high speed the assumption is
made that almost all the heat generated at the interface goes
into the disc. This is assumed because the bulk temperature
of the disc is very low (essentially room temperature) which
leads to a very steep thermal gradient between the interface
and the disc. When the disc surface first contacts the pin it
is always cool. The pin effectively receives heat from a
stationary heat source and its bulk temperature therefore
rises. This reduces its temperature gradient, and because
heat flow (16)

$$q_x = -kA\frac{dT}{dx}$$

is directly related to the thermal gradient less heat flows
into the pin. Sideways flow of heat is neglected; all heat
flows in a radial direction. The depth to which heat
penetrates into II during the time of contact is small
compared to the dimensions of the contact. The sideways flow
of heat is therefore neglected and the problem becomes one of
linear heat flow.

Based on these assumptions the interfacial temperature
can be calculated as (15)

$$T_f = \frac{fLV^{1/2}}{3.6(\rho c r^3 k)^{1/2}}$$

where

> T_f = equilibrium mean interface temperature
>
> f = coefficient of friction
>
> L = normal load, pounds
>
> V = velocity, inches/second
>
> ρc = volumetric specific heat, pounds/inch^2-$^\circ$F
>
> k = thermal conductivity, pounds/second-$^\circ$F
>
> r = radius of contact junction, inches

Let a one-eighth inch pin be used for testing and assume r to be .062 inches. At 500 fps, 5 pounds normal load, and f = .5, T_f is indicated to be 55°F or 87°F depending upon whether the thermal constants for brass or steel were used. Since test results show definite temperatures above 1000°F there is some doubt as to the validity of this calculation. An incorrect value of friction coefficient could change the answer, probably by as much as a factor of 2. Changes in friction during a test should also be taken into account. This dependence on friction alone would still indicate an insufficient temperature rise.

The one factor that is really in question is r. The area of contact at the interface can be taken to be either the apparent area (pin cross-sectional area) or the real area. The apparent area gives a very low temperature rise, as seen before. If the real area of contact is taken to be

$$a_r = \frac{L}{P}$$

where   P = penetration hardness, about 3 times the yield strength for metals

a_r is independent of pin size and only depends on load and yield strength of the material. Taking this into account and suitably reducing r, $T_f = 2160°F$ if $P = 30,000$ psi. This is at least in the range of interest. However, yield stress can vary considerably with temperature. One value of stress could not be used to characterize a test with large temperature variation. The real area of contact is also dependent upon shear stress, although not in a well defined way. r is not exactly a constant.

To summarize, temperature rises can be calculated. They are very inaccurate, and if situations such as surface melting are to occur and be verified they will have to be measured. A hundred degrees in the vicinity of the melting range could result in a large change in friction and wear characteristics. Accuracies of this level are best achieved empirically.

The value of temperature rise calculations is significant if used together with experimental results. For example, heat transfer considerations prescribe that the temperature varies as the square root of the velocity. If some experimental data points are determined, it is acceptable to use them to determine the nature of a variable such as r.

Extrapolation can then be made with a large degree of accuracy.

APPENDIX G

Optical Pyrometer Circuit
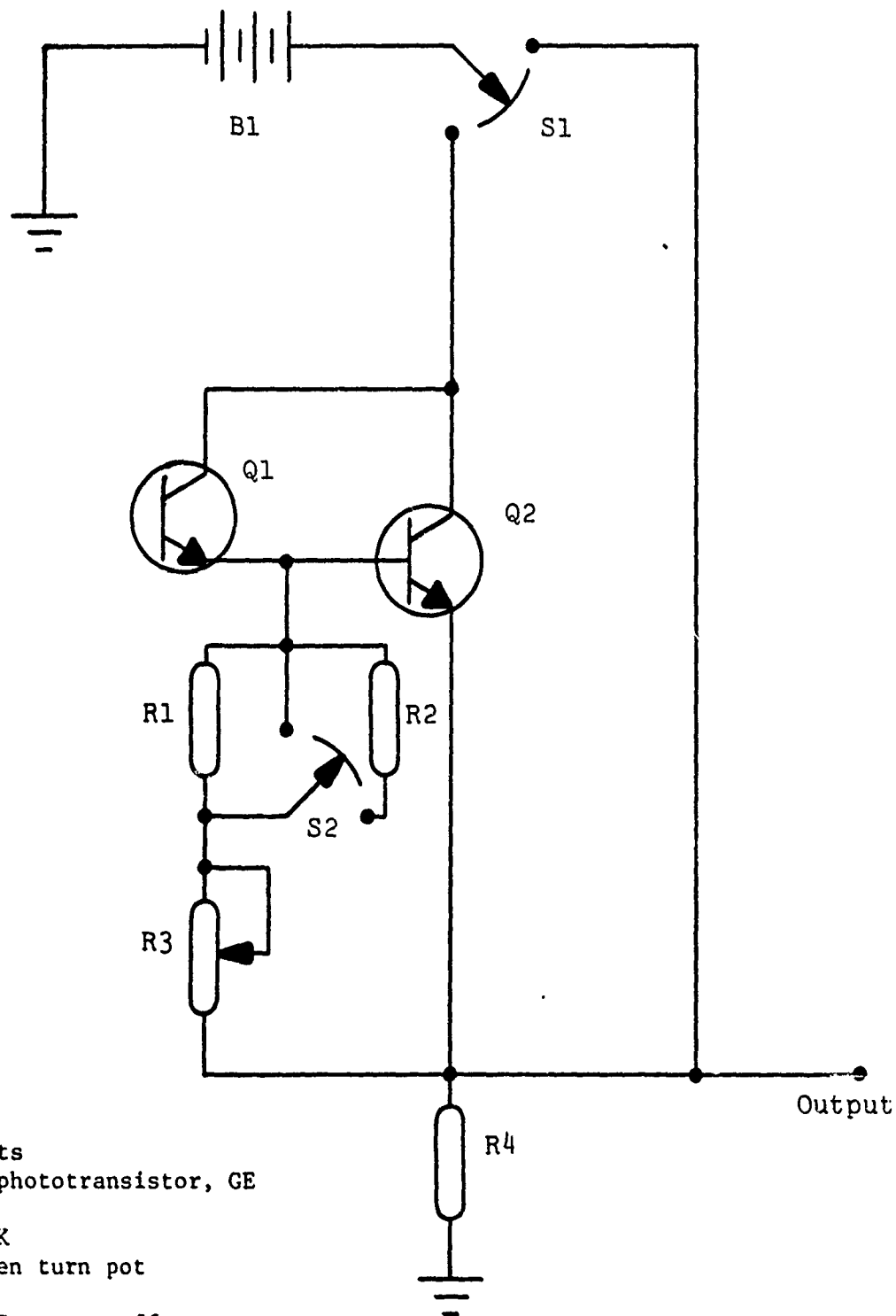
B1--22 volts
Q1--L14G2 phototransistor, GE
Q2--2N2222
R1-R2--200K
R3--100K ten turn pot
R4--4.7K
S1-S2--SPDT center off

S1--On, Off, Battery check
S2--Low, High, Medium gain

Figure G1. Optical pyrometer circuit

APPENDIX H

Test Materials

Appendix H

70-30 Brass, Cartridge Brass
Cu-70%, Zn-30%
Solidus 915 °C, 1680 °F

Liquidus 955 °C, 1750 °F

ρ = .308 lbs/in^3
P = 199,000 psi

Gilding Metal, Commercial Bronze
Cu-90%, Zn-10%
Solidus 1020 °C, 1870 °F

Liquidus 1045 °C, 1910 °F

ρ = .318 lbs/in^3
P = 107,000 psi

Constantan
Cu-55%, Ni-45%
Solidus 1220 °C, 2230 °F

Liquidus 1290 °C, 2355 °F

ρ = .323 lbs/in^3
P = 151,000 psi

Copper
Melting Point 1083 °C, 1981 °F

Heat of Fusion = 30 BTU/in^3

ρ = .324 lbs/in^3
P = 140,000 psi

84% Copper, 16% Lead

ρ = .25 lbs/in^3
P = 64,000 psi

Iron, 99.9+
Ferrovac-E
Melting Point 1534 °C, 2793 °F

ρ = .28 lbs/in^3
P = 117,000 psi

Zinc
Melting Point 420 $^\circ$C, 788 $^\circ$F
Heat of Fusion = 11.2 BTU/in^3

ρ = .258 lbs/in^3
P = 54,000 psi

4140 Steel
ρ = .28 lbs/in^3
P = 299,000 psi

DQ3, from the Glacier Metal Co. Ltd., Middlesex, England
Teflon-Lead Oxide-Bronze Composite

ρ = .128 lbs/in^3
P = 8,500 psi　*

National Vulcanized Fiber
Phenolic
ρ = .053 lbs/in^3
P = 25,000 psi　*

Nylon, Type 101
ρ = .041 lbs/in^3
P = 10,000 psi　*

Rulon A, from Dixon Corp., Bristol, R.I.
Teflon composite

ρ = .081 lbs/in^3
P = 6,400 psi　*

*   Hardness is not well-defined for some materials due to their viscoelasticity. The scales used to determine the hardness of metals are often unsuitable for non-metals like vulcanized fiber. A hardness measuring method was therefore used in which a 1/2 inch diameter ball was pressed into the test material and the indentation measured. The hardness can be calculated by the following equation:

$$P = \frac{L}{(\pi/2)D(D - \langle D^2 - d \rangle^{1/2})}$$

where   L = load, pounds
        D = indenter diameter, 1/2 inch
        d = indentation diameter, inches
        P = hardness in psi

All hardness values given are measured.

ref.   Metals Handbook, Volume 1, 8th edition

APPENDIX A.VII.I

Disc Surface Cooling Calculations

The exact solution to the problem of disc surface cooling with an error function initial condition can be found by solving two formidable integrals (5). If we are willing to approximate the erfc initial temperature distribution with an exponential distribution, the problem becomes manageable. The approximation is good over a large portion of the erfc curve (Figure I1). This is especially true near $x = 0$.

The problem can be modeled as a semi-infinite solid with a $T_o e^{-cx}$ initial temperature distribution. There is convection at the surface ($x = 0$) into air at $25^{\circ}C$ (Figure I2). The governing equations are

$$\frac{\partial^2 T}{\partial x^2} = \frac{1}{K} \frac{\partial T}{\partial t}$$

and

$$\frac{\partial T}{\partial x} = H(T - T_a) \qquad \text{convection boundary condition}$$

where
    K . thermal diffusivity
    h = heat transfer coefficient
    k = thermal conductivity
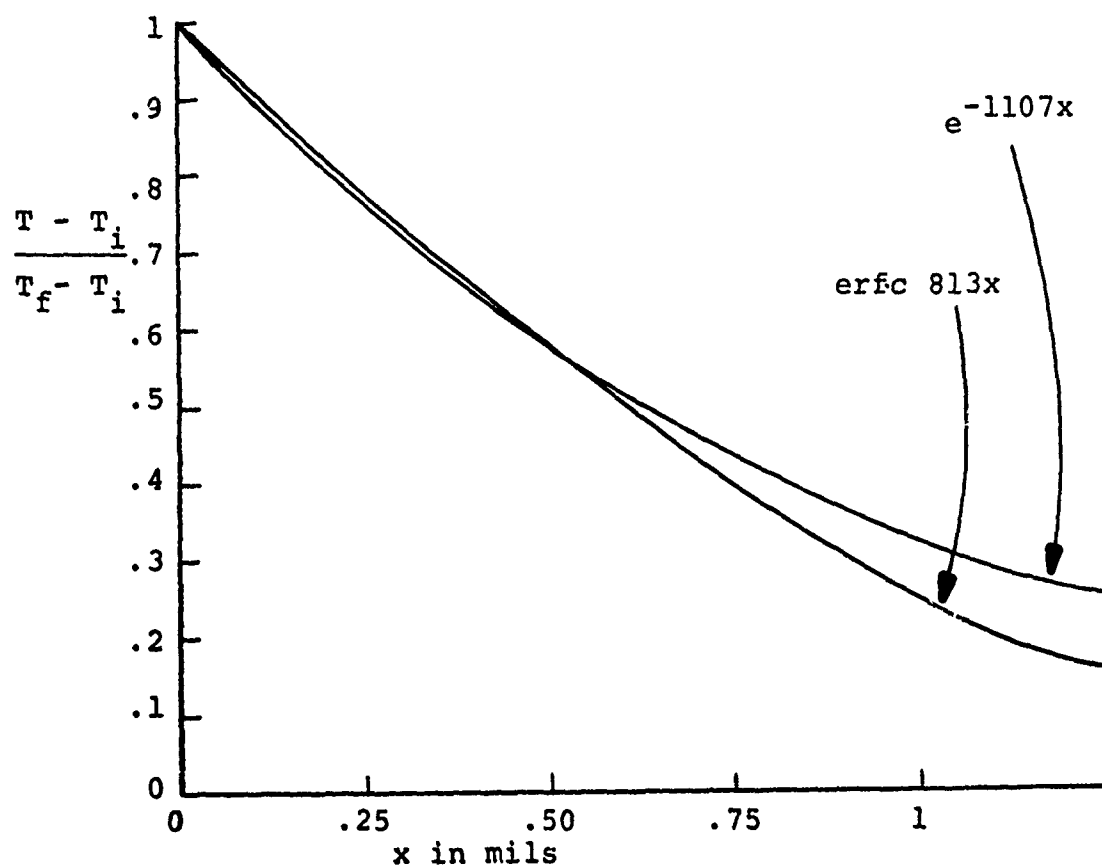   H = h/k

we have to solve for $T(t)$ at $x = 0$.

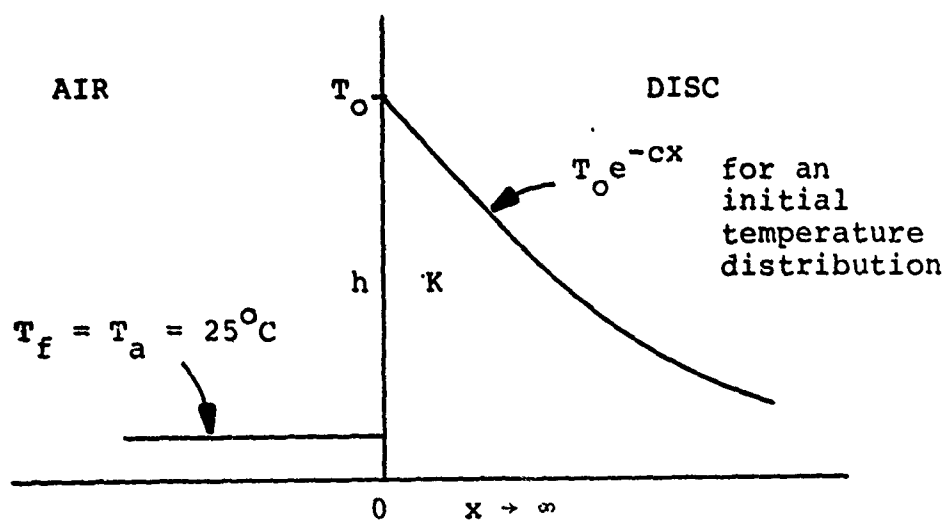Figure I1. Exponential approximation of a complimentary error function

Figure I2. Heat transfer model

Solve by LaPlace Transform method ().

$$\frac{d^2 T}{dx^2} - q^2 T = -\frac{T_o}{K} e^{-cx} \qquad \text{where } q^2 = p/K$$

and

$$\frac{dT}{dx} - HT = -\frac{HT_a}{p} \qquad \begin{array}{l}\text{transformed boundary} \\ \text{condition}\end{array}$$

This is now an ordinary differential equation instead of a partial differential equation.

solution $T = T_{homogeneous} + T_{particular}$

$$T = Ae^{-qx} - \frac{T_o e^{-cx}}{K(c^2 - q^2)}$$

A can be found by using the boundary condition at $x = 0$.

$$A = \frac{HT_a}{p(H+q)} + \frac{(H+c)T_o}{K(c^2-q^2)(H+q)}$$

which gives

$$T = \frac{HT_a e^{-qx}}{p(q+H)} \qquad +$$

$$\frac{(H+c)}{K} T_o e^{-qx} \left[\frac{1}{(c^2-H^2)(H+q)} + \frac{1}{(2cH-2c^2)(c+q)} + \frac{1}{(2cH+2c^2)(c-q)} \right]$$

$$- \frac{T_o e^{-cx}}{K(c^2-q^2)}$$

Taking the inverse Laplace transform and simplifying

$$T = T_a \, \text{erfc} \, \frac{x}{2\sqrt{Kt}} - (T_a + \frac{T_o h}{c-h}) \, e^{hx + Kh^2 t} \, \text{erfc}(\frac{x}{\sqrt{Kt}} + h\sqrt{Kt}) +$$

$$\frac{c+h}{2(c-h)} \, e^{cx + Kc^2 t} \, \text{erfc}(\frac{x}{2\sqrt{Kt}} + c\sqrt{Kt}) + T_o e^{-cx} \, e^{Kc^2 t} \, -$$

$$\frac{T_o}{2} \, e^{-cx + Kc^2 t} \, \text{erfc}(\frac{x}{2\sqrt{Kt}} - c\sqrt{Kt})$$

It can be checked that at $t = 0$, $T = T_o e^{-cx}$

and at $x = 0$, $t = 0$, T becomes T_o

This is a general solution for any x. If we only want
the solution at $x = 0$ the solution can be simplified. It is
found from the resulting equation that >99% of the disc
surface temperature drop is due to conduction into the disc.
This is true for values of h even greater than 1000
$BTU/hr-ft^2 - °F$. The actual h can be estimated to be less than
100 in all test cases. That the solution is virtually
independent of h is fortunate because h is not known. The air
flow conditions over the surface of the disc right above the
specimen govern h, and the actual air velocity is unknown.
With these simplifications, the equation becomes

$$T = \frac{T_o c}{c-H} \, e^{Kc^2 t} \, \text{erfc} \, c\sqrt{Kt}$$

T depends strongly upon the initial temperature distribution, the disc thermal diffusivity, and the cooling time. This equation can be applied to the example given in Figure 45.

let K = .018 in^2/sec

c = 1107 in^{-1} (intersects erfc curve at x=0 and x=.0005 inches)

t = 17 microseconds (.1 inch travel at 500 fps)

T_a = 25°C

T = 730°C (indicated by pyrometer #1)

Solving for T_o, we find it is 1280°C.

Appendix B. Experimental testing subsequent to that described in Appendix A

BI. Tests using a high-speed low melting surface

In the past nine months of the project, the main emphasis has been on studying effects associated with softening and melting of interfacial layers during sliding. It is known that in high speed pin on disk friction tests melting of test materials can occur. It has been argued that, if the pin has a lower melting point than the disk, it is not likely that full fluid lubrication at the sliding interface will occur because the leading edge of the pin is not molten. However, if the disk melts at a lower temperature than the pin, full hydrodynamic lubrication can occur more readily. To check on the existence of any differential effect, a layer of eutectic solder was cast around a 4140 steel disk to produce a low melting point surface moving at a high velocity. Low friction values were indeed observed, but they were not low enough to indicate hydrodynamic lubrication. Disk runout greater than the thickness of a hydrodynamic fluid film are a possible explanation of this result.

B II. Thermoelectric temperature measurements

Thermoelectric temperature measurement techniques do not work well for most combinations of test materials. A non-linear temperature-EMF relationship exists for many material combinations, and that effect combined with a low EMF output makes it difficult to accurately determine the temperature.

However, some test materials, bismuth in particular, produce large linear thermoelectric outputs against ordinary metals. It seems that reliable temperature measurements can be made with bismuth sliding against 4140 steel or eutectic solder.

In tests of bismuth sliding against eutectic solder, thermoelectric measurements indicate a maximum temperature of 130°C with an average of 90°C. Eutectic solder melts at 183°C and bismuth melts at 271°C. A ternary bismuth alloy known as Malotte's metal has tin and lead in the same ratio as eutectic solder, and it melts at about 120°C. During a sliding test this low melting point alloy is formed and the maximum sliding temperature is therefore limited.

In tests of bismuth sliding against 4140 steel, the thermocouple method indicates that the average temperature is 260°C which is essentially the melting point of bismuth. Low values of the friction coefficient were obtained with this combination.

These tests indicate that the method of using dissimilar metals at an interface as one arm of a thermocouple does indeed give sensible values for the interfacial temperature. One of the problems we encountered with low melting metals was that of determining their melting points, latent heats, and compositions.

A way of determining these properties consisted of extracting heat from a molten sample at a constant rate and plotting its temperature versus time. The resulting curve gives the solidus-liquidus temperature from changes in the slope, and the heat of fusion of the metal can be calculated from the length of the flat region. For some unknown reason the experimentally determined heats of fusion are lower than published values by a factor of at least two. Since no critical calculations involving the heat of fusion have been made, this discrepancy has not been resolved.

B. III. Optical pyrometer measurements

The optical pyrometer can be used if the test material melts at a temperature of at least 1000°C. Using our method, the temperature is measured

downstream of the interface and a multiplication factor is used to compute the interfacial temperature. We have recently computed improved values of the multiplication factors. Since the multiplication factors are based upon the disc cooling rate, any sparks produced during a test will give an indicated temperature which is higher than that which actually exists. Often tests with ferrous materials produce sparks and saturate the electronics of the pyrometer, but in practice the presence of the sparks seems to indicate that the test material has melted.

B.IV. Tests in which bulk plastic deformation was made especially easy

Some tests were conducted in which the specimen was pushed against a narrow projection on the disc. This resulted in high contact pressures and increased the PV value of the test by a factor of 3.5 above normal tests. A large shear stress is introduced in the pin but no plastic flow has been observed from tests using pins of gilding metal or Wood's metal. The friction coefficient is lower for these 'projection' tests than it is for ordinary tests because of the higher PV values.

The large amount of scatter in the wear data for sintered iron led to an improvement in the test apparatus. A means of precisely controlling the duration of a test was devised so that all tests could be run for an equivalent sliding distance. The effect of material transfer on wear rate during different tests would therefore be minimized. Otherwise some tests would retrace a wear track many times and material adhered to the disc would produce very large wear rates. Now a 500 fps test lasts 1/5 as long as a 100 fps test. The test duration is presetable from 0 to 1 sec with 10 millisecond accuracy.

Many tests were conducted in an attempt to uncover materials with low

friction coefficients. The test apparatus was adapted to conduct tests at speeds as low as 10 fps to extend the usable PV test range. Even with this, materials known for their low friction coefficients exhibit high values of f. Teflon composites typically give f values of .3 instead of .1. The PV values investigated are still much higher than those normally used.

It was suspected that the lower the melting point of one of the test materials, the lower a PV value would be necessary to produce low friction. This was not found to be the case. Over the velocity range of 100 to 500 fps individual friction coefficients do not vary by much more than a factor of 2. Almost all tests were conducted using 1/8" diameter specimens under a 4.8 lb normal load. Average friction coefficient values for materials tested were as follows.

Table B.1. Average friction coefficients against a 4140 steel disk

Material	Friction coefficient f
Bismuth	.35 → .14
Copper	.85 initial, > 1 later
Delrin	.85
DQ3	.30 at low speeds, 10 fps
Eutectic Solder	.80
Gilding metal	.85 → .35 Scattered
Graphite	.35 10 fps
Iron	.9 → .6
Sintered Iron	.85 → .4
Polycarbonate	.55
Rulon A	.30 @ 10 fps, .2 for lower speeds
Steel and soap	.20 @ fps
Ultra-high molecular weight polyethylene	.55
Wood's metal	.85 → .4

<u>Table B.2 Average friction against a eutectic solder disk</u>

                   1/2" steel ball   .25

                   Bismuth   .30 (.15 initial peak)

Some of the friction-velocity, wear-velocity and temperature-velocity plots obtained are shown in figures B1 - B10.
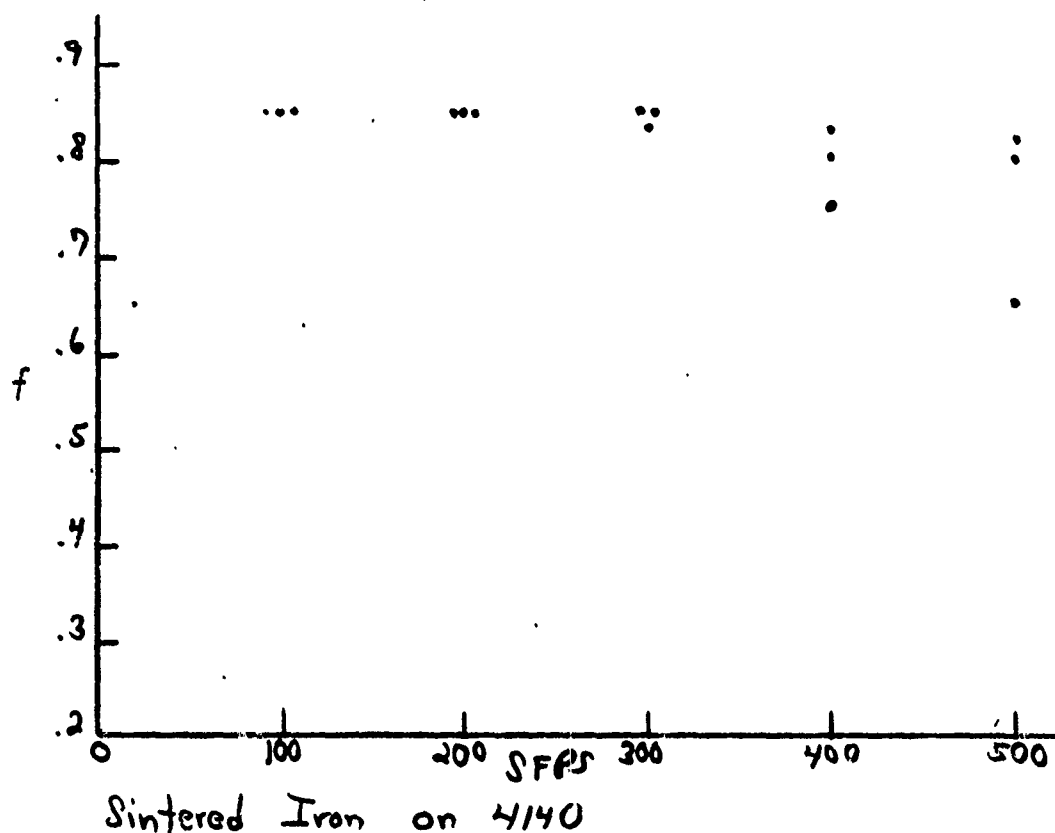
Figure B1. Friction coefficient obtained using a sintered iron pin on a 4140
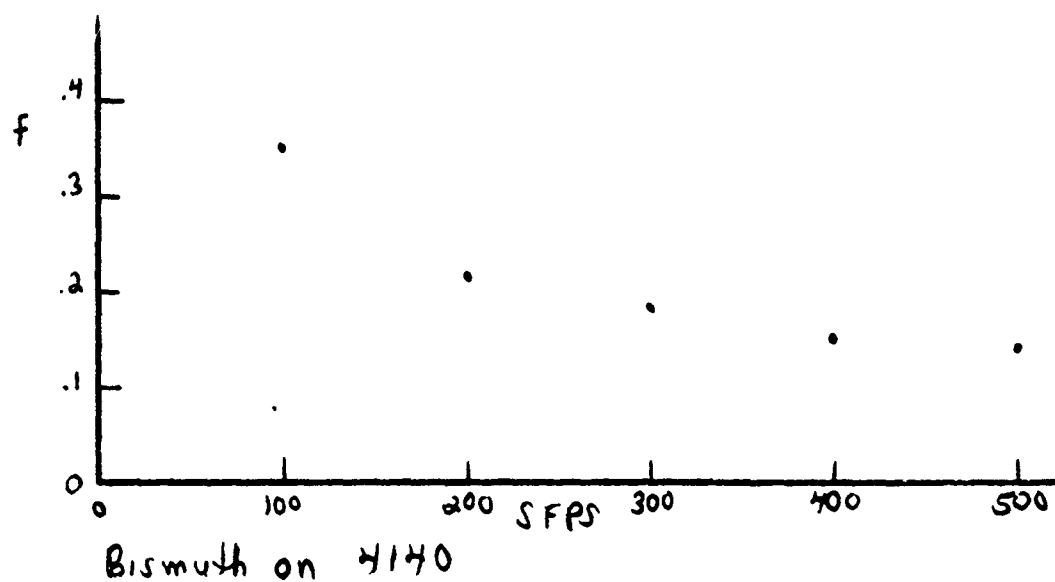steel disk. The friction is high, but drops off slightly as the speed increases.

Figure B2. Friction coefficient using a bismuth pin on a 4140 steel disk.
Some of the lowest friction values encountered in this project were observed
with this combination.
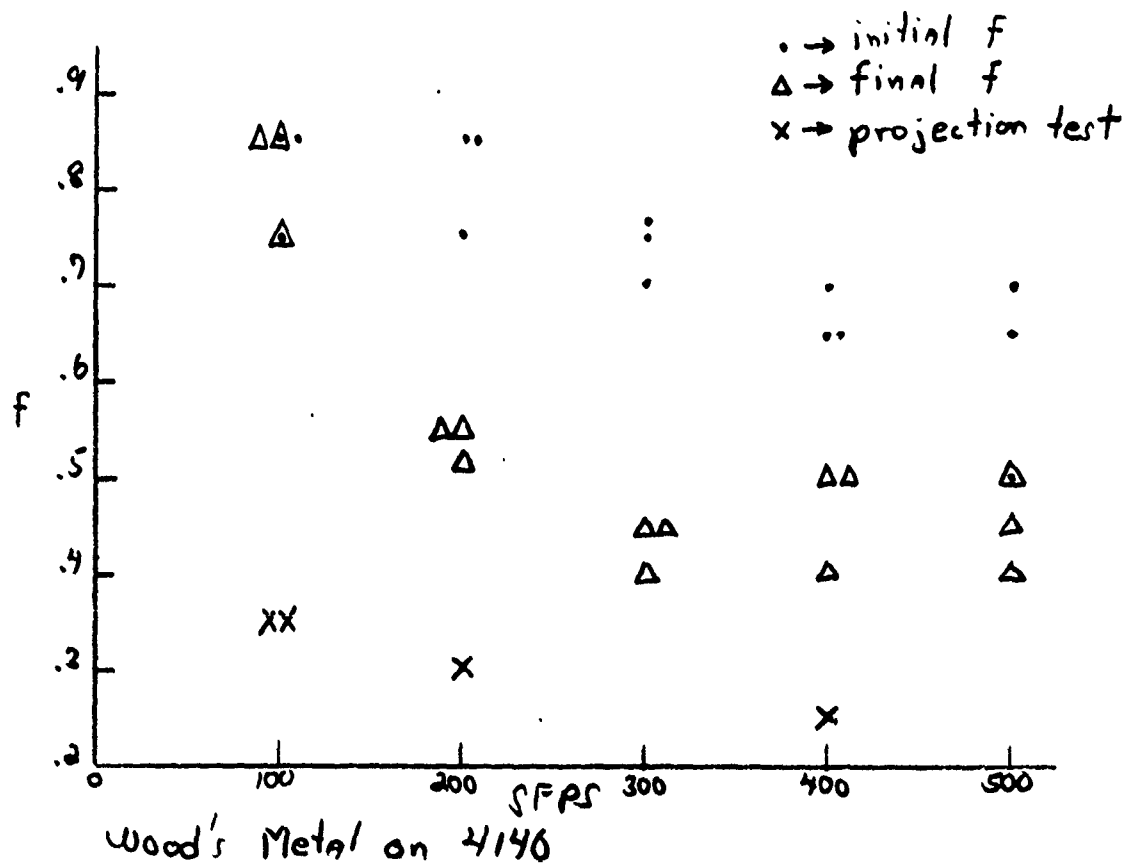
Figure B3. Friction coefficient values using Wood's metal on 4140 steel. The lowest friction was observed when the disk had a sharp projection.
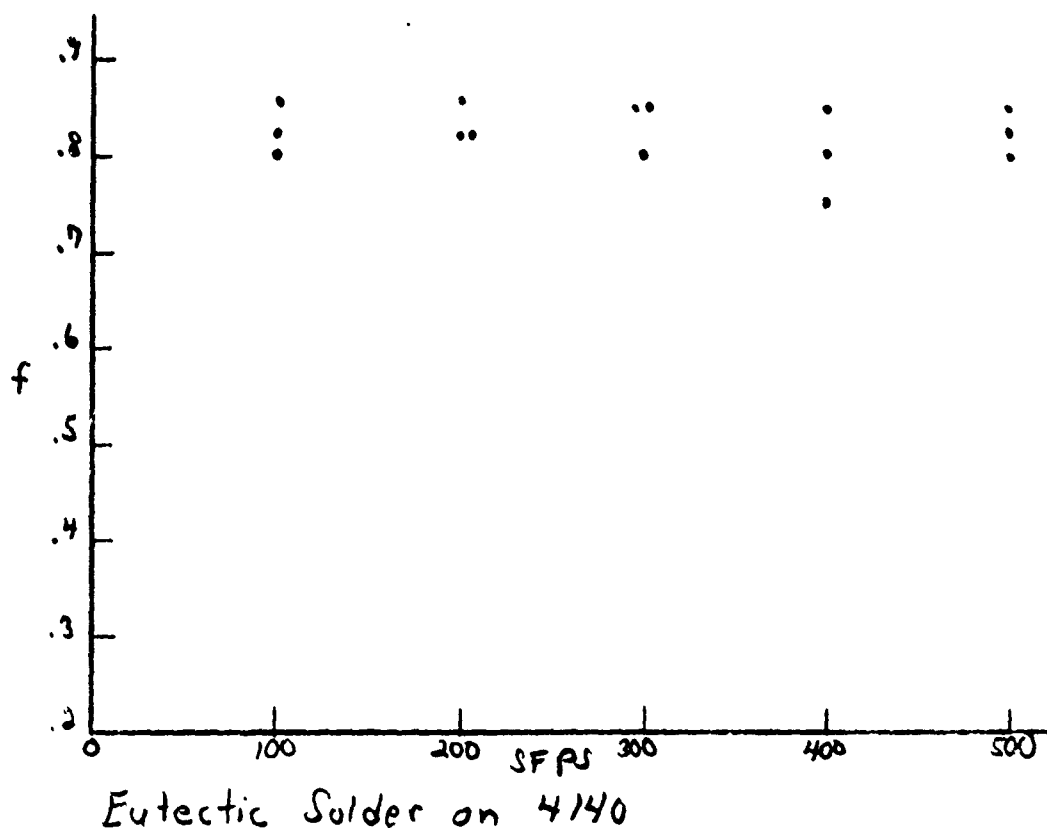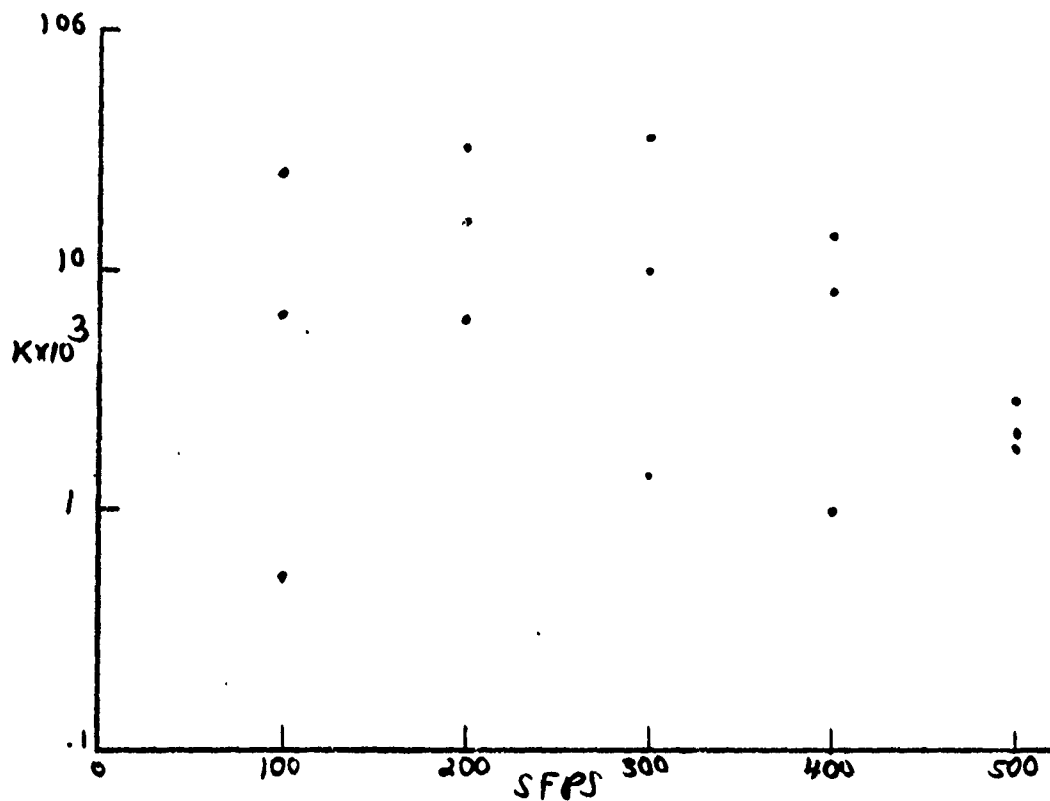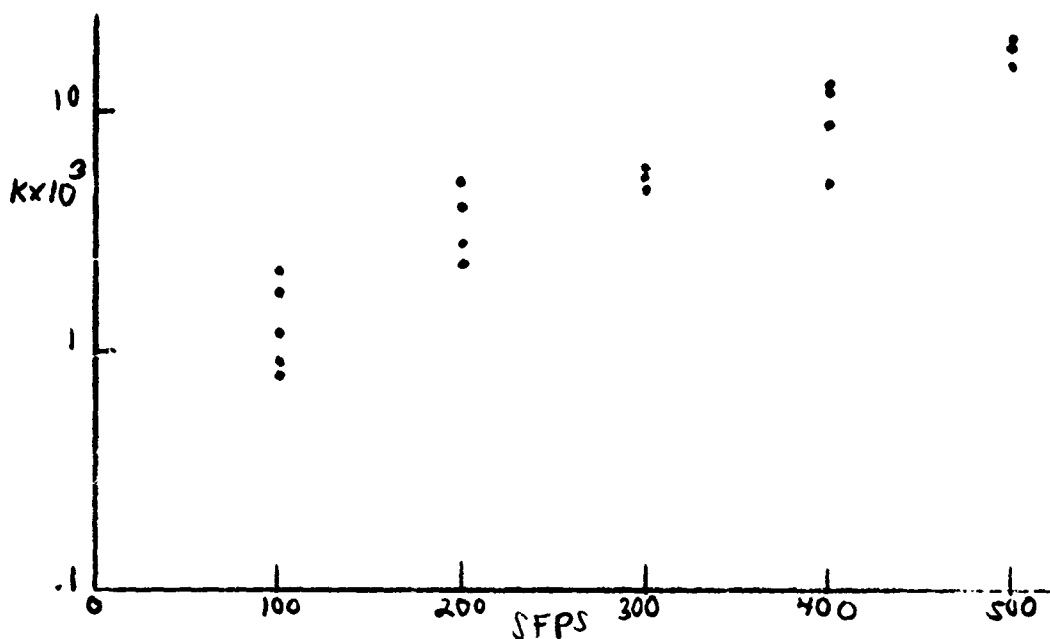

Figure B4. friction coefficient using a tin-lead solder on 4140 steel. The friction was surprisingly high.
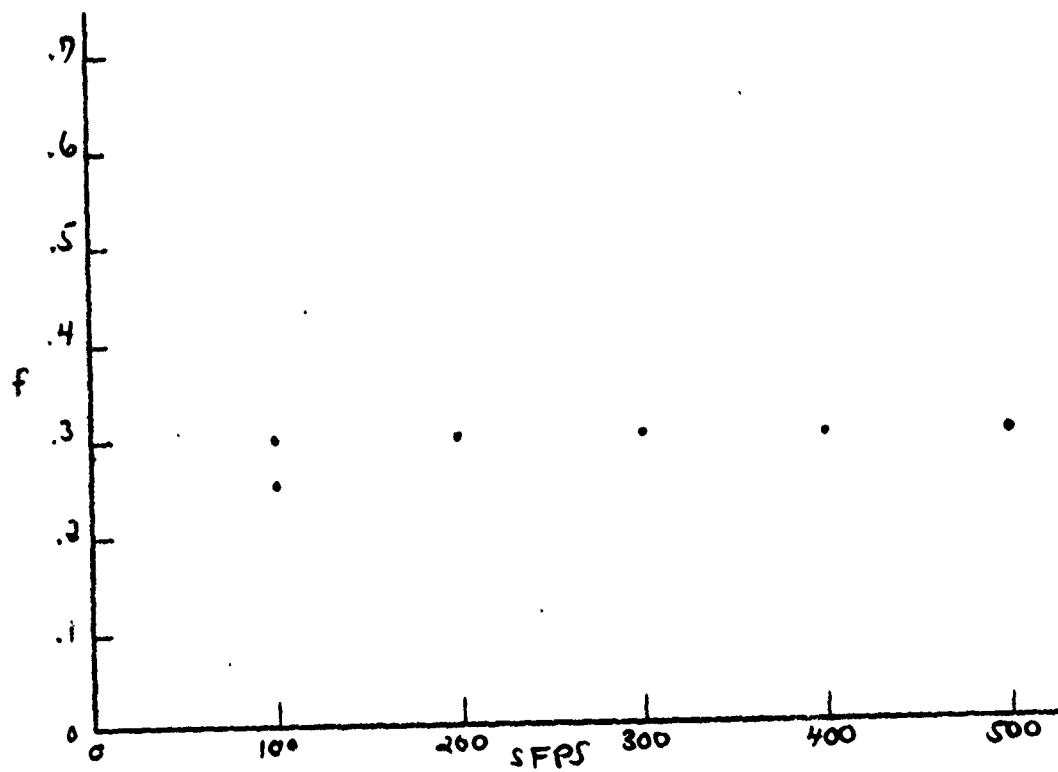
Sintered Iron on 4140

Figure B5. Wear coefficient for sintered iron on 4140 steel as a function of sliding speed. The wear is high, but decreases as sliding speed increases.
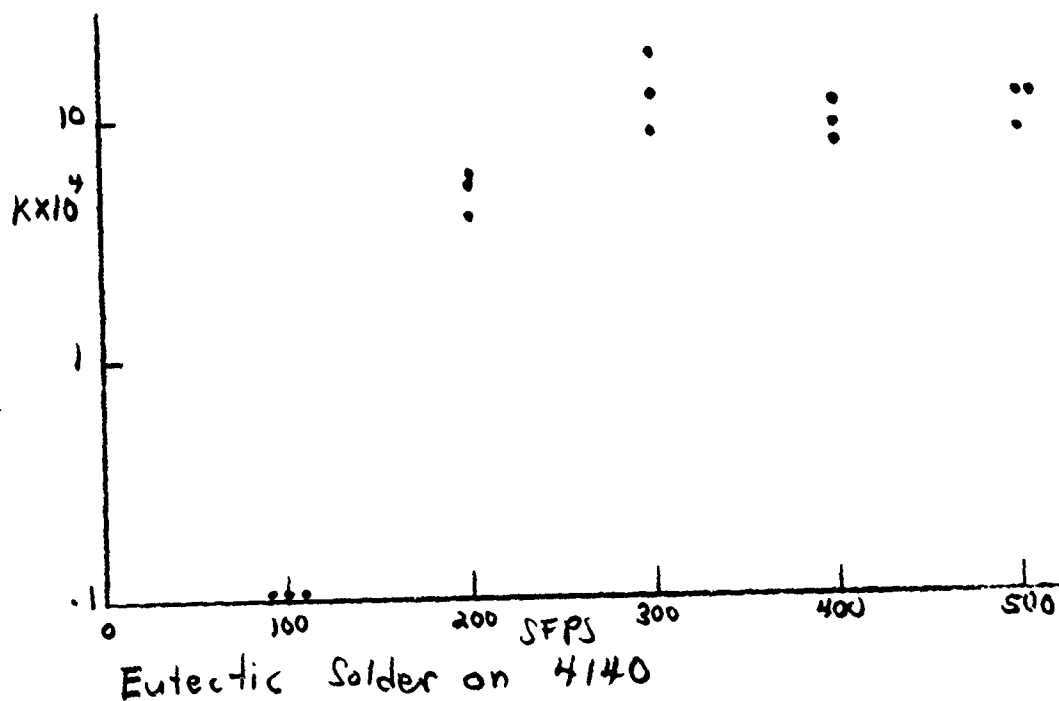

Wood's Metal on 4140

Figure B6. Wear coefficient for Wood's metal against 4140 steel. The increase in wear at high sliding speeds is associated with melting of the Wood's alloy.

Bismuth on Eutectic Solder Disc

Figure B7. Friction of a bismuth pin on a steel disc coated with tin-lead solder.

Eutectic Solder on 4140

Figure B8. Wear coefficient of a tin-lead solder pin on a 4140 steel disk. A great increase in wear seems to be associated with melting at the interface.
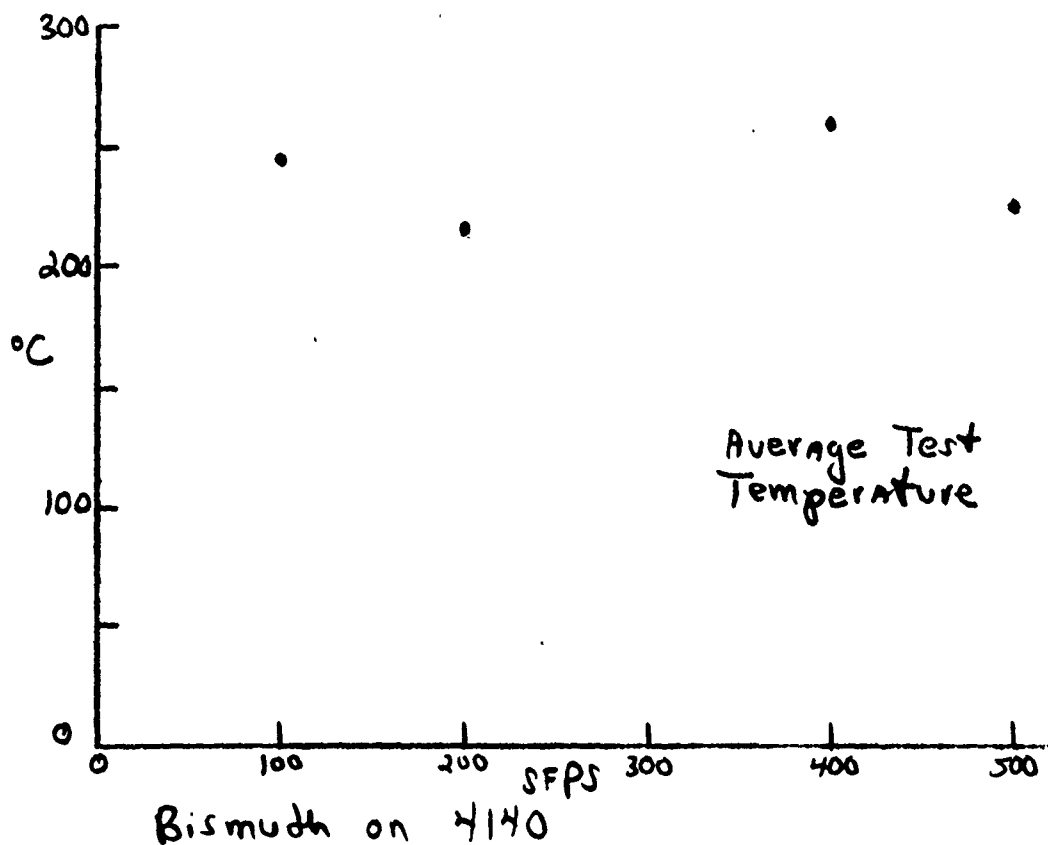
Figure B9. Surface temperature (measured by the thermocouple method) as a function of sliding speed for a bismuth pin on a 4140 steel disk. The interface readily reaches a temperature close to the melting temperature of bismuth.
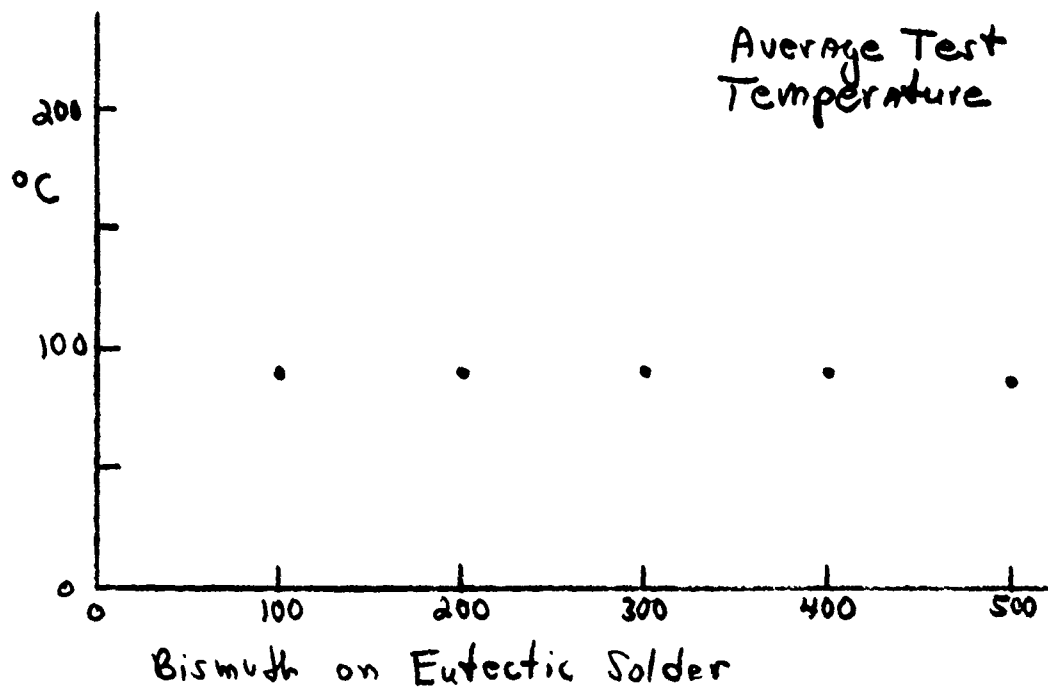

Figure B10. Temperature as a function of sliding speed for a bismuth pin on a tin-lead disk. The temperature is limited by the melting of a low melting ternary alloy.